



NASW-4435

111-23-172

204-83

1521

NASA/USRA UNIVERSITY
ADVANCED DESIGN PROGRAM
1992-1993

PROJECT CENTER MENTOR:
NASA-AMES DRYDEN FLIGHT RESEARCH FACILITY

FINAL DESIGN PROPOSAL

The Blue Emu

A Simulated Commercial Air Transportation Study

April 1993

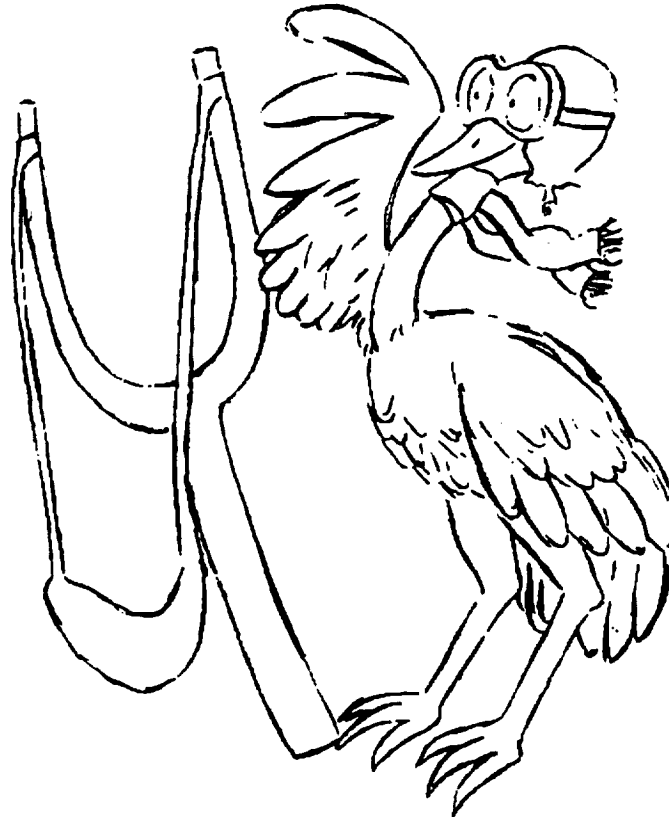
Department of Aerospace and Mechanical Engineering
University of Notre Dame
Notre Dame, IN 46556

(NASA-CR-195535) THE BLUE EMU
Final Design Proposal (Notre Dame
Univ.) 125 p

N94-24817

Unclass

50/50 Aeronautics presents:



the Blue Emu

FINAL PROPOSAL

Submitted: April 8, 1993 by...

**Doug Descalzi
John Gillett
Karl Gordon
Ed Keener
Ken Novak
Laura Puente**

**PROPULSION
STABILITY AND CONTROL
PERFORMANCE
AERODYNAMICS
WEIGHTS
STRUCTURES**

**AE441: Aerospace Design
UNIVERSITY OF NOTRE DAME**

Table of Contents

A. Executive Summary	
A.1 Summary	A-1
A.2 3 View External/Isometric View/2 View Internal.....	A-4
A.3 Tabular Summary of Specifications	A-7
A.4 Critical Technical Areas	A-8
A.5 Critical Data Summary	A-9
B. Design Requirements and Objectives and Mission Definition Study	
B.1 Mission Evaluation Study.....	B-1
B.2 Design Requirements and Objectives.....	B-3
B.2.1 Marketing and Economics	B-3
B.2.2 Propulsion System	B-3
B.2.3 Performance.....	B-4
B.2.4 Stability and Control.....	B-4
B.2.5 Aerodynamics.....	B-4
B.2.6 Structures and Weight	B-4
C. Concept Selection Studies	
C.1 Introduction	C-1
C.2 Fuselage Concepts	C-1
C.3 Wing Design Concepts	C-4
C.4 <i>The Blue Emu</i>	C-6
C.5 Influencing Factors.....	C-7
D. Aerodynamics	
D.1 Summary	D-1
D.2 Requirements and Objectives.....	D-1
D.3 Wing Design.....	D-2
D.4 Airfoil Selection and Characteristics.....	D-5
D.5 Drag Prediction.....	D-6
D.6 Aerodynamic Performance.....	D-9
E. Propulsion	
E.1 Summary	E-1
E.2 Requirements, Objectives, and Propulsion Mission Analysis	E-1
E.3 Motor Selection.....	E-1
E.4 Propeller Selection.....	E-3
E.5 Battery Selection.....	E-6
E.6 Speed Control	E-7
E.7 System Performance	E-8
F. Weight Analysis	
F.1 Introduction and Tabular Summary	F-1
F.2 Center of Gravity: Movement and Compensation	F-3
F.3 Weight Conservation of the Tapered Wing	F-7
F.4 Competitive Weight Design with the <i>HB-40</i>	F-9
G. Stability and Control	
G.1 Summary	G-1
G.2 Design Requirements and Objectives.....	G-1
G.3 Center of Gravity and Static Margin	G-2
G.4 Longitudinal Stability.....	G-3
G.5 Longitudinal Control	G-5
G.6 Lateral Stability	G-8
G.7 Lateral Control	G-10
G.8 Control Mechanisms.....	G-11

H. Performance	
H.1 Takeoff and Landing Estimates.....	H-1
H.2 Range and Endurance.....	H-2
H.3 Climbing and Gliding Performance	H-6
H.4 Turning	H-7
H.5 Performance Summary	H-9
I. Structural Analysis	
I.1 Producibility.....	I-1
I.2 V-n Diagram	I-1
I.3 Wing Structure	I-2
I.4 Vertical and Horizontal Tail Structure.....	I-3
I.5 Fuselage	I-4
I.6 Landing Gear Design	I-5
J. Economic Analysis	
J.1 Introduction and Tabular Summary.....	J-1
J.2 Depreciation Costs.....	J-2
J.3 Fuel Costs	J-5
J.4 Fuel Cost per Passenger.....	J-6
J.5 Brief Economic Comparison with <i>HB-40</i>	J-8
K. References	K-1

Appendices

Appendix I. Concept Selections.....	I-1
Appendix II. Aerodynamics	II-1
Appendix III. Stability and Control	III-1
Appendix IV. Performance.....	IV-1
Appendix V. Economics.....	V-1

A. Executive Summary

A.1 Summary

The Blue Emu is a 60 passenger, 4.79 lb. commercial aircraft with a design range of 17,000 ft (including a two minute loiter) and a cruise speed of 30 ft/sec. The total cost of the aircraft is \$1,690.34. *The Blue Emu* is designed to compete with the existing aircraft, the *HB-40*, and to successfully capture the short- to mid-range market of Aeroworld.

The primary goal in designing *the Blue Emu* was to provide an airline with a cost efficient and profitable means of transporting passengers between the major cities in Aeroworld. The design attacks the market where a demand for inexpensive transportation exists, and for this reason *the Blue Emu* is an attractive investment for any airline. In order to provide a profitable aircraft, special attention was paid to cost and economics. For example, in manufacturing, simplicity was stressed in structural design to reduce construction time and cost. Aerodynamic design employed a tapered wing which reduced the induced drag coefficient while also reducing the weight of the wing. Even the propulsion system was selected with cost effectiveness in mind, yet also to maintain the marketability of the aircraft. Thus, in every aspect of the design, consideration was given to economics and marketability of the final product.

From these primary, qualitative considerations evolved a set of secondary, specific objectives. Many of these objectives were set to exceed the performance and marketability of the competition, the *HB-40*. A takeoff objective of 32 feet was set in order to service all cities of Aeroworld except C and O which have much shorter runway distances. A simple tail-dragger, high wing, monoplane concept was selected to reduce complexity in design and construction. *The Blue Emu* is not a particularly innovative aircraft. Rather than attempt to compete with a risky and revolutionary design, the *Blue Emu* attempts to improve on simple, existing concepts. By studying the competition, areas of weakness can be capitalized upon without radically changing conventional aircraft shape and design. This simplicity, and in a sense redundancy, lead to ease and confidence in construction. All these factors were considered in order to reduce the primary measure of economic merit, the CPSPK of the aircraft.

Economic considerations focused largely on reducing the manufacturing and operating costs of the aircraft. The DOC for *the Blue Emu* is \$6.10 with a CPSPK of \$0.0061 as compared to the \$0.009 CPSPK of the *HB-40*. As previously mentioned, the total cost of the aircraft is \$1,690.34. The greater passenger payload capacity and

reduction in CPSPK give *the Blue Emu* a economic marketing advantage over the *HB-40*.

The propulsion system for *the Blue Emu* consists of a single, front mounted, Astro Cobalt 15 electric motor, a Top Flight 12-6 propeller, and 11 P-90SCR batteries. The propulsion system was selected by finding the components that would most efficiently meet the takeoff objectives yet not suffer weight and cost penalties in overpowering the aircraft. The Astro 15 - Top Flight 12-6 combination provided the necessary power and thrust to takeoff in 32 feet, yet remain cost effective and perform efficiently in cruise. Smaller motors were considered but did not provide enough power. Likewise, larger or multiple motor systems motors provided unnecessary, excessive power and were more expensive. The Top Flight 12-6 was the smallest and most efficient propeller that provided the thrust required for the takeoff objective. In addition, the Astro 15 - Top Flight 12-6 combination allowed for use of the P-90SCR 900 mAhr batteries, which happen to be the least expensive battery cells available.

The Wortmann airfoil was selected because it exhibited high lift, low drag, and favorable stall characteristics in this low Reynolds number regime. The wing size was chosen as 10 square feet to attain an advantageous wing loading and to produce similar lift characteristics of the Wortmann airfoil section for the finite wing of the aircraft. The wing employed a taper ratio of 0.6 to increase the aspect ratio, which ultimately narrows the difference between airfoil section and finite wing lift characteristics, as well as to approximate an elliptic wing planform. By using a tapered wing concept and thus modeling an elliptic wing shape, a 6% reduction in the induced drag coefficient over a rectangular wing was realized. Further, the wing employed by *the Blue Emu* produces 57% less induced drag in cruise than the *HB-40*. Wing design was a critical technology of *the Blue Emu*. This reduction in drag will improve the economic characteristics of the aircraft and allow it to successfully compete in Aeroworld.

Longitudinal and lateral control surfaces allow *the Blue Emu* to maneuver. *The Blue Emu* utilizes a elevator-rudder, two servo control system. Ailerons were not included in the control system to avoid the complexity and weight of added servos. Flat plates were used for the horizontal and vertical tail to ease construction. The combination of rudder deflection and dihedral was the mechanism chosen to turn the aircraft. A static margin of 20% was allowed to permit the pilot longer response times when controlling from the ground.

The Blue Emu successfully met design requirements and objectives set forth by the request for proposals as well as by the design group. The aircraft has several distinct advantages over the existing competition, the *HB-40*. First and most obvious, *the Blue*

Emu has a greater passenger capacity than the *HB-40*. Second, the extended range of *the Blue Emu* adds to flexibility in use of the aircraft. Third, the wing design offered by *the Blue Emu* reduces the induced drag of the aircraft. Finally, *the Blue Emu* has a CPSPK 34.4% lower than that of the *HB-40*, making it a more economical aircraft. For these reasons, upon completing construction, *the Blue Emu* should successfully compete in the market it was designed for.

Figure A.2-1: EXTERNAL CONFIGURATION

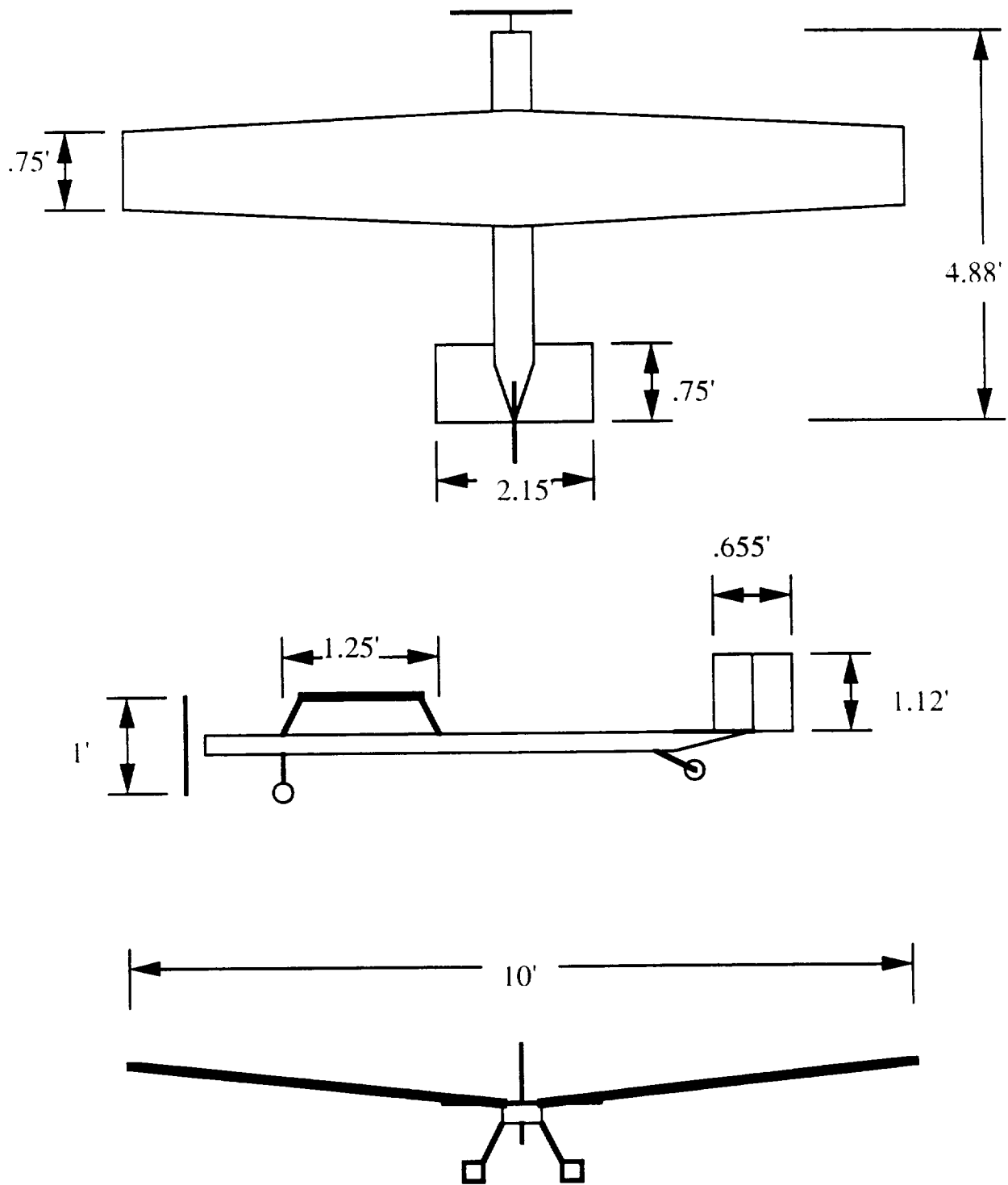


FIGURE A.2-2: ISOMETRIC VIEW

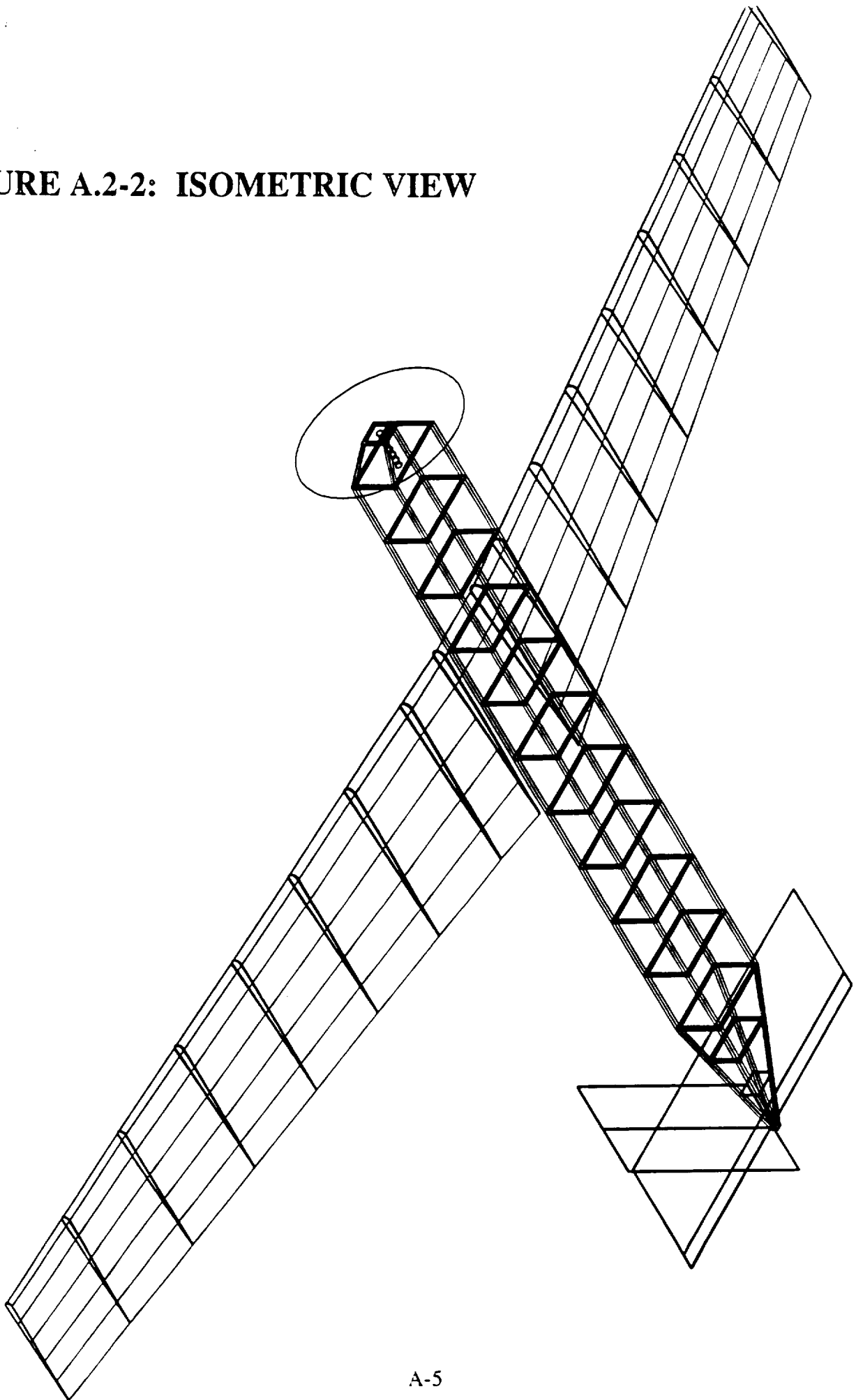
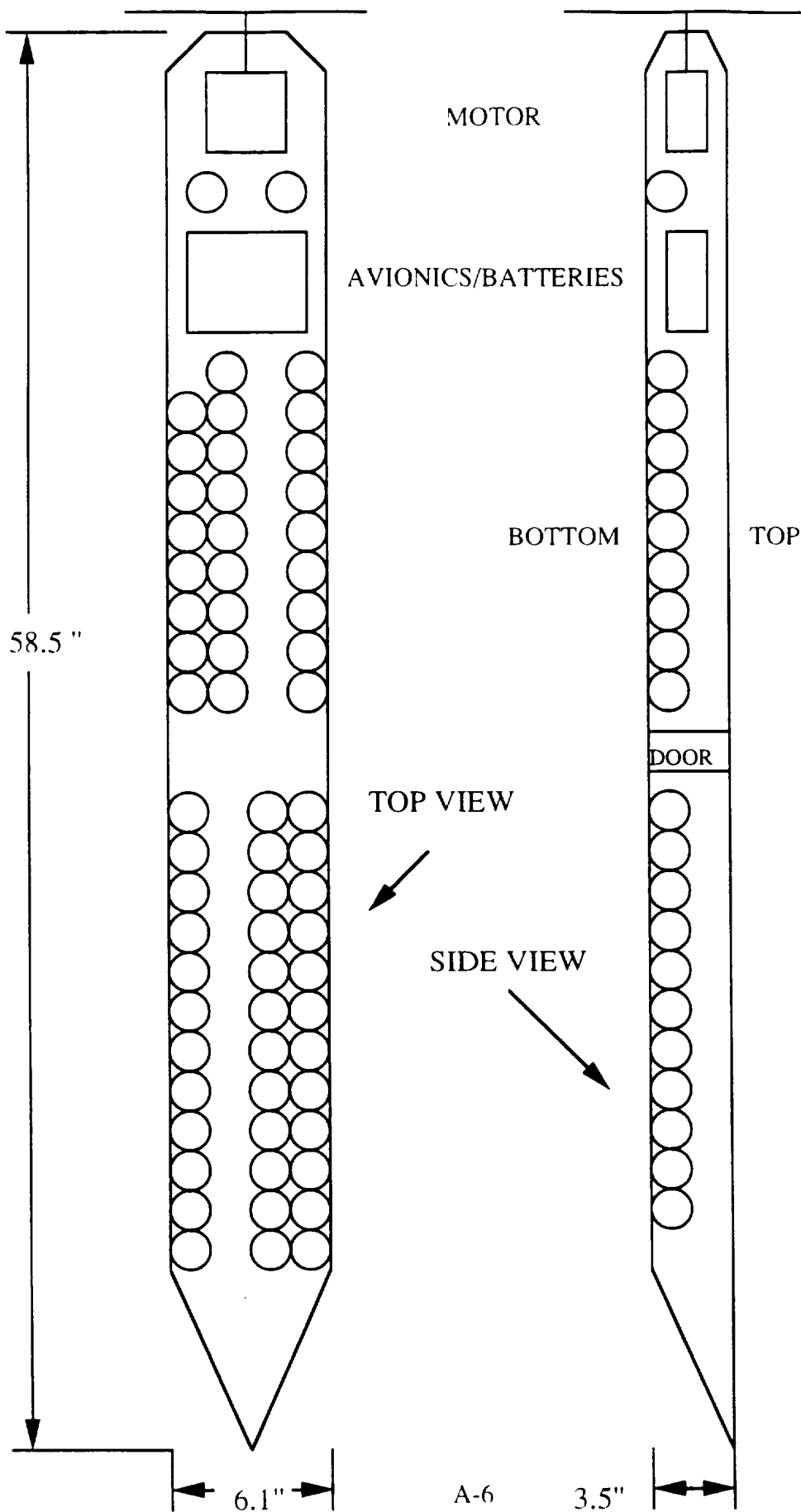


Figure A.2-3: INTERNAL LAYOUT



POST FLIGHT MANAGEMENT REVIEW:

Blue Emu

April 30, 1993

The following observations were made during the flight test validation for this aircraft design. This assessment is obviously quite qualitative and is based primarily upon the pilot's comments and instructor's observations.

1. Some problems were encountered with the flexibility of the vertical stabilizer and the rudder hinge. Also it was brought to the test flights with excessive asymmetric twist in the wings due to a recent repair of the main wing carry-through as a result of an accident during taxi testing.
2. Left rudder was very ineffective, possibly due to the hinge and inadequate stiffness.
3. Seemed to stall in the turns.
4. Marginally controllable. The pilot would fly into the turns, wings would stall, and he had to use the throttle to pull out of the turns.
5. Successful validation of basic flight concept. Flew under control through entire closed course at approximately the required loiter speed. Landing and take-off performance was acceptable based upon the requirements.

A.3 Summary of Specifications

AERODYNAMICS		PERFORMANCE	
Wing Area	10 ft ²	Takeoff distance	30.96 ft
Aspect Ratio	10	Velocity @ Takeoff	25.32 ft/sec
Mean Chord	1.0 ft	Velocity @ cruise	30.0 ft/sec
Span	10 ft	Range (cruise)	23,170 ft
Taper Ratio	0.6	Endurance (cruise)	12.87 min
Sweep	0.0 degrees	Max Range	23,667 ft
Dihedral	9.0 degrees	Max Endurance	14.3 min
C _{do}	0.015	Max Rate of Climb	11.32 ft/s
Airfoil Section	Wortmann FX63-137	Turn Radius	53.3 ft
Wing Mount Angle	0.0 degrees		

EMPENNAGE		PROPULSION	
Horiz Tail Airfoil	Flat Plate	Engine	Astro 15
Horiz Tail Area	1.61 ft ²	Propeller	Top Flight
Vert Tail Airfoil	Flat Plate	# of Batteries	11
Vert Tail Area	0.68 ft ²	Battery Pack Voltage	13.2 Volts
Elevator δ max	- 15/+10 degrees	Battery Capacity	900 mAh
Elevator Area	0.32 ft ²	Motor Cruise rpm	8042 rpm
Rudder δ max	+/- 25 degrees	Prop Cruise rpm	3380 rpm
Rudder Area	0.37 ft ²		

STRUCTURE		ECONOMICS	
Weight	4.79 lbf	DOC	\$6.10
Fuselage Length	60.5 inches	CPSPK	\$.006
Fuselage Width	6.1 inches	Cost of Aircraft	\$1690.34
Fuselage Height	3.5 inches		

A.4 Critical Technologies

The major critical technology incorporated into the design of *the Blue Emu* was the tapered wing. The tapered wing was constructed with benefits in the areas of aerodynamics, weight savings and reduced structural strength at the tip chord. The only significant risk involved will be in the production of the different size airfoil sections.

The first objective in the area of aerodynamics was to improve upon the aerodynamic performance of the *HB-40*. The area of the wing was set at 10 ft² in order to produce low wing loadings. By tapering the wing, the span must increase in order to maintain this desired wing area. This translated into an increased aspect ratio. Induced drag varies inversely with aspect ratio and therefore, *the Blue Emu*, with a higher aspect ratio than the *HB-40* managed a lower induced drag.

A further benefit of the tapered wing is the fact that the wing tip is not as strong as the wing root. The lift distribution over the span of the wing reduces as the wing tip is reached. Therefore, the wing tips do not have to be constructed to be as strong as the wing root. A typical rectangular wing has the same strength characteristics at the root as at the tip, thus representing an inefficient use of material.

By having a tapered wing, a reduction in wing weight was achieved. By gradually reducing the sizes of the airfoil sections, a weight savings was attained. Smaller wing spars correspond to less weight.

As mentioned earlier, the main disadvantage of the tapered wing is realized in the manufacturing of the different size airfoil sections which will have to be scaled properly. In previous years the tapered wing concept was apparently shunned because of this difficulty. Therefore, venturing into this uncharted area does present a certain amount of risk. However, it is believed that with the aid of a Xerox machine the difficulty of reproducing the scaled spar webs will be reduced, as will the necessary manufacturing time.

A second critical area was a keen observance of weight reduction in all possible areas. Inspection of the competition, the *HB-40*, showed inefficient use of material in areas aside from the wing construction. Structural redundancies in the fuselage were eliminated, wider wing spar spacing was employed, and lighter materials were used. These considerations resulted in a lower aircraft weight per passenger ratio.

The overall aircraft sought to excel in aerodynamic performance, to provide a structure which preserved integrity and accomplished efficient weight conservation, and to facilitate manufacturing so as to keep costs low. A final disadvantage of the overall design is the fact that *the Blue Emu* attacks a market that is already serviced by existing aircraft. Therefore, to be successful, *the Blue Emu* must not only fulfill the mission, but perform better than the competition, specifically, the *HB-40*.

Parameter Initials of RI:
 *[all distances relative
 to aircraft nose
 and in common units]*

DESIGN GOALS:

V cruise	30 ft/s
Max # of passengers	60
# passenger-coach	60
# passengers - 1st class	0
# crew	4
Max Range at Wmax	23,000
Altitude cruise	20 ft
Minimum turn radius	55 ft
Max Range at Wmin	23,000
Maximum TO Weight-WMTO	4.79 lb
Minimum TO Weight - Wmin	4.43 lb
Total Cost per Aircraft	\$1,690.34
DOC	\$6.10
CPSPK (max design conditions)	0.0061

A.5 CRITICAL DATA SUMMARY

BASIC CONFIG.

Wing Area	10 ft ²
Maximum TO Weight - WMTO	4.79 lb
Empty Flight Weight	4.43 lb
Wing loading(WMTO)	9 oz/ft ²
max length	4.9 ft
max span	10 ft
max height	3.5 in
Total Wetted Area	33.7 ft ²

WING

Aspect Ratio	10
Span	10 ft
Area	10 ft ²
Root Chord	1.25 ft
Tip Chord	0.75 ft
taper Ratio	0.6
C mac - MAC	1.0 ft
leading edge Sweep	0.0 degrees
1/4 chord Sweep *	0.0 degrees
Dihedral	8.0 degrees
Twist (washout)	0.0 degrees
Airfoil section	Wortmann
Design Reynolds number	200,000
t/c	13.59%
Incidence angle (root)	0.0 degrees
Hor. pos of 1/4 MAC	30 in
Ver. pos of 1/4 MAC	5.95 in
e- Oswald efficiency	0.95
CDo - wing	0.07
CLo - wing	0.53
CLalpha - wing	0.089/degree

FUSELAGE

Length	4.9 ft
Cross section shape	square
Nominal Cross Section Area	21.35 in ²
Finess ratio	16.8
Payload volume	736 in ³
Planform area	10 ft ²
Frontal area	21.35 in ²
CDo - fuselage	0.00394
CLalpha - fuselage	

EMPENNAGE

Horizontal tail	
Area	1.613 ft ²
span	25.8 in
aspect ratio	2.867
root chord	9 in
tip chord	9 in
average chord	9 in
taper ratio	1
i.e. sweep	0.0 degrees
1/4 chord sweep	0.0 degrees
incidence angle	0.0 degrees
hor. pos. of 1/4 MAC	33.25 in
ver. pos. of 1/4 MAC	1.75 in
Airfoil section	flat plate
e - Oswald efficiency	0.63
CDo -horizontal	0.000855
CLo-horizontal	0.0041/ degree
CLalpha - horizontal	0.063/ degree
CLde - horizontal	0.0002/ degree
CM mac - horizontal	0.041

Vertical Tail	
Area	0.681 ft ²
Aspect Ratio	1.59
root chord	7.86 in
tip chord	7.86 in
average chord	7.86 in
taper ratio	1
i.e. sweep	0.0 degrees
1/4 chord sweep	0.0 degrees
hor. pos. of 1/4 MAC	38.78 in
vert. pos. of 1/4 MAC	1.75 in
Airfoil section	flat plate

SUMMARY AERODYNAMICS

Cl max (airfoil)	1.6
CL max (aircraft)	1.1
lift curve slope (aircraft)	0.089/degree
CDo (aircraft)	0.015
efficiency - e (aircraft)	0.829
Alpha stall (aircraft)	11 degrees
Alpha zero lift (aircraft)	7.0 deg (neg)
L/D max (aircraft)	17.4
Alpha L/D max (aircraft)	2.75 degrees

WEIGHTS

Weight total (empty)	4.79 lb
C.G. most forward-x&y	17.8 in
C.G. most aft- x&y	18 in
Avionics	5.92 oz
Payload-Crew and Pass-max	5.64 oz
Engine & Engine Controls	24.28 oz
Propeller	0.5 oz
Fuel (battery)	13.53 oz
Structure	
Wing	14.74 oz
Fuselage/emp.	14.54 oz
Landing gear	3.5 oz
lcg - max weight	17.95 in
lcg - empty	16.6 in

PROPULSION

Type of engines	Astro 15
number	1
placement	front
Power max at cruise	80 W

Preq cruise	14.158 W
max. current draw at TO	10.82 A
cruise current draw	4.11 A
Propeller type	Top Flight 12-6
Propeller diameter	12 in
Propeller pitch	6 degrees
Number of blades	2
max. prop. rpm	9000 rpm
cruise prop. rpm	3380 rpm
max. thrust	2.8 lb
cruise thrust	0.33 lbs
battery type	P90SCR 900
number	11
individual capacity	900 mAh
individual voltage	1.2 V
pack capacity	900 mAh
pack voltage	13.2 V

STAB AND CONTROL

Neutral point	0.5 c
Static margin %MAC	20%
Hor. tail volume ratio	0.53
Vert. tail volume ratio	0.22
Elevator area	9.8 in ²
Elevator max deflection	20 degrees
Rudder Area	57.50%
Rudder max deflection	20 degrees
Aileron Area	N.A.
Aileron max deflection	N.A.
Cm alpha	0.0176/deg (neg)
Cn beta	0.069/deg
Cl alpha tail	3.616
Cl delta e tail	0.0002/degree

PERFORMANCE

Vmin at WMTO	22 ft/s
Vmax at WMTO	51.3 ft/s
Vstall at WMTO	22 ft/s
Range max at WMTO	23,600 ft
Endurance @ Rmax	13.14 min
Endurance Max at WMTO	13.14 min
Range at @Emax	23,600 ft
Range max at Wmin	23,600 ft
ROC max at WMTO	5.55 ft/s
Min Glide angle	2.9 degrees
T/O distance at WMTO	26.19 ft

SYSTEMS

Landing gear type	Conventional
Main gear position	forward
Main gear length	7 in
Main gear tire size	2.5 in
nose/tail gear position	15 in/45.3 in
n/t gear length	8 in/2 in
n/t gear tire size	2.5 in/1 in
engine speed control	TEKIN
Control surfaces	rudder, elevator

TECH DEMO

Max Take-Off Weight	
Empty Operating Weight	
Wing Area	
Hor. Tail Area	
Vert Tail Area	
C.G. position at WMTO	
1/4 MAC position	

Static margin %MAC
V takeoff
Range max
Airframe struct. weight
Propulsion sys. weight
Avionics weight
Landing gear weight

ECONOMICS:

raw materials cost	\$100
propulsion system cost	\$142
avionics system cost	\$210
production manhours	95
personnel costs	\$950
tooling costs	\$294
total cost per aircraft	\$1,690
Flight crew costs	\$0.20
maintenance costs	\$0.07
operation costs per flight	\$0.27
current draw at cruise WMTO	4.11 A
flight time - design Range max	13.14 min
DOC	\$6.10
CPSPK	0.0061

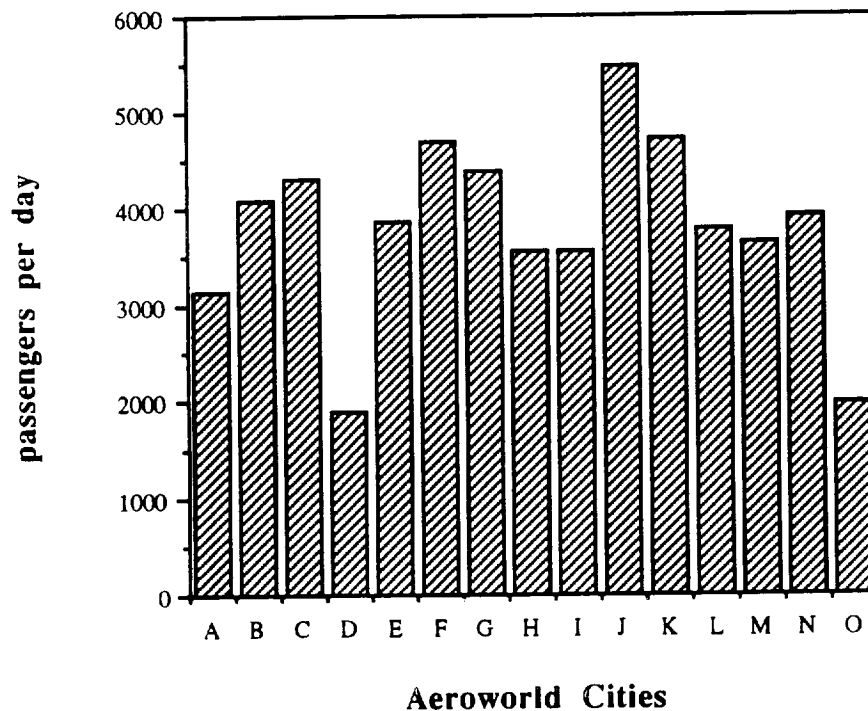
B. Mission Definition Study and Design Requirements and Objectives

B.1 Mission Evaluation Study

A mission evaluation study was performed in order to determine which specific market in Aeroworld could be successfully captured by a new aircraft. In mission selection, three primary questions were asked. First, it had to be determined which cities, if any, should be excluded from the cities that *the Blue Emu* could serve. Second, a design range had to be selected for the aircraft. Finally, the maximum passenger capacity needed to be determined for the aircraft.

From the market data given in the AE441 handout (ref. 10), the passenger traffic for each city (each city in Aeroworld was given an arbitrary name A through O) was calculated and is shown in Figure B.1-1.

Figure B.1-1: Aeroworld Air Traffic per Day by City

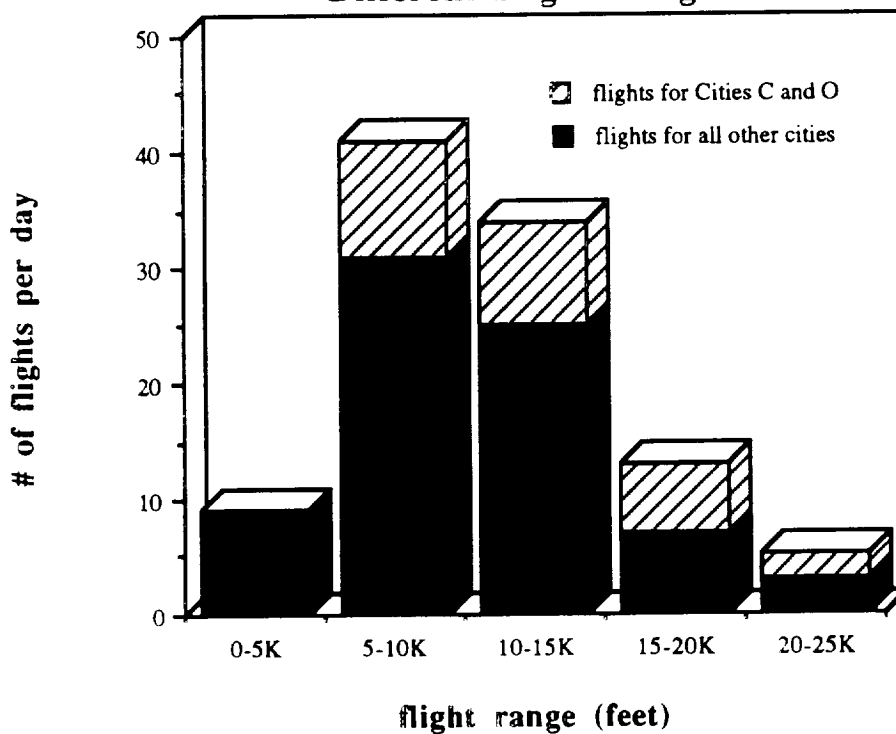


Cities C and O, which comprise 11.0% of the total Aeroworld passenger traffic per day, have runways 60% and 50% shorter than the average Aeroworld runway. Thus, in order

to serve this 11.0% of the market, the aircraft must have additional power and lift to takeoff in the shorter distance plus the capability of landing in this distance as well. It was concluded that the 11.0% of the market in question did not justify the weight and cost penalties associated with buying/installing a larger propulsion system and/or incorporating high lift devices on the aircraft. Thus, in an effort to remain cost efficient, *the Blue Emu* will not serve all of Aeroworld.

The second task in mission selection was to determine the design range for the aircraft. Figure B.1-2 shows the number of flights for each category flight range.

Fig. B.1-2: No. of Flights per Day for Different Flight Ranges



The top portion on each bar represents the flights into Cities C and O and therefore will not be served by *the Blue Emu*. From the chart, the greatest flight density lies between ranges of five and fifteen thousand feet. Specifically, a design range of 15,000 feet was chosen to add some flexibility to the aircraft. By selecting the furthest possible distance within the high flight density range, the aircraft may be used to travel shorter distances and therefore compete for more flights. If a shorter design range were selected, the aircraft may not be able to travel longer distances.

The final major task in mission selection was to determine the passenger capacity for the aircraft. A sixty passenger full-capacity was chosen for two reasons. First, it was

considered important to carry more passengers than the competition, the *HB-40*. Second, in order to keep the plane profitable, the capacity of *the Blue Emu* was kept down to keep the aircraft full for as many flights as possible. In studying the passenger demand for routes between each city, the demand is below 60 passengers for only 18.1% of the routes. Therefore, by increasing the payload of the aircraft, *the Blue Emu* would incur greater losses due to empty seats.

The only disadvantage to the mission selected for *the Blue Emu* is that the *HB-40* targets as very similar market. Table B.1-1 summarizes the target markets for each aircraft.

Table B.1-1: Market Summary for Both Aircraft

<u>Aircraft</u>	<u>% of Aeroworld capable of serving</u>	<u>Design Range</u>	<u>Full Passenger Capacity</u>
<i>the Blue Emu</i>	89.0%	15,000 feet	60
<i>the HB-40</i>	89.0%	17,000 feet	40

B.2 Design Requirements and Objectives

B.2.1 MARKETING AND ECONOMICS

Requirements:

- full capacity of 60 passengers with 4 crew members: 2 stewards, 2 pilots (see mission selection for discussion).
- employ coach seating only to provide cheapest and most economic transportation.
- total passenger volume of 717.36 cubic inches based on passenger capacity (this includes volume for: seating + aisle + doorway).

Objectives:

- reduce overall cost through improved wing design and relative ease in construction.
- **PRIMARY ECONOMIC OBJECTIVE:** achieve a CPSPK significantly below that of the *HB-40* through reduced cost.

B.2.2 PROPULSION SYSTEM

Requirements:

- utilize electric power plant with propeller supplying thrust due to weight and range objectives.
- capable of being installed and removed in 20 minutes or less (by imposed requirement).

Objectives:

- provide necessary power and thrust to takeoff in objective distance.

B.2.3 PERFORMANCE

Requirements:

- capable of sustaining 60 ft. radius turn at 25 ft/s (by imposed requirement).
- capable of loitering for two minutes in the case of airport technical difficulties, inclement weather, etc. (by imposed requirement).

Objectives:

- capable of taking off in 32 feet or less to serve market identified.
- minimum speed of 20-25 ft/s to avoid stall at higher speeds.
- cruise speed of 30 ft/s to compete with *HB-40* which has an identical cruise speed.
- design range of 15,000 feet (see mission selection; this does not include loiter time).

B.2.4 STABILITY AND CONTROL

Requirements:

- controlled by 4-channel RC system with 4 servos (by imposed requirement).
- maneuver using only two control surfaces: a rudder and an elevator, to maintain simplicity.
- provide for static and dynamic stability for easy control during flight.

Objectives: NONE

B.2.5 AERODYNAMICS

Requirements: NONE

Objectives:

- achieve a lift-to-drag ratio greater than 12 (which is the L/D for the *HB-40*).
- achieve a maximum aircraft lift coefficient of 1.1 to improve L/D ratio.

B.2.6 STRUCTURES AND WEIGHT

Requirements:

- design safe life of 50 hours (by imposed requirement).

Objectives:

- total aircraft weight of 5 lbs. to maintain feasibility in achieving performance objectives.

C. Concept Selection Studies

C.1 Introduction

Prior to the submission of the individual concept selections, the group met in order to set a common goal. While this allowed members of the group to become familiar with one another and to begin to focus toward one goal, it also severely limited the number of innovations incorporated into each individual design. This in turn limited the availability of designs to choose from; primarily, the high wing, monoplane aircraft.

The high wing, monoplane aircraft has been proven to be successful in the Aeroworld market that the *Blue Emu* has been designed to acquire. This is evidenced by the success of the *HB-40*. Therefore, in order to capture a share of, and eventually win, this market, the *Blue Emu* must exceed the *HB-40* in terms of aerodynamic performance and economics. Based on this fact, two major areas of innovation were considered: a different fuselage design, and an improved wing design.

Note: The following concept drawings represent only those innovative technologies as opposed to each individual concept. This was done due to the lack of variance between the original individual concepts.

C.2 Fuselage Concepts

C.2.A Triangular Fuselage

This concept was originally considered because it was believed to be a more structurally sound design than the typical rectangular fuselage. This assumption was based on the fact that triangular cross sections are simple, yet they exhibit high strength characteristics. This structural advantage would best be used during landing since this is the flight stage during which the greatest loads are incurred on the fuselage. In the proposed design, the two beams on the top would be sufficient to withstand the compressive loads while the lower beam could successfully withstand the tensile load. The lack of a fourth load-bearing beam in the fuselage structure would reduce the weight of the aircraft. This would lead to an economic savings for the airline, and subsequently, the Aeroworld passenger.

The major problem with this proposed innovation was the internal volume requirements for the passengers. In order to produce the necessary volume for the passengers, the external surface area of the aircraft would be enormous. Due to the fact that the drag on a body is increased with increasing surface area, this penalty would outweigh any weight benefits from the internal structure.

In order to fully appreciate the penalties of this design, consider a section of the fuselage for six passengers. For the *Blue Emu*, this corresponds to two rows of passengers. At 8 in³ per coach seat, this compartment would require 48 in³. The dimensions for the *Blue Emu* for this section are 6.1 in wide, 3.5 in high, and 3.2 in long. These dimensions correspond to 68.3 in³ of space. The excess space will be used for placement of avionics, adequate aisle space, as well as improved passenger comfort. The corresponding external surface area is 65.1 in².

For the same seating arrangement in the triangular concept, the *Tri-Emu*, these dimensions increase dramatically. Due to “headroom” considerations, the top width was assumed to be 8 inches. This value was assumed so that even after two passenger widths, approximately 3.2 inches, there would be 1.5 inches of “headroom” for the window passenger. Solving for similar triangles, a triangle height of 7.5 inches was determined for the fuselage, yielding overall dimensions of 7.5 in high, 8 in wide, and 3.2 in long. These dimensions produce an internal volume of 192 in³, an increase of 280% over the *Blue Emu* and four times the necessary volume. This represents a grossly inefficient use of space. Further, the external surface area is 80 in², an increase of approximately 120% over the *Blue Emu*. Since skin friction drag is dependent upon the external surface area, much more drag is produced by the *Tri-Emu* than the *Blue Emu*. Calculations are presented in Appendix I.

No trade studies were actually performed in order to determine whether or not the triangular fuselage was a structural improvement on the rectangular fuselage. However, due to the enormous increase in both internal volume and external surface area, this innovation was rejected.

C.2.B Circular Fuselage

The main benefit for the use of a circular fuselage configuration in real world aircraft is the fact that it is an ideal pressure vessel. However, this class of RPV will not be pressurized. Since the aircraft will not be pressurized, this real world benefit is not applicable to this Aeroworld design.

A second benefit of circular fuselages is that they are more streamlined than the rectangular fuselage. This streamlined nature is a result of the absence of sharp corners. However, this potential benefit of the reduction in body drag was outweighed by the necessary increase in manufacturing time to sand the edges of the fuselage. No trade study was performed in order to determine the potential benefits of the circular fuselage, but due to the time constraints of this course, it was decided that the benefits would be minimal at best. Therefore, this concept was not selected.

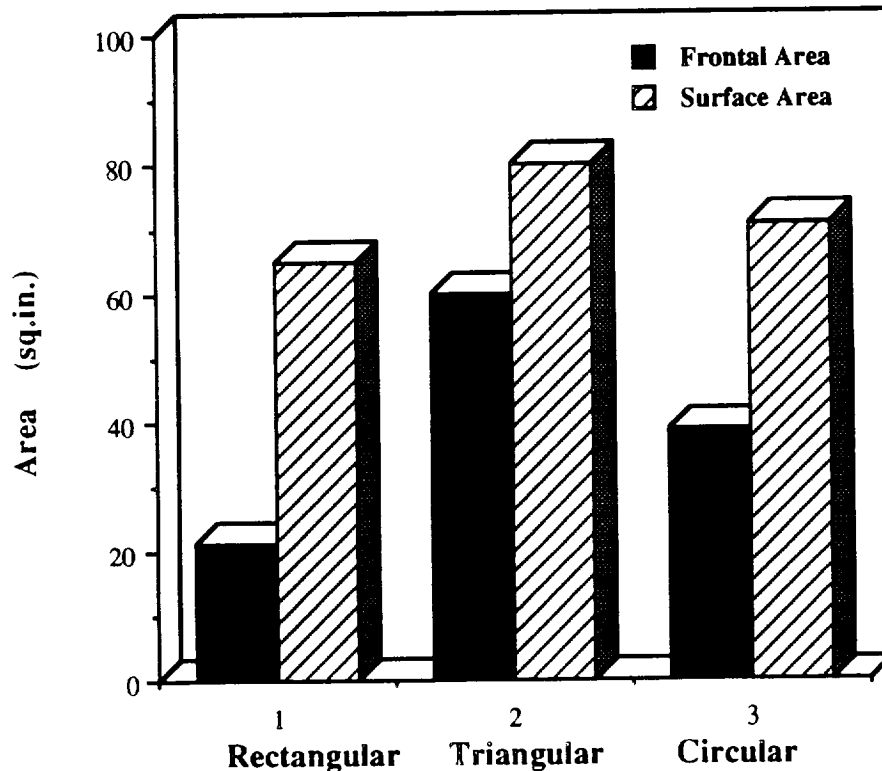
C.2.C Rectangular Fuselage

The most attractive feature of the rectangular fuselage is the relative ease in construction as compared to the circular fuselage concept discussed in section C.2.B above. This fuselage construction also facilitated an easier passenger entrance than the circular fuselage. Furthermore, this fuselage has lower drag penalties than the triangular fuselage concept of section C.2.A. This combination of benefits clearly made this concept the most logical one to select.

The major disadvantage of selecting the rectangular fuselage for the *Blue Emu* is the fact that it represented no improvement over the competition, the *HB-40*. Therefore, it was desired to achieve this aerodynamic improvement through the selection of a better wing design.

Figure C.2-1 demonstrates the aerodynamic disadvantages of the innovative fuselage concepts.

Figure C.2-1: Fuselage Concepts Study



C.3 Wing Design Concepts

C.3.A High, Rectangular Wing

The major advantage of constructing a high, rectangular wing is its ease of manufacture. Once an airfoil is selected, the group must only cut out one geometrically similar section for each wing spar. Production of this wing is slowed only by the number of desired wing spars, as more wing spars increases the amount of manufacturing hours.

Two disadvantages result from the design of a rectangular wing. First, this design represents an inefficient use of material. Due to the spanwise lift distribution, the outer sections of the wing must not be as strong as the root sections. However, it is typically the case that a rectangular wing is as strong at the tip as it is at the root. In other words, the designers of a rectangular wing use too much material at the tip, and a potential weight saving is not realized.

The second disadvantage of the design of a rectangular wing for this concept is the more critical one. The use of a rectangular wing for the *Blue Emu* represents no aerodynamic advantage over the *HB-40*. It is the production of an aerodynamically superior aircraft that is the ultimate goal of this design team. The *HB-40* has already captured the target market of the *Blue Emu*. Therefore, in order to capture the market, the *Blue Emu* must outperform the *HB-40* in order to attract airlines to purchase it. Based on this criterion alone, the rectangular wing concept was rejected.

C.3.B Swept Wing

Two advantages to the swept wing concept exist. First, a swept wing is used in order to reduce the compressibility effects encountered at high Mach numbers. Second, a swept wing can be used to aid in the adjustment of the position of the center of gravity. However, neither of these benefits was great enough to consider the swept wing concept too seriously.

Although the swept wing reduces the compressibility effects encountered at high Mach numbers, this is not the flight regime of the *Blue Emu*. Compressibility effects and the resulting drag penalties become problems at Mach numbers approaching 1.0 and higher. The flight Mach number of the *Blue Emu* and this class of aircraft is 0.027, hardly a high Mach number. Furthermore, this design team had already decided to enable an adjustment of the location of the battery pack to compensate for motion of the center of gravity. Therefore, the swept wing concept was not selected because it represented no aerodynamic improvement over the rectangular wing employed by the *HB-40*.

C.3.C Tapered Wing

Tapering a wing influences one of two parameters with beneficial results. By tapering a wing, either the span increases, or the planform area decreases depending on which parameter is held constant. It is desirable to allow the span of the wing to increase because this causes the aspect ratio of the wing to increase.

An increase of the aspect ratio is beneficial for two reasons. First, the induced drag of the wing is reduced as can be seen from

$$C_{D_i} = \frac{C_L^2}{\pi e A} \quad (\text{C.3-1})$$

Furthermore, the Oswald efficiency factor, e , is also influenced by an increase in aspect ratio as can be seen from Figure 5.18 of reference 1. Using this information, a taper ratio of 0.6 for a wing with an aspect ratio of 10 results in a 6% reduction in the induced drag coefficient over a rectangular wing with an aspect ratio of 10 and a taper ratio of 1.0.

Secondly, as the aspect ratio increases, the correlation between the lift characteristics of the airfoil section to those of the finite wing improves. The lift curve slope of an airfoil is higher than that for a finite wing due to the presence of downwash on the finite wing. Therefore, in order to predict the lift characteristics of a finite wing from data for an airfoil, a correction factor, k , is required. Reference 7 suggests a suitable correction factor to be

$$k = \frac{A}{A + \left[\frac{2(A+4)}{(A+2)} \right]} \quad (\text{C.3-2})$$

As equation C.3-2 indicates, as the aspect ratio increases, k increases. This means that the lift curve slope for the high aspect ratio wing reaches a peak similar to that of the airfoil. In other words, the wing more efficiently uses the airfoil to produce lift by minimizing the downwash on the wing.

Added benefits of the tapered wing include the more efficient use of material at the wing tip as well as a reduction in the weight of the wing. This weight reduction results from the reduced amount of material used to construct the wing.

The major disadvantage in constructing a tapered wing is the problem of accurately manufacturing tapered wing spars. This problem will be eliminated through the use of a copier machine. One "master" drawing of the airfoil section will be drawn. Subsequent tapered airfoil sections will be created by reducing the drawing by the appropriate scaling factor based on the location of the section relative to the location of the "master" section.

Although the initially apparent benefits of the tapered wing seem minimal, the innovative technique to construct the tapered airfoil sections greatly reduces the risk involved in producing a tapered wing. In addition to this consideration, the primary goal in manufacturing the *Blue Emu* is to gain an aerodynamic advantage in order to produce a better, more economical aircraft. Therefore, the *Blue Emu* will use a tapered wing in order to produce this aerodynamic improvement on the *HB-40*.

C.4 The *Blue Emu*

The final concept for this aircraft involves a rectangular fuselage with a high, tapered wing. This aircraft will possess a low wing loading due to the large planform area, 10 ft². The use of a taper ratio of 0.6 increases the aspect ratio to 10. This combination of taper ratio and high aspect ratio leads to a reduction in the induced drag coefficient of the wing as well as improved correlation between the lift curve slope of the airfoil section and the lift curve slope of the finite wing. All of these factors lead to an aerodynamically superior aircraft than the *HB-40*.

Placement of major aircraft components, the motor, passenger payload, battery pack, etc., was determined by a desire to place the center of gravity at 30% of the chord due to stability considerations. As passengers are removed, the position of the center of gravity moves forward only slightly. However, in order to compensate for potentially larger movement of the center of gravity, space was set aside within the fuselage to facilitate moving the battery pack.

Only one seating arrangement was considered due to the nature of the desired mission for the *Blue Emu*. If this aircraft was targeted to attack the long-range flight traffic, then first-class seating would have been considered. However, the *Blue Emu* is designed to compete in the short- to mid-range market, the business traveler market. Travelers in this market want to get to their destination as quickly as possible. The *Blue Emu* accomplishes this with some added passenger room over typical coach seating. In order to carry the passenger load of 60 passengers, a 3x20 seating arrangement was selected with two passengers sitting on one side of the aisle and a lone passenger across from them. An innovative technology was used in this seating arrangement by switching the seating halfway down the passenger compartment. This technique was used in order to maintain the alignment of the center of gravity with the longitudinal axis of the aircraft.

C.5 Influencing Factors

The major influencing factor in the design of the *Blue Emu* was the desire to produce a more efficient aircraft in terms of aerodynamic performance and cost. Since most aerodynamic improvements result from an improved wing design, this component of the aircraft was most influenced by this factor.

The improved efficiency of the wing through the use of taper also had an effect on the weight and cost of the aircraft. With the use of taper, less material will be used in the construction of the wing. This will result in a lighter aircraft. In addition, the reduction in raw materials directly influences the overall cost of constructing the wing. Although construction of the tapered wing may increase the necessary manhours to produce the aircraft, innovative techniques such as the use of a copier machine should reduce these labor costs. Therefore, the *Blue Emu* will be an aerodynamically superior aircraft that also holds an economic advantage over the *HB-40*.

D. Aerodynamics

D.1 Summary

In real world passenger aircraft, the major improvement in aircraft results from improved aerodynamic characteristics of the wing. Since the *Blue Emu* is attempting to overtake the market of the *HB-40*, the goal of this design team is to outperform the *HB-40* aerodynamically. This improved aerodynamic performance will result from better airfoil section characteristics and a more efficient wing design, the tapered wing. Tables D.1-1 and D.1-2 summarize the major aspects of the wing and aircraft aerodynamic design.

Table D.1-1 Wing Data Summary

Wing Area	[ft ²]	10.0
Wing Span	[feet]	10.0
Aspect Ratio		10.0
Taper Ratio		0.6
Dihedral	[degrees]	9.0
Root Chord	[feet]	1.25
Tip Chord	[feet]	0.75
Oswald efficiency factor (wing)		0.95

Table D.1-2 Aerodynamic Summary

$C_{l\max}$ (airfoil)	1.62
$C_{L\max}$ (aircraft)	1.31
C_{Do}	0.015
Oswald efficiency factor	0.829
Lift to Drag Ratio (maximum)	17.4
Lift to Drag Ratio (cruise)	16.4
$C_{L\alpha}$ (aircraft) [per degree]	0.089

D.2 Requirements and Objectives

The following were the driving forces behind the design of the wing section for the *Blue Emu*: in order to produce an aerodynamic advantage over the *HB-40*:

- 1) Produce a lift to drag ratio greater than 12
- 2) Reduce the induced drag coefficient of the wing

D.3 Wing Design

In the production of real world aircraft, it is desirable for passenger aircraft to have high wing loadings in order to minimize the effects of turbulence on passenger comfort. However, for these RPV's, a low wing loading is desired in order to enable an easy takeoff as well as to allow the aircraft to remain aloft as easily as possible. Turbulence effects on passenger comfort are eliminated in the confines of the test area, Loftus Sports Center.

In order to produce low wing loadings for a variable range of aircraft weights, the wing planform area was set at 10 ft². For the projected weight of 5.6 pounds, this produced a wing loading of approximately 9^{oz}/ft² for the *Blue Emu*. Furthermore, this area also simplified many future calculations.

By solving the lift equation for a coefficient of lift at a selected stall speed of 22 ft/s with a weight of 5.6 pounds and a wing area of 10 ft², the wing must produce a coefficient of lift of at least 1.1. In this low Reynolds number regime, between 150,000 and 200,000, few airfoils produce a section lift coefficient greater than 1.2. Therefore, it was necessary to produce a close correlation between the lift characteristics of the airfoil section and the finite wing.

Due to the presence of downwash on the finite wing, its lift curve slope is less than that of the airfoil section. Therefore, a correction factor is needed in order to predict the lift characteristics for the finite wing constructed from a particular airfoil section. Reference 7 suggests a suitable correction factor to be

$$k = \frac{A}{A + \left[\frac{2(A+4)}{A+2} \right]} \quad (\text{D.3-1})$$

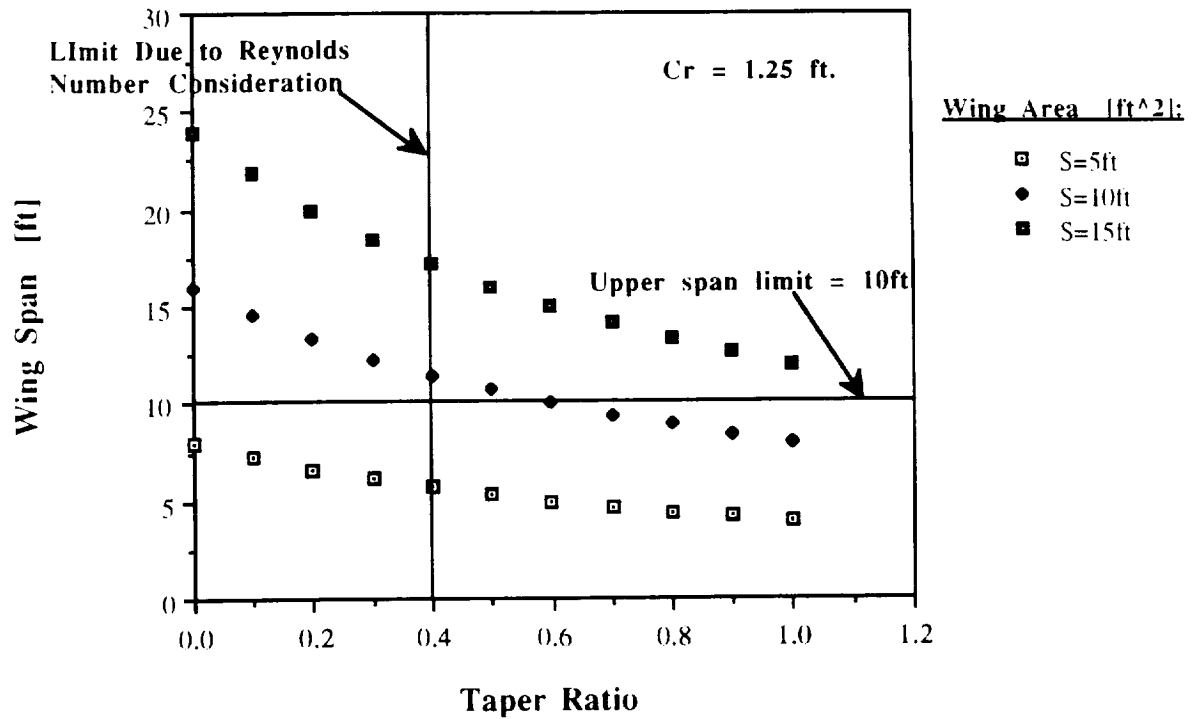
where A is the aspect ratio of the wing. Inspection of equation D.3-1 indicates that as the aspect ratio of the wing is increased, the correction factor approaches unity. Therefore, a high aspect ratio wing was desired.

From the **Concept Selection Studies** section, it had been decided to use a tapered wing in order to produce aerodynamic benefits over the *HB-40*. Trade studies determined that the use of taper increased the aspect ratio of the wing by increasing the wing span.

Figure D.3-1 indicates that for a constant wing area, the wing span is increased as the taper ratio decreases. For a planform area of 15 ft² and a taper ratio of 0.2, the wing span must be approximately 20 feet. A taper ratio of 1.0 for the same wing only requires about a 12 ft. wing span. The lower bound on the taper ratio was a result of the fact that data for airfoils in this low Reynolds number regime were only tabulated for Reynolds numbers between 100,000 and 200,000. For a cruise speed of 30 ft/s, this corresponded

to a maximum root chord of 1.25 feet and a minimum tip chord of 0.75 feet. These parameters produce the limiting value of 0.4 for the taper ratio. In addition to this limit, a limit of 10 feet was imposed on the wing span. This limit resulted from a desire to produce an aircraft that could maneuver within the confines of Loftus.

Figure D.3-1: Effect of Taper Ratio on Wing Span

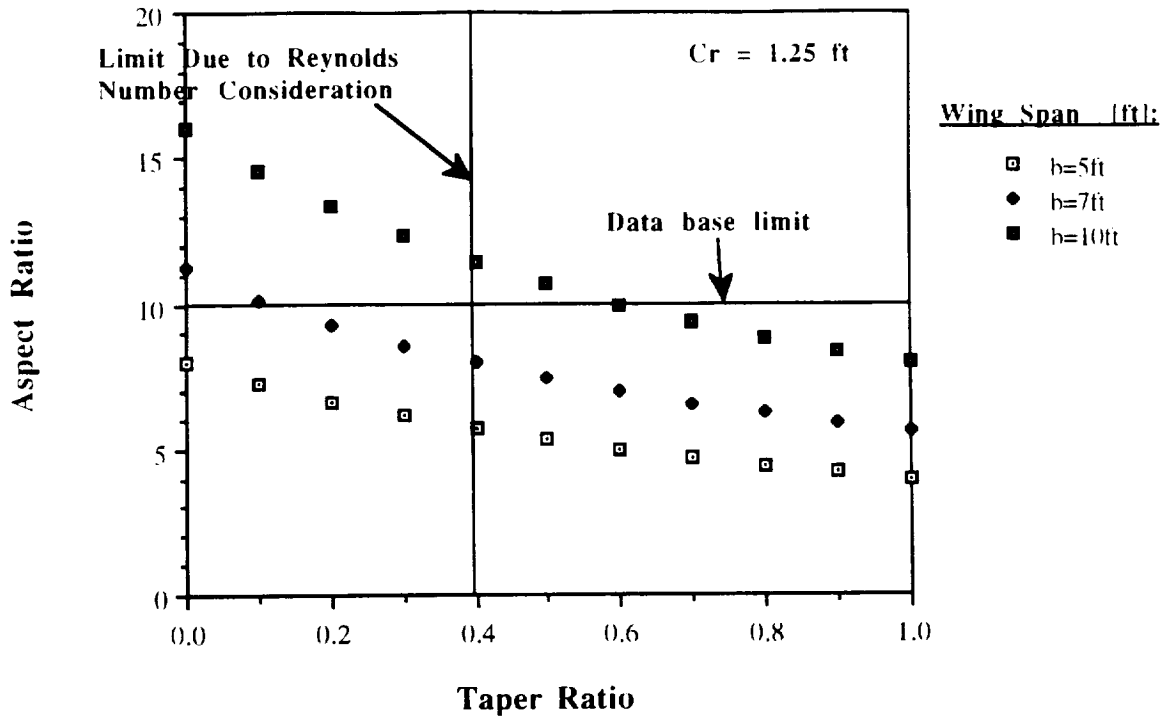


From the relation

$$A = \frac{b^2}{S} \quad (D.3-2)$$

it is clear that as the wing span is increased, the aspect ratio will also increase. Figure D.3-2 displays this result. Once again, the limitations for Figure D.3-1 were imposed on this Figure.

Figure D.3-1: Effect of Taper Ratio on Aspect Ratio



While the initial benefit of tapering the wing is a better correlation between the airfoil section lift characteristics and the finite wing lift characteristics, a performance benefit is also achieved. This aerodynamic advantage is the reduction of the induced drag coefficient of the wing. The induced drag coefficient is calculated using

$$C_{D_i} = \frac{C_L^2}{\pi e A} \quad (D.3-3)$$

where e is the Oswald efficiency factor, and A is the aspect ratio. From equation D.3-3, it is clear that as the aspect ratio of the wing is increased, the induced drag coefficient is decreased. Furthermore, from reference 1, the Oswald efficiency factor is also a function of taper ratio. The Oswald efficiency factor reaches a maximum value at a taper ratio of approximately 0.6. This peak value at a taper ratio of 0.6 is representative of the fact that this taper ratio closely approximates an elliptic wing because an elliptic wing yields the optimum wing loading due to its lower induced drag. Simple calculations demonstrate that a wing with a taper ratio of 0.6 has a 6% reduction in the induced drag coefficient from a wing of the same aspect ratio and a taper ratio of 1.0, a rectangular wing.

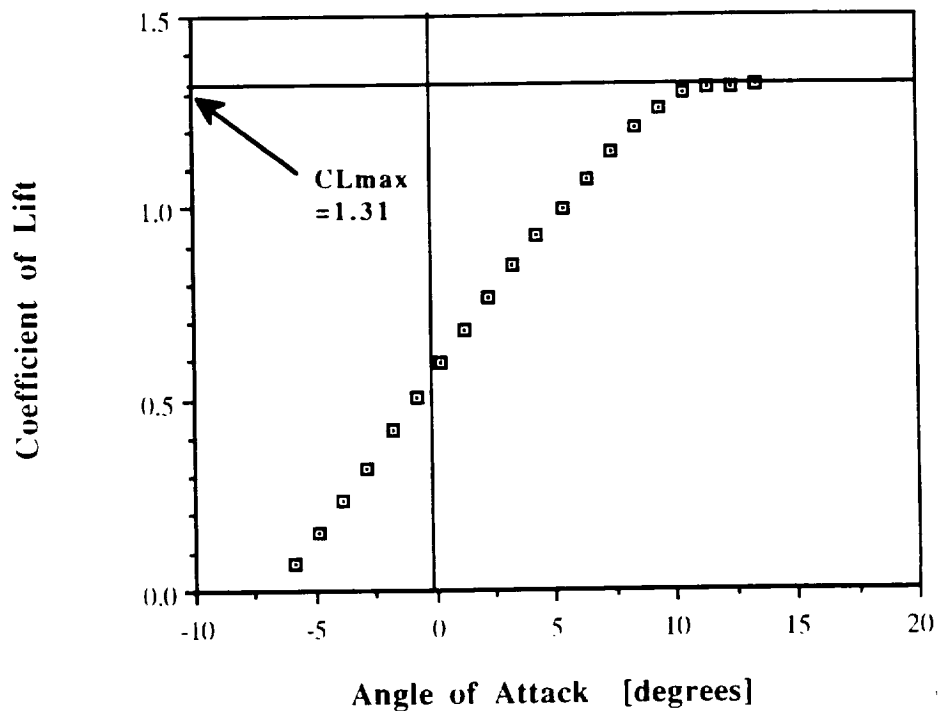
A further benefit of tapering the wing was the possibility of reducing the wing weight. The lift distribution across a wing is not uniform. Instead, it is greatest at the

root and least at the tip. Therefore, the tapered tip will not have to be constructed to be as sturdy as the wing root, and the wing weight will be reduced.

As with all design parameters, tapering the wing does have some disadvantages. The most noteworthy of these disadvantages is the fact that an elliptic wing stalls over its entire span, not at particular sections. This condition is a result of the fact that an elliptic wing produces the same amount of downwash, and the same induced angle of attack, at all points on the wing. Therefore, when the aircraft reaches stall, the entire wing stalls.

The final wing design consists of a wing with an area of 10 ft² having a root chord of 15 inches. The taper ratio of 0.6 results in a tip chord of 9 inches, and a wing span of 10 feet. These values result in an aspect ratio of 10. Using these inputs, the aircraft lift curve was plotted. The result is figure D.3-3.

Figure D.3-3: Aircraft Lift Curve

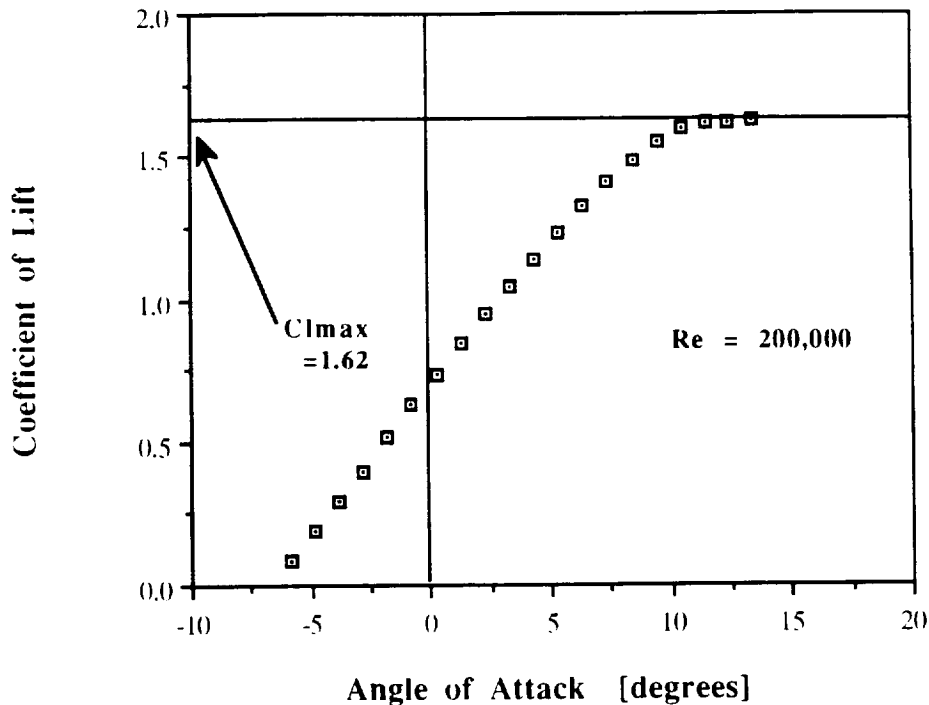


D.4 Airfoil Selection and Characteristics

In this low Reynolds number regime, approximately 150,000, very few airfoils produce a C_l greater than 1.2. This problem limited the number of available airfoil sections to approximately three or four. These airfoil sections were further reduced to only two, the Wortmann and the Clark-Y, as a result of the desire for an airfoil section

with good stall characteristics and low section drag characteristics. Both airfoil sections exhibit low section drag characteristics, but the Wortmann airfoil does not stall abruptly. Inspection of figure D.4-1 displays the favorable stall characteristics of the Wortmann airfoil.

Figure D.4-1: Lift Curve For the Wortmann Airfoil



The second problem involved the correction factor for a finite wing. Lift characteristics of an airfoil are better than those for a finite wing employing the particular section due to the absence of downwash. Therefore, as discussed in section D.3 above, a correction factor is required. By solving equation D.3-1 with the data for this aircraft, the resulting factor was 0.811. Therefore, the airfoil section had to produce a C_l of approximately 1.3 in order for the finite wing to produce the necessary lift coefficient.

Based on this overall analysis, the Wortmann airfoil was selected for the final design concept.

D.5 Drag Prediction

D.5.A. Method I

An initial drag calculation was performed using

$$C_{D0} = \sum \frac{C_{D\pi} A \pi}{S_{ref}} \quad (D.5-1)$$

where $C_{D\pi}$ is the C_D based on the component area, A_π , and S_{ref} is the wing planform area. Values for $C_{D\pi}$ were located in references 4 and 7. Values for A_π and $C_{D\pi}$ are located for each component in table D.5-1.

Table D.5-1 Method I Component Drag Breakdown

<u>Component</u>	<u>$C_{D\pi}$</u>	<u>A_π</u>	<u>total</u>	<u>Source</u>
Fuselage	0.9	0.148	0.1332	Hoerner
Wing	0.007	10.0	0.07	Nelson
Horiz. Tail	0.008	1.613	0.013	Nelson
Vert. Tail	0.008	0.681	0.00545	Nelson
Landing Gear	0.017	0.013	0.000663	Nelson
		$\Sigma=$	0.026	

A summation of these values resulted in an overall C_{D0} of 0.026. This value also includes an additional 15% that is suggested in order to compensate for interference between the wing and the fuselage. Although this estimate agrees well with values in the data base, a more detailed component drag breakdown was performed in order to achieve a more accurate value of the parasite drag coefficient.

D.5.B. Method II

In reference 8, the second method presented involves the calculation of such important parameters as the critical Reynolds number for each component, the skin friction coefficient, and form factors. In order to determine the parasite drag coefficient for the aircraft, the following equation was used:

$$\overline{C_{D0}} = \sum \frac{C_{f\pi} FF_\pi S_{wet\pi}}{S_{ref}} + C_{D0,aux} \quad (D.5-2)$$

Equations for $C_{f\pi}$ and FF_π are located in Appendix II.

This method was more involved than Method I, and as such, it was expected to produce a more accurate value for the parasite drag coefficient. Calculations for $C_{f\pi}$, FF_π , and $S_{wet\pi}$ are located in Appendix II. Computed values of $C_{f\pi}$, FF_π , and $S_{wet\pi}$ are tabulated in table D.5-2 below.

Table D.5-2 Method II Component Drag Breakdown

<u>Component</u>	<u>C_{fπ}</u>	<u>FF_π</u>	<u>S_{wetπ} (ft²)</u>	<u>total</u>
Fuselage	0.0045	1.091	7.99	0.0394
Horiz. Tail	0.0035	0.746	3.23	0.0084
Vert. Tail	0.0038	0.752	1.36	0.0039
Wing	Same as for	Method I		0.07
Landing Gear	Same as for	Method I		0.0093
			Σ=	0.015

Based on the fact that the calculations necessary to achieve these values were more rigorous, it was expected that the resulting parasite drag coefficient would be more accurate. In other words, it was expected that the C_{D0} would increase slightly to agree better with values in the data base. However, the C_{D0} actually dropped to a new value of 0.015. Although this value is much lower than values in the existing data base, the areas upon which this calculation were based are closer to the final values than the original values were. Further, all recalculations of this parameter have yielded the same value. It is believed that the major source for this “low” estimate is an inaccurate model of the landing gear. The landing gear is a high drag producer, and it is expected that this will drive the C_{D0} up slightly. With this in mind, this is an area of concern for the final aircraft design.

D.5.C Drag Due to Lift

Once the parasite drag coefficient, C_{D0}, for the entire aircraft has been determined, the entire drag coefficient may be calculated using

$$C_D = C_{D0} + \frac{C_L^2}{\pi e A} \quad (D.5-3)$$

where the second term of equation D.5-3 represents the drag due to lift. In this second term, e is the Oswald efficiency factor. Reference 8 suggests the following equation for calculating e:

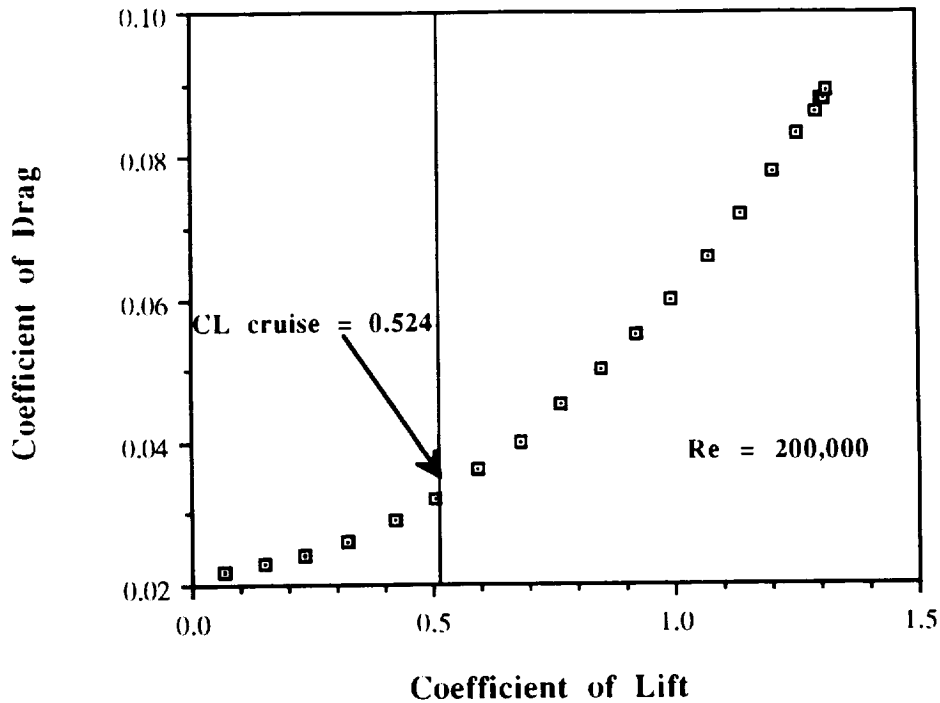
$$\frac{1}{e_{aircraft}} = \frac{1}{e_{wing}} + \frac{1}{e_{body}} + \frac{1}{e_{other}} \quad (D.5-4)$$

The calculation for this parameter for the *Blue Emu* is presented in Appendix II. Using equation D.5-4, the Oswald efficiency factor for this aircraft is 0.829. By substituting in values for e and A, the drag coefficient was calculated using

$$C_D = 0.015 + 0.0384 C_L^2 \quad (D.5-5)$$

From this information, the drag polar for the entire aircraft was plotted. Figure D.5-1 is the resulting plot.

Figure D.5-1: Aircraft Drag Polar



D.6 Aerodynamic Performance

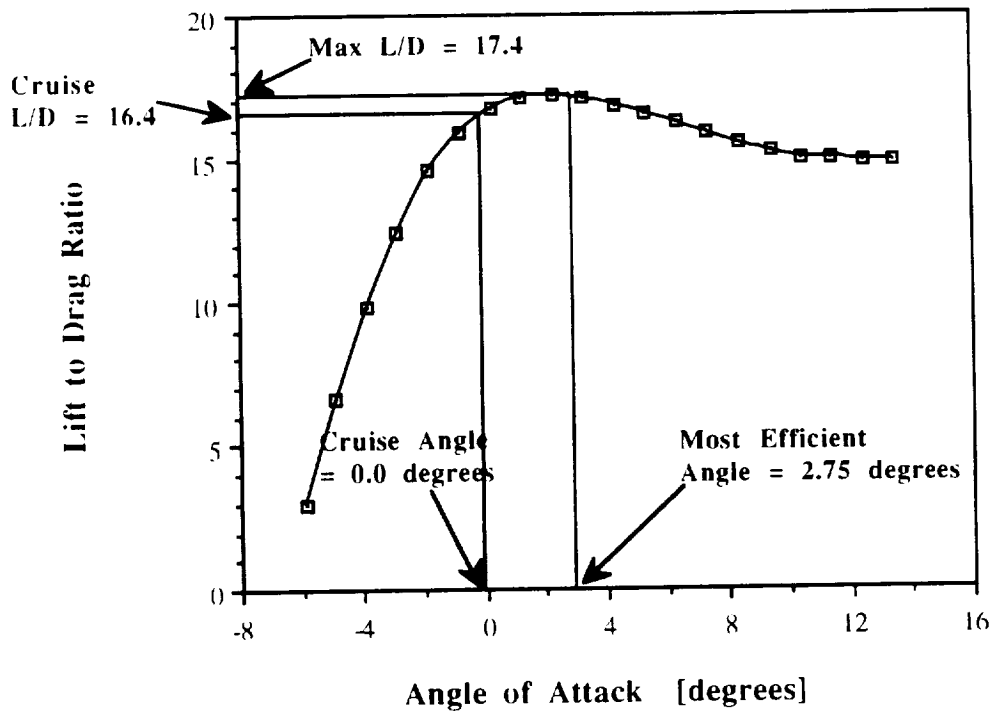
The goal of the wing design was to improve on the aerodynamic performance of the *HB-40* in order to produce a better, more efficient aircraft. Inspection of some parameters of the two aircraft show that this has been attained.

By using a tapered wing, the induced drag coefficient of the *Blue Emu* is significantly lower than the *HB-40*. For the *HB-40*, the induced drag coefficient is $0.07C_L^2$ while this parameter is only $0.03C_L^2$ for the *Blue Emu*, a 53% reduction for the *Blue Emu*. Furthermore, at cruise, this difference is increased. The *HB-40* cruises at a lift coefficient of 0.548 while the *Blue Emu* cruises at a lift coefficient of 0.524. The lower value of C_L for the *Blue Emu* is a direct result of the larger wing area. This corresponds to an induced drag coefficient at cruise of 0.021 for the *HB-40* and 0.0091 for the *Blue Emu*, a 57% reduction.

The major measure of the efficiency of the aircraft is its lift to drag ratio. For the *HB-40*, this ratio is 12. A primary goal of this design team was to exceed this value. This was accomplished as the maximum lift to drag ratio for the *Blue Emu* is 17.4. In addition to this, the lift to drag ratio at the cruise condition is 16.4, only 5.7% lower than

the maximum value. The lift to drag ratio curve for the *Blue Emu* is presented as Figure D.6-1. It should be noted that the lift to drag ratio for the *Blue Emu* is extremely high as compared to other aircraft of this class. This is a direct result of the low value for the parasite drag coefficient. (See Section D.5.B) Once again, this is an area of concern for the final aircraft design.

Figure D.6-1: Aircraft Lift to Drag Ratio



E. Propulsion

E.1 Summary

Table E.1-1 summarizes the propulsion system components for *the Blue Emu*.

Table E.1-1: Propulsion System Summary

Motor / Rated Power Output	Astro 15 / 200 Watts
Propeller	Top Flight 12-6
Battery / Capacity	P-90SCR / 900 mAh
No. of Batteries / Pack Voltage	11 / 13.2 V

E.2 Requirements, Objectives, and Propulsion Mission Analysis.

From the market information provided concerning Aeroworld, *the Blue Emu* mission was defined and analyzed. There were several major requirements and objectives placed on the propulsion system of the aircraft in order to accomplish the selected mission:

- (1) the aircraft will utilize an electric driven propeller propulsion system
- (2) the propulsion system must provide sufficient power to takeoff in 32 ft.
- (3) the propulsion system must be removable and be capable of being installed in 20 minutes or less

The greatest influence in the selection of the propulsion system was meeting the takeoff objective. Although the aircraft was required to takeoff in less than 40 feet, an objective of the design was to takeoff in 32 feet in order to service all of Aeroworld except for cities C and O, which have runway lengths of 24 and 20 feet, respectively. From the market data provided, only 11% of the total Aeroworld traffic per day flies into or out of Cities C and O. Since the primary goal of the aircraft was to provide cost efficient air transportation, it was concluded that this 11% did not justify the weight and cost penalties associated with taking off and landing in 20 feet or less. Further, since only 11% of the total Aeroworld traffic per day flies through Cities C and O, the decision to exclude this portion of the market does not significantly hurt the marketability of the aircraft. For these reasons, the driving objective of the propulsion system for the *Blue Emu* was to provide the necessary thrust and power for a maximum weight takeoff ground roll distance of 32 feet.

E.3 Motor Selection

Motor selection was limited to electric power in order to achieve the objective range and cruise speed specified by the mission. All previous aircraft studied employed electric power; therefore, no other means of propulsion was seriously considered. It was noted that combustion engine systems require heavier components such as the piston engine and

liquid fuel, and also that these engines emit harmful exhaust gases into the environment. Any form of potential or stored mechanical energy was also unrealistic due to the required range and overall weight of the aircraft. An electric system was therefore feasible and advantageous for the goals set for *the Blue Emu*.

Multiple engines were considered for the propulsion system, but a single engine design was selected. This eliminated the difficulty of coordinating multiple power plants. Additional engines also add to the overall weight and cost and therefore have the disadvantage of increasing the CPSPK of the aircraft. The average weight and cost of the motors considered (shown in Table E.3-1) was 10.79 oz. and \$128.28, respectively. Thus, based on design weight and cost, each an additional motor would cause an increase of 14.1% in aircraft weight and an increase of 7.6% in aircraft cost. It was also determined that for the performance required, the coordination difficulties and cost disadvantages of multiple engines outweigh the advantages in speed and takeoff distance. Further, enough power could be produced by one motor. Therefore, a single electric motor was selected for the propulsion system of the aircraft and determined sufficient for the mission specified.

The three electric motors that were considered for *the Blue Emu* are shown in Table E.3-1:

Table E.3-1: Motors Considered for Propulsion System

<u>Motor</u>	<u>Rated Power Output</u>	<u>System Weight</u>	<u>Engine Cost</u>
Astro Cobalt 05	125 Watts	16 oz.	\$109.95
Astro Cobalt 15	200 Watts	25 oz.	\$124.95
Astro Cobalt 25	300 Watts	38 oz.	\$149.95

This information was provided by Astro Flight Inc. and can be found in the group data book. It should be noted that the *System Weight* includes the recommended battery pack for a model aircraft. This parameter is simply shown for comparison since a battery pack will be designed specifically for the aircraft. Motors with rated power output above and below those listed in Table E.3-1 are available. However, through preliminary takeoff calculations and studies of previous years, a takeoff power of 120 to 170 Watts was expected. Therefore, only these three geared motors were considered.

As previously mentioned, the takeoff requirements for the aircraft were the primary influence on the selection of the propulsion system. Thus, in selecting a motor, the goal was to select a motor with sufficient power to takeoff in the required distance yet not overpower the aircraft and suffer a weight and cost penalty. Therefore, the methodology adopted for motor selection was to start with the least expensive and lightest motor and continue to analyze takeoff performance for motors with increasing power output until the

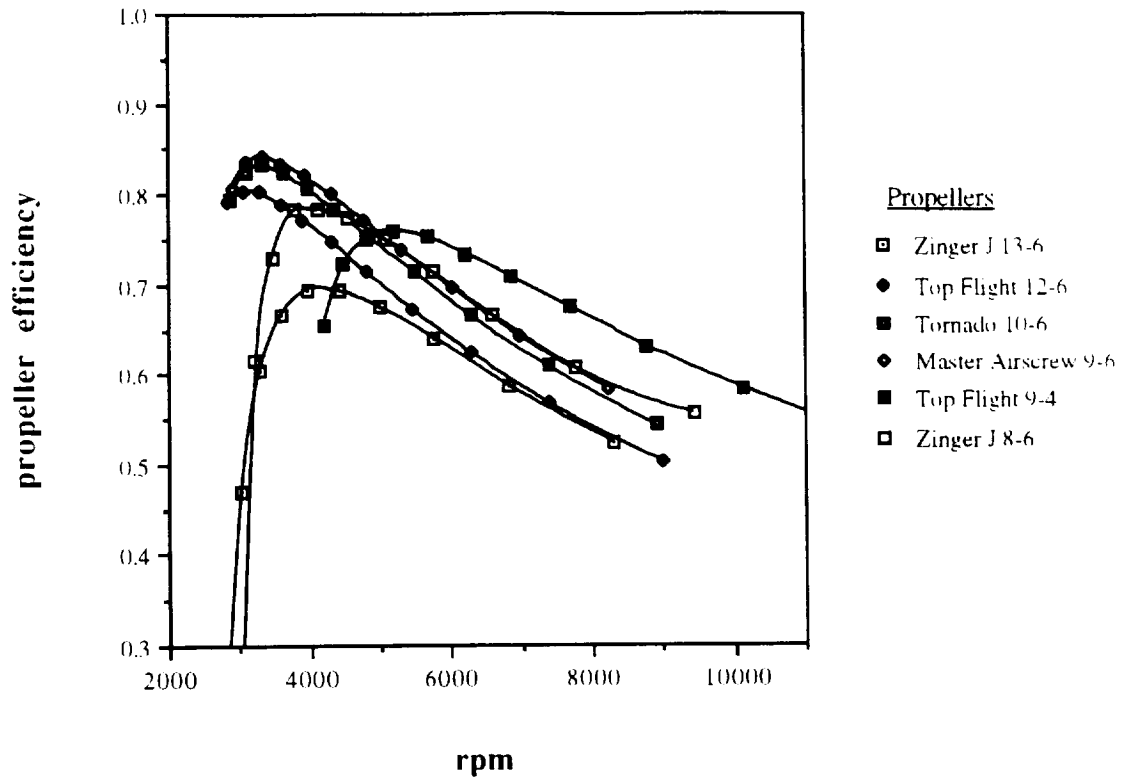
ground roll takeoff objective could be achieved. Takeoff performance was studied using the software tool, TAKEOFF (ref.2). From this analysis, it was concluded that the Astro Cobalt 05 could not produce sufficient power to takeoff in the objective distance of 32 feet. Therefore, the Astro 05 was eliminated from further consideration. The first motor to satisfy the takeoff ground roll objective was the Astro 15 (see Table E.7-2). Since greater power is superfluous and would induce weight and cost penalties, the Astro Cobalt 15 was selected for the propulsion system of the *Blue Emu*.

E.4 Propeller Selection

Several propellers were considered for the propulsion system of the aircraft. Once again, the takeoff portion of the flight regime had the greatest influence in the selection decision. Propeller data was studied using the software tool, PROPELLER (ref. 9). The propellers considered were limited to those stored within the software database. Manufacturing or analyzing other propellers not in the software database was not considered due to time constraints and the minimal payoff since props in the database have been successful in the past. The software accepted the following as input: the blade airfoil data, flight conditions, and blade dimensions. Using simple blade element theory including induced velocity and tip losses, the thrust coefficient, the power coefficient, and the prop efficiency as a function of advance ratio were calculated. As a method of reducing the number of choices, possible selections were narrowed to six by grouping the propellers by common diameters and then selecting the prop with the highest peak efficiency as a representative from the group. The six propellers that comprised this group were: the Zinger 13-6, the Top Flight 12-6, the Tornado 10-6, the Master Airscrew 9-6, the Top Flight 9-4, and the Zinger 8-6. Two props were selected with 9 inch diameters because it was initially suspected that a 9 inch propeller would be selected.

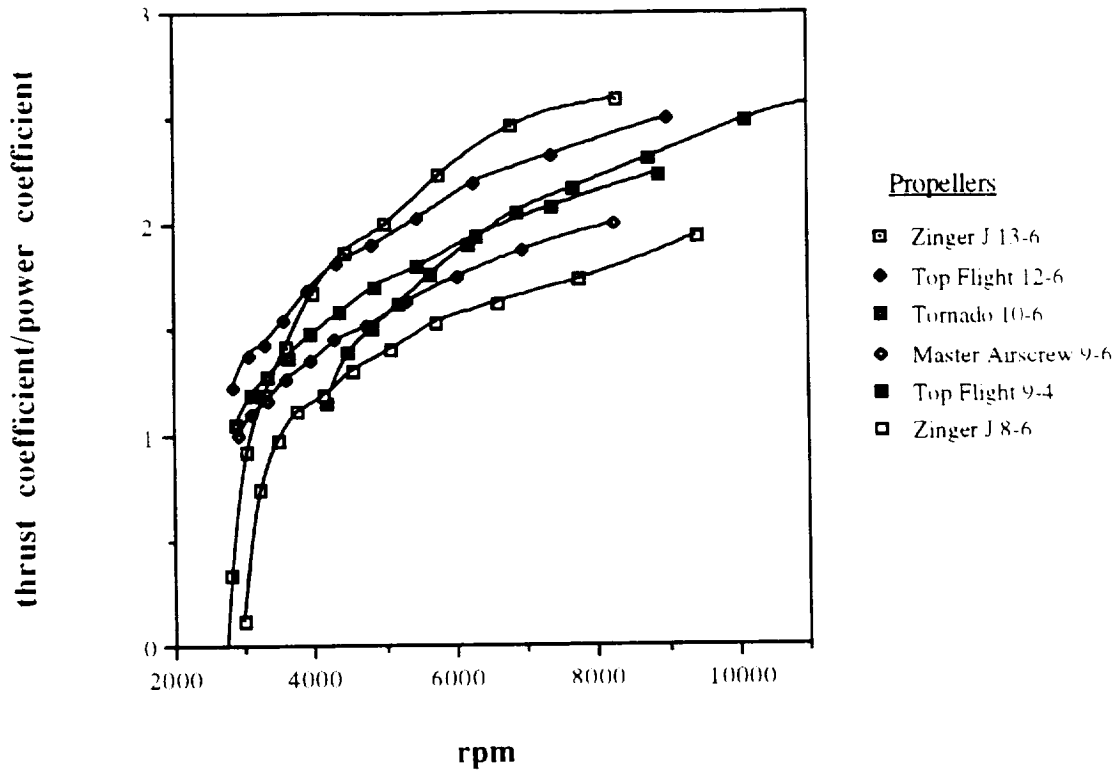
The primary measures of merit for propeller selection were the peak efficiency and thrust produced. Figure E.5-1 shows the relationship between propeller efficiency and propeller rpm for the props considered.

Figure E.5-1: Propeller Efficiency vs. RPM for Various Propellers



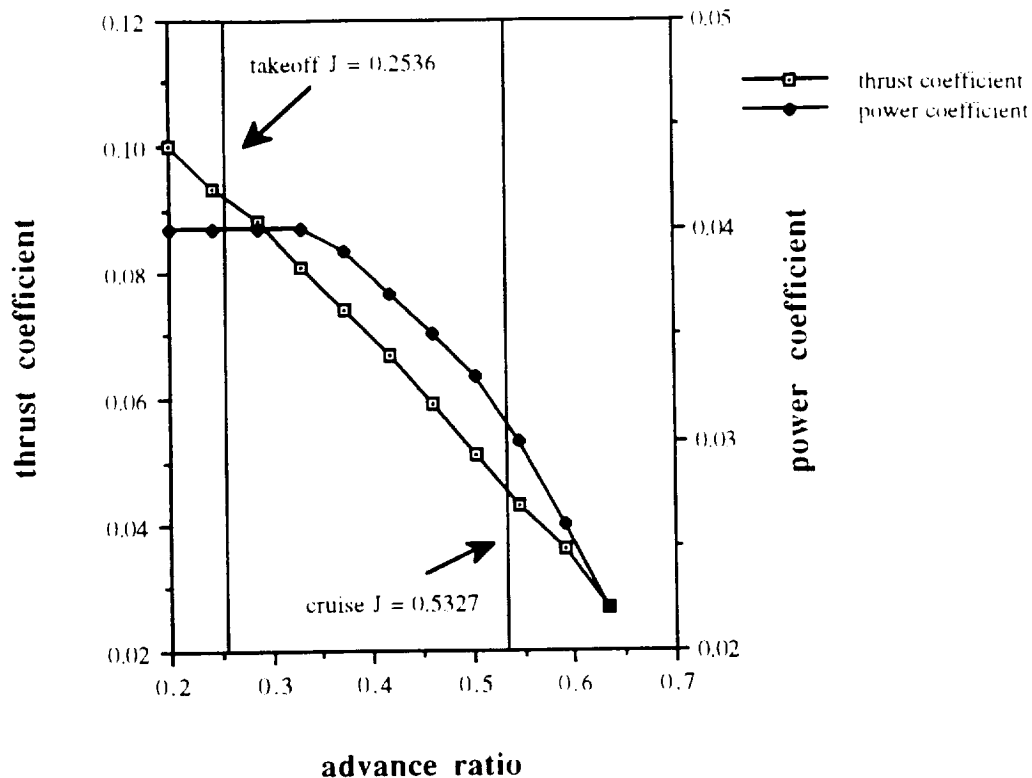
A general decrease in efficiency with decreasing propeller diameter was noted. However, Figure E.5-2 shows the variation in C_T/C_p with propeller rpm for the six props studied.

Figure E.5-2: Thrust Coefficient/Power Coefficient vs. RPM for Various Propellers



From this figure, it is obvious that the larger diameter propellers produce the greatest thrust for the power input to the prop. Thus, a compromise was necessary to select a propeller for the propulsion system of the *Blue Emu*. Once again, the deciding factor in component selection was takeoff. Since the Astro Cobalt 15 was already chosen as the power plant of the aircraft, the software tool TAKEOFF (ref. 2) was used to determine which Astro 15 - propeller combinations would provide the necessary thrust to takeoff in 32 feet. The Astro 15 motor could not be paired with the Zinger 13-6 due to the power necessary to overcome the torque to spin the 13 inch prop at takeoff. The Top Flight 12-6 combined with the Astro 15 engine provided the thrust to takeoff in 30.96 feet, one foot under the design goal. Stepping down to the 10 inch Tornado 10-6 propeller caused an increase in takeoff ground roll distance to 60.174 feet, twice the distance of the Top Flight 12-6 propeller. Thus, no further analysis was required. The Top Flight 12-6 was chosen for the *Blue Emu* propulsion system to meet the takeoff design objective. For further reference and added information, Figure E.5-3 shows the variation of power and thrust coefficients with advance ratio.

Figure E.5-3: Thrust and Power Coefficients vs. Advance Ratio for Top Flight 12-6



E.5 Battery Selection

Unlike the motor and propeller selection, battery selection was dependent upon cruise conditions and range objectives. Using a Microsoft Excel spreadsheet, the current draw necessary for cruise was found using motor, propeller, and aerodynamic information as input. The current necessary to cruise at 30 ft/s was 4.11 A. Using the cruise velocity of 30 ft/s and the design range of 17,000 feet, the design endurance was calculated as 0.1574 hours. Thus, the necessary battery capacity for the aircraft was simply the current multiplied by the maximum flight time: 647 mAhr. From the software tool TAKEOFF (ref. 2), the battery drain during takeoff is 7.364 mAhr. As a simple estimate, the takeoff battery capacity required will be used to estimate the climb portion of the flight profile as well. Thus the total battery capacity requirement is:

$$\text{total battery capacity} = \text{cruise capacity} + \text{takeoff capacity} + \text{climb capacity}$$

From this expression, the necessary battery capacity is 661.7 mAh. Batteries with rated capacities between 600 and 1000 mAh are shown in Table E.5-1.

Table E.5-1: Batteries Considered for Propulsion System

<u>Designation</u>	<u>Nominal Capacity</u>	<u>Cost per Cell</u>	<u>Weight per Cell</u>
N-600SCR	600 mAh	\$4.50	1.02 oz.
P-90SCR	900 mAh	\$3.00	1.23 oz.
P-100SCR	1000 mAh	\$3.50	1.46 oz.
N-1000SCR	1000 mAh	\$3.50	1.52 oz.
N-1400SCR	1000 mAh	\$5.50	na

Since more than 600 mAh capacity was required for the Blue Emu, only the 900 mAh and 1000 mAh batteries could be considered. From Table E.5-1, the P-90SCR battery was the logical choice since any greater capacity was unnecessary and the P-90SCR was also the least expensive cell. Therefore, although this battery significantly exceeds the 17,000 foot design range goal of the aircraft, a battery with a smaller acceptable capacity is currently unavailable and thus the battery selection for the *Blue Emu* propulsion system was quite simple.

The number of batteries on board the aircraft was determined by the voltage necessary for takeoff in the 32 foot objective. Eleven batteries connected in series produced a combined voltage of 13.2 V (1.2 V/battery). From TAKEOFF (ref. 2), 11 P-90SCR batteries produced enough voltage to takeoff in 30.96 feet. Rerunning the code for a 10 battery series it was obvious that 10 batteries, which sum to a total of 12 V, was only enough to takeoff in 41.24 feet. The 1.2 V drop in maximum voltage led to a 33.2% increase in takeoff ground roll length. Therefore, to meet the takeoff distance requirement of 40 feet as well as the takeoff distance objective of 32 feet, 11 P-90SCR batteries were used in series.

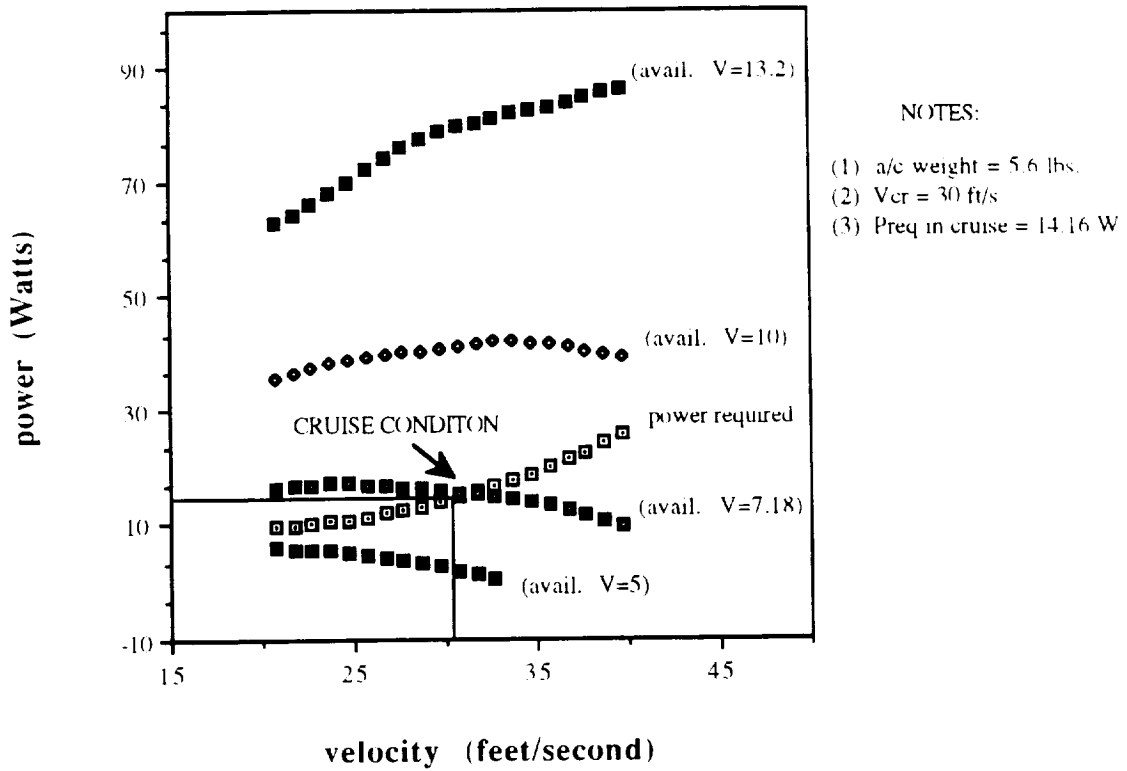
E.6 Speed Control

A speed controller will be required to control the propulsion system selected. The pilot of the aircraft must be able to throttle back after takeoff and climb to achieve a steady level cruise condition. Although the takeoff and climb phases of the mission will be performed at full throttle, only about 54.4% (battery voltage of 7.18 V) of full power will be required in the cruise condition. Additional power may be necessary for maneuvering (e.g. turning) since the aircraft is banked in a turn and thus the lift is not vertical.

E.7 System Performance

The performance of the propulsion system met the goals for the mission selected. Figure E.7-1 shows the power available and power required vs. velocity for different nominal voltages applied to the motor.

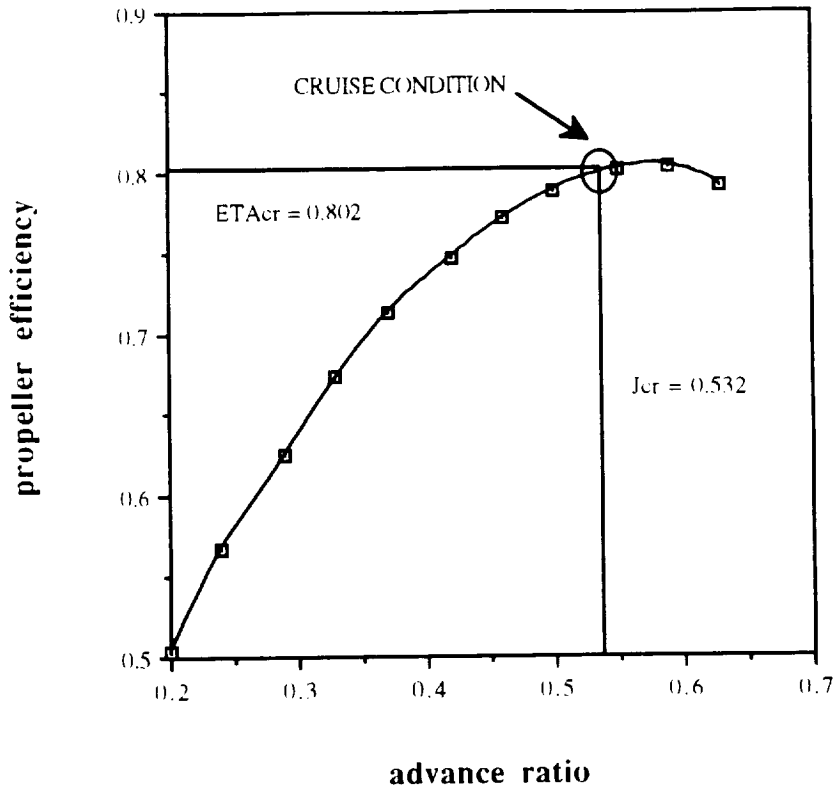
Figure E.7-1: Power Available and Power Required vs. Velocity at Various Voltage Settings



For cruise at a velocity of 30 ft/s, a nominal voltage of 7.18 V is necessary. This corresponds to roughly 54% of maximum throttle. The maximum power available at the cruise velocity of 30 ft/s is approximately 80 Watts which is well above the power required in cruise of 14.16 Watts.

Figure E.7-2 shows the propeller efficiency at different advance ratios.

Figure E.7-2: Propeller Efficiency vs. Advance Ratio for Top Flight 12-6 Propeller



The Top Flight 12-6 propeller operates at 0.802 efficiency in cruise which is over 90% of the peak efficiency of the propeller.

Cruise and takeoff parameters are given in Table E.7-1 and Table E.7-2.

Table E.7-1: Propulsion Performance Parameters in Cruise

power required	14.16 Watts
motor power out	18.69 Watts
motor rpm	8043
propeller rpm	3380
advance ratio	0.5327
propeller efficiency	0.802
nominal voltage	7.18 V

Table E.7-2: Propulsion Performance Parameters at Takeoff

velocity at takeoff	25.32 ft/sec
takeoff distance	30.96 feet
battery drain	7.364 mAhr
advance ratio at takeoff	0.2536
thrust at takeoff	2.0853 lbs
current draw at takeoff	10.8214 A
static thrust	2.817 lbs
static current draw	10.801 A
static propeller rps	97.82

Since the selection of the primary components of the propulsion system was dictated by takeoff performance, many of the decisions made in regard to propulsion were relatively simple. *Everything depended on whether the aircraft could takeoff, and how inexpensive the component was.* Although takeoff performance of the aircraft was the primary influence in propulsion component selection, cost efficiency was considered as well. The Astro Cobalt 15, the Top Flight 12-6 Propeller, and the P-90SCR batteries provide the required capability of *the Blue Emu* in the most inexpensive manner possible.

F. Weight Analysis

F.1 Introduction and Tabular Summary

The earliest weight estimate for this aircraft was 5.6 lbf. The earliest weight estimates, which were based upon relative size-weight data found in similar aircraft, suggested a larger battery weight than was required for *The Blue Emu*. *The Pale Horse* had a total weight of 4.98 lbf and required 22.08 oz for batteries. The *El Toro*, a 5.0 lbf aircraft which used the Astro15 engine, had a battery weight of 24 oz. The *HB-40* with a total weight of only 4.3 lbf and also an Astro15 engine customer used 9 batteries which totaled 17.8 oz. The earliest battery weight estimate of 22 oz exceeded the actual battery weight by 8.47 oz or 0.5 lbf. The design philosophy, "heavier on paper is better than heavier on taxi", encouraged and supported a weight estimate of 5.6 lbf which included a high battery weight estimate and allowed for unseen weight additions attributed to possible amendments to structure. The newest weight estimation is 4.79 lbf.

The newest weight component estimations were remarkably close to the earlier weight estimates. The empennage and the fuselage estimates differ less than 0.3 ounces from their earlier estimates. The wing is 2.3 oz lighter than its previous prediction. The point which is being made here is the following. Careful examination of the database by comparison and sizing of previous designs can lead to fairly accurate component predictions without knowledge of your design's exact "structural blueprints". However, interdisciplinary communication between the design team's engineers is also a crucial aspect of validating estimates. Communication is essential when informing other engineers of the current technology. In other words, if the technology has become more weight efficient, it is important to make yourself aware of the lighter, current systems in use. Also, early estimations can be made on some structural aspects which must exist: longerons, airfoils, spar caps and webs etc. Below is presented a pie chart (Figure F.1-1) of the weight fractions as well as a tabular summary of component weights (Table F.1-1).

Figure F.3-1 Aircraft Weight Percentages

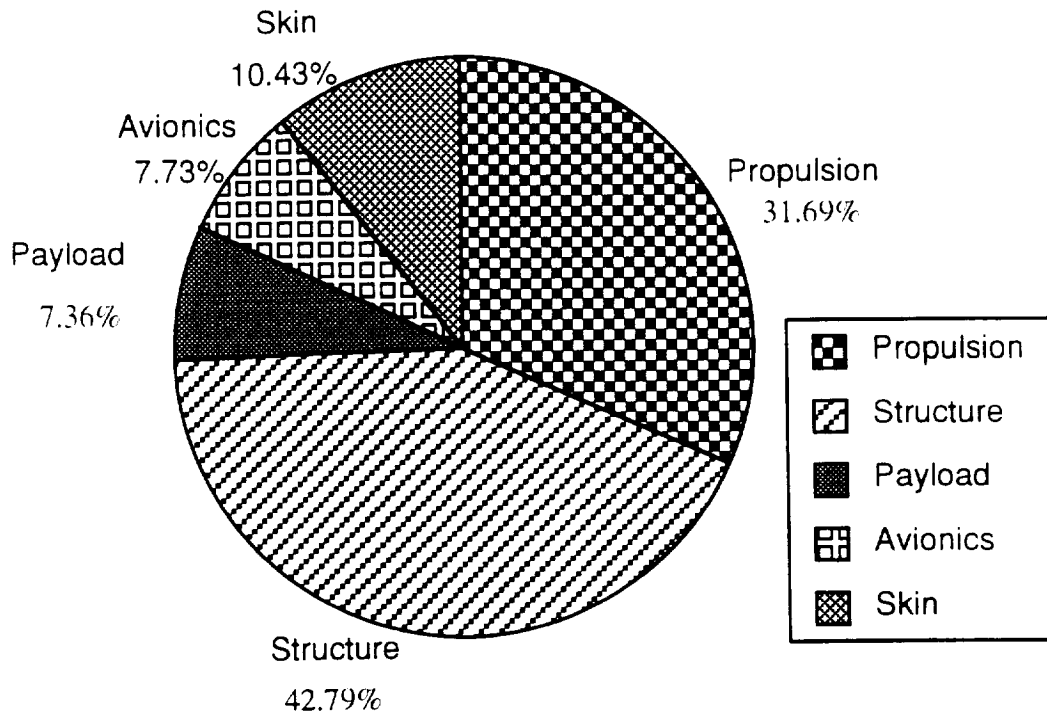


Table F.1-1 Component Weights and Total Weights

Payload	5.64 oz
Motor, Gbox, Mount	10.24 oz
Batteries	13.53 oz
Fuselage	10.44 oz
Landing Gear	3.50 oz
Empennage	4.10 oz
Wing	14.74 oz
Propeller	0.50 oz
Servos [2]	1.2 oz
Receiver	0.95 oz
System Battery	2.00 oz
Speed Controller	1.77 oz
Monokote	7.99 oz
Maximum Weight	75.69 oz or 4.79 lbf
Empty Weight	70.95 oz or 4.43 lbf
Weight/Passenger	1.2 oz

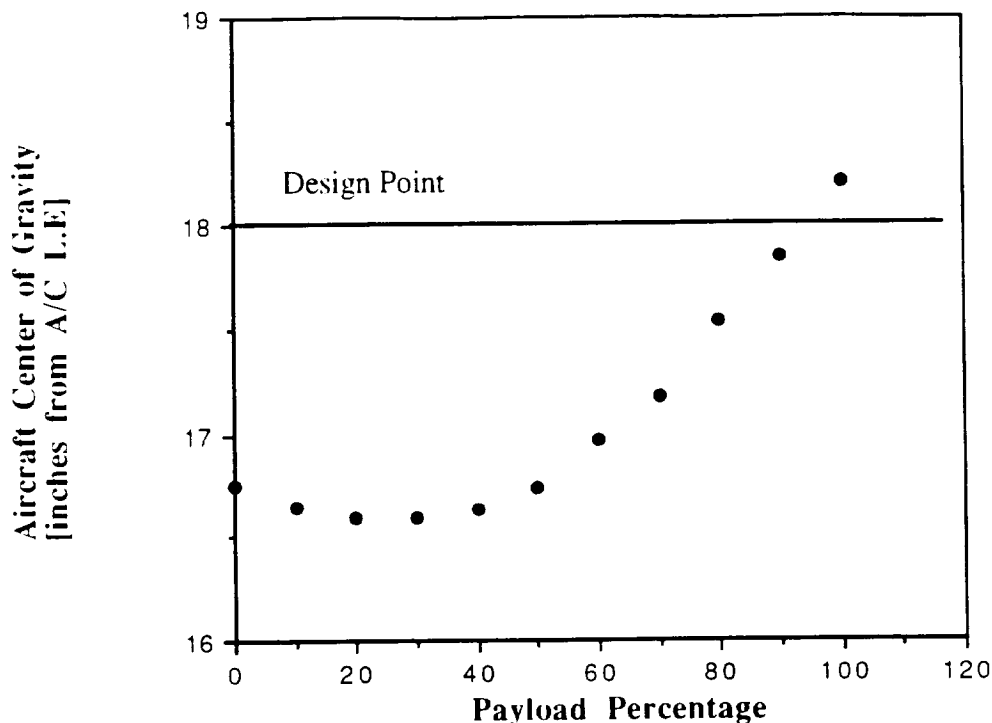
F.2 Center of Gravity: Movement and Compensation

The design center of gravity (c.g.) is $0.3c_{\text{mean}}$. This value was suggested since the aircraft is predicted to show the best longitudinal stability and control characteristics at this location. The leading edge of the wing is positioned 14 inches aft of the nose. A 12 inch mean chord locates the aircraft's c.g. 18 inches from the leading edge of the aircraft (nose).

Two components, the battery/avionics package and the wing, were chosen to have variable positions. Restrictions on placement of the battery/avionics package are forced by the limited 14 inch compartment located directly behind the "cockpit". The wing's leading edge is preferably located right after the 12 inch compartment, since this would allow room for a service door located on top of the compartment. Too great an infringement on this space reduces the service door size which must be a minimum of 6 inches long for ease of maintenance. Positioning the c.g. of the battery/avionics package 11.25 inches aft of the nose allows for the wing to keep its desired position directly behind the compartment and attain a c.g. for the fully-loaded aircraft of $\sim 0.3c$ (17.9 inches).

The center of gravity moves as the payload decreases. The direction which it moves is dependent upon how many passengers are seated. Figure F.2-1 illustrates the c.g. movement while assuming the aircraft is loaded from the front to the rear and the battery/avionics package c.g. is located at an intermediate distance 12 inches. Observation reveals a forward c.g. of 16.6 inches around 20% payload. In other words, when the aircraft is more than 80% empty the c.g. will have its largest displacement, 1.4 inches from design c.g. location $0.3c$. Once the cabin is filled past 20% the center of gravity begins to move aft.

Figure F.2-1 Weight Balance Diagram

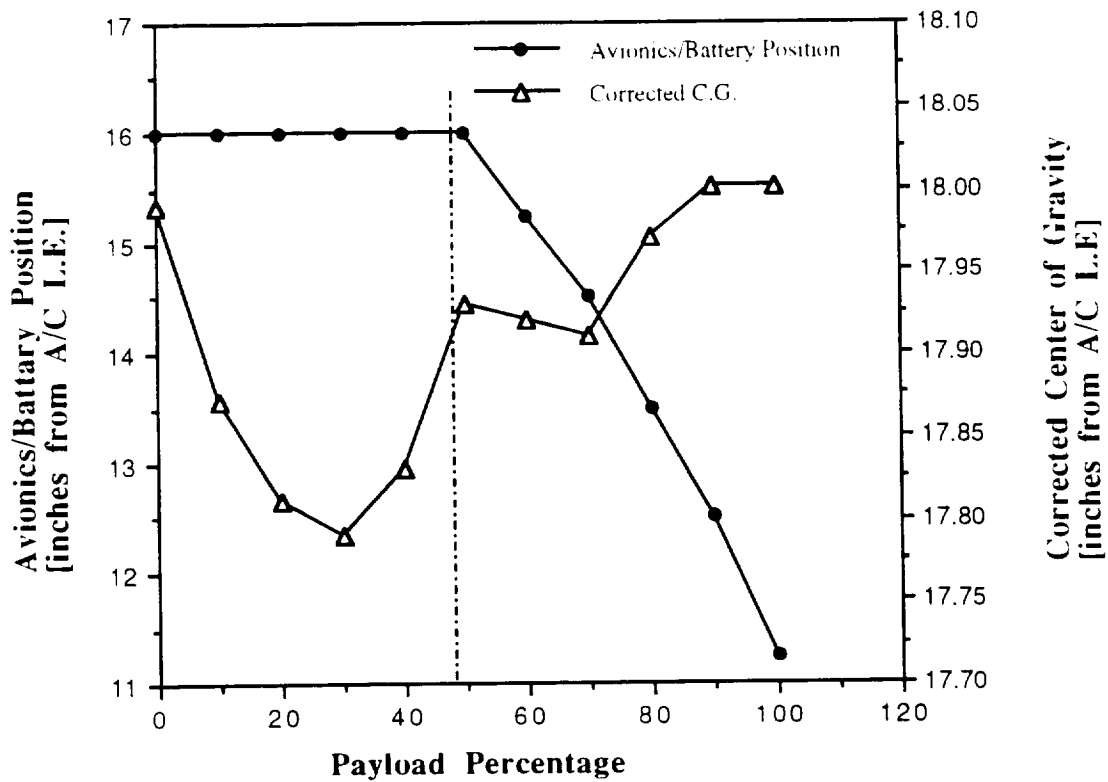


In reality, the movement of the center of gravity cannot be compensated for by moving or reassembling the structure. As mentioned above the center of gravity for the aircraft can move 1.4 inches from its design location. The effect of this motion is measured by control and stability characteristics and is not mentioned here. The scale of Aeroworld allows for an interesting new technology or possibility. This new technology is the movement of the avionics/battery package along a variable location system. In Aeroworld, this system is best constructed with strips of Velcro on the floorboard and on the package. The package is simply “stuck” at the desired location. Again, in reality, such a system would not only be costly, but also, the fuel tanks or avionics would not be the variable weight but rather some other mass which would be redistributed. Aeroworld provides the luxury of repositioning the battery/avionics package to compensate for c.g. travel.

Figure F.2-2 shows the effect of moving the package and maintaining the desired c.g. of 18 inches. A 0.25 inch tolerance from a c.g. of 18 inches is respected as the battery/avionics package's c.g. is varied from 16 inches to 11.25 inches over a full range of payload percentages. After the aircraft is filled 50%, the package position is required

to move more forward. Up to the 50% point the package c.g. can be kept 16 inches to keep the aircraft c.g. at approximately 0.3c. The corrected c.g. movement is much different from that of the fixed-package. Again, the package is fixed before the 50% payload point and the curve is quite similar; however, the curve loses continuity when it is influenced by the changing c.g. of the package.

Figure F.2-2 Center of Gravity Correction via Avionics/Battery Position



Remember the aircraft was loaded from the front. Also remember the asymmetric seating configuration in the internal layout. The center of gravity in the transverse direction is put off the centerline of the aircraft a maximum distance at the 50% capacity point. The asymmetric seating is then mirrored for the remaining 50% of the payload and the c.g. returns to the centerline at 100% capacity. At the 50% mark, the weight shifted to the one side is only 2.5% of the total aircraft weight. Such a weight distribution does not affect the aircraft overall c.g. since the distance is small and the weight is nominal. If a solution was desired, assigned seating could compensate for the small c.g. misalignment. Center of gravity in both the z (vertical) and y (transverse) directions

were not presented here since 1) the vertical distance to the component center of gravities is so small it is contained inside the aircraft structure and 2) a fully loaded aircraft produces a transverse c.g. on the centerline (symmetry line).

Below, Table F.2-1 and Figure F.2-3 present the component center of gravities. The center of gravity of the wing was complicated by its tapered geometry and the compound-material-structure which consists of spruce, birch, and balsa. The traditional "hang and mark" technique was used on a scaled cutout of the tapered wing. The center of gravity is 3.75 inches from the leading edge root which appeared to be a fair estimation.

Table F.2-1 Component Center of Gravities

Component	inches from nose
Payload	33 (full)
Motor,Gbox,Mount	2.50
Battaries/Avionics	11.25
Cockpit (structure)	1.33
Fuselage (cabin)	25.25
Front Landing Gear	15.00
Rear Landing Gear	45.29
Fuselage Empennage	52.25
Vertical Tail	59.69
Wing	15.75
Propeller	0.06
Fully Loaded Aircraft	17.95
Empy Aircraft	16.60 (uncorrected by package postion)

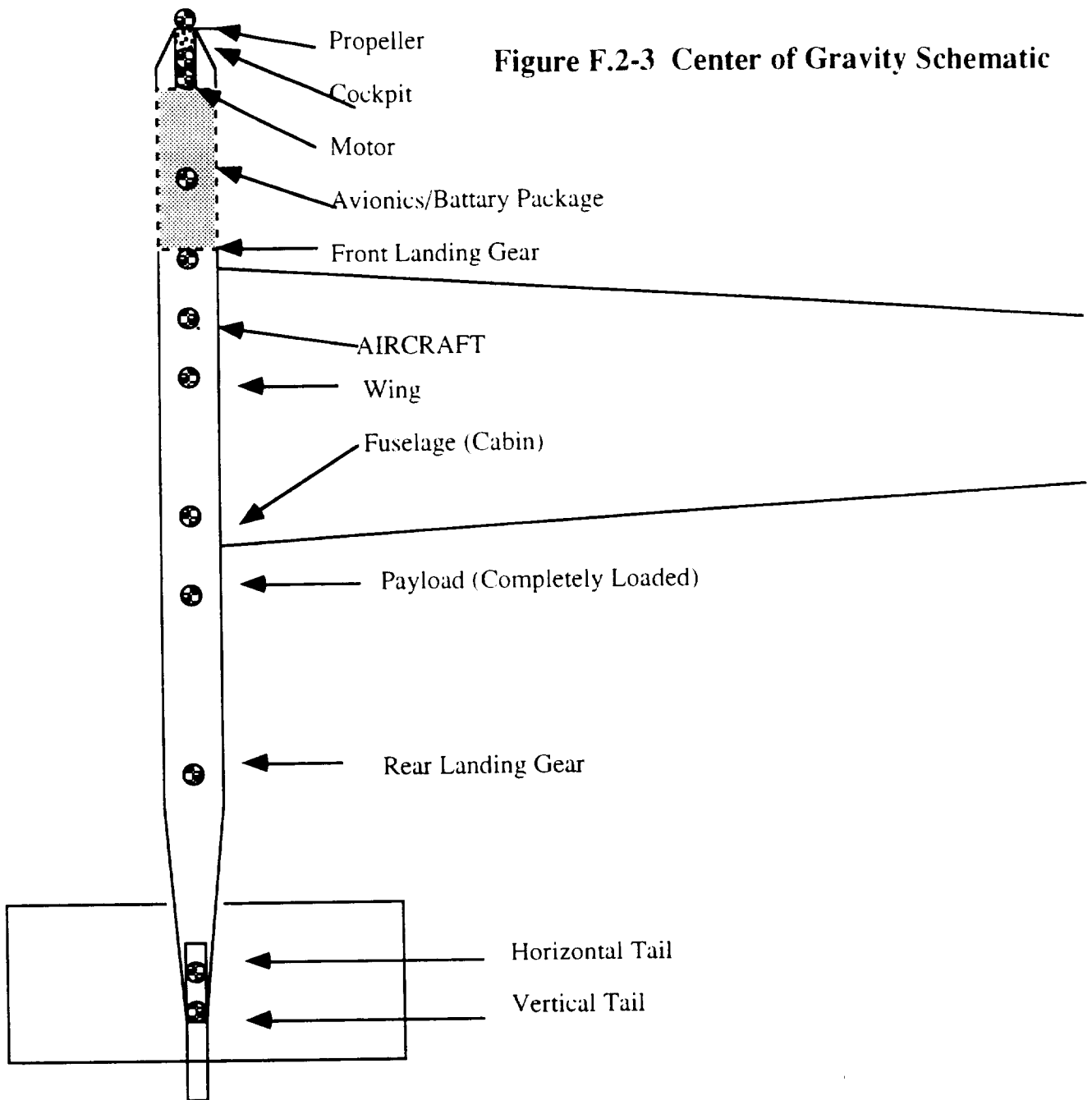


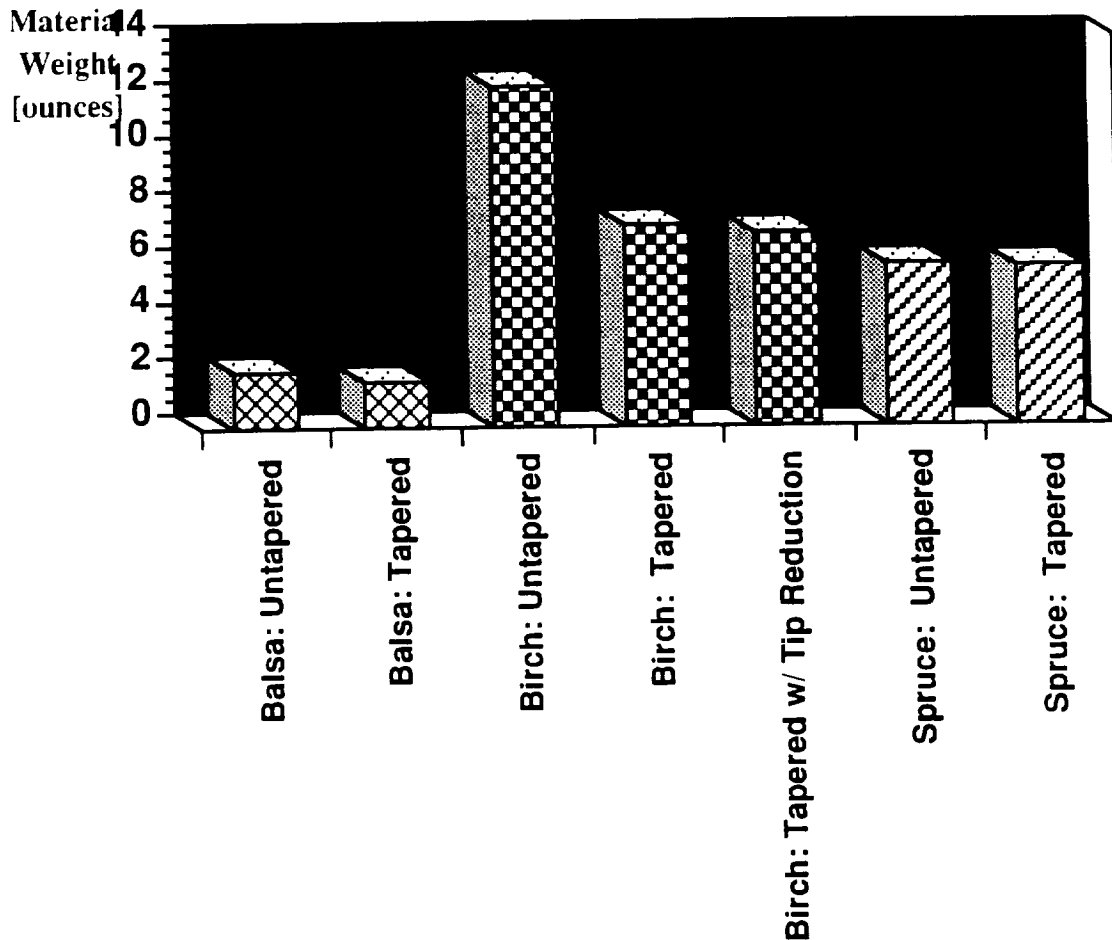
Figure F.2-3 Center of Gravity Schematic

F.3 Weight Conservation of the Tapered Wing

The wing has a taper ratio of 0.6. It incorporates a total of 3 different types of structural materials: spruce spar caps, balsa airfoils, and birch spar webs. Figure F.3-1 shows small savings due to taper in the balsa section and hardly any in spruce. Such minimal change is due to the light weight of balsa and the small changes in the length of the spruce spar caps. The largest conservation results from the 1/16 inch thick birch spar webs.

In a tapered wing, the birch spar webs which are located near the root are larger than those at the tip. Since the untapered wing has the same size spar webs throughout the wing, the tapered wing yields a reduction in weight due to the decreased size of the birch spar webs. In fact, Figure F.3-1 shows the tapered wing enjoys a 40% weight decrease over the untapered wing in this area.

Figure F.3-1 The Weight Conservation of a Tapered Wing



Since the tapered wing approximately generates an elliptical lift distribution, the lifting power at the tip of the tapered wing is not as strong as at the root. Conversely, the untapered wing provides a uniform lifting distribution and requires the wing structure to be just as strong at the root as at the tip. The elliptical lift distribution of the tapered wing allows for the removal of the birch spar webs near the tip. The absence of the spar webs for 15 inches from the tip decreases the tapered-birch spar webs weight by 1/10 of its original 40% reduction. This is not a tremendously significant reduction, but any weight conservation is favorable.

F.4 Competitive Weight Design with HB-40

The present aircraft which *The Blue Emu* would compete against is the *HB-40*. Below, Table F.4-1 communicates the advantages *The Blue Emu* has over its competitor via an effective conservative weight design.

Table F.4 Comparison of Weight Design with HB-40

Criteria	<i>The Blue Emu</i>	<i>The HB-40</i>	<i>The Blue Emu</i> has
Weight/Passenger	1.2 oz/passenger	1.63 oz/passenger	36% less wt/psngr
Wing Weight	14.74 oz	13.2 oz	26% larger wing
Payload Weight	5.64 oz	3.7 oz	22 more passengers
Battery Weight	13.53 oz	17.8 oz	2 more batteries
Fuselage Weight	9.90 oz	7.83 oz	~40% more volume

G. Stability and Control

G.1 Summary

The following is a list of important design variables and stability coefficients for our final aircraft design.

Table G.1-1: Summary of Longitudinal Stability and Control Parameters

neutral point	0.5 c	horizontal volumetric tail ratio	0.53
$C_{m\alpha}$	-0.0177/deg.	horizontal tail surface area	1.54 sq. ft.
C_{m0}	0.041	horizontal tail span	24.6 in.
$C_{m\delta_e}$	0.00816/deg.	horizontal tail surface moment arm	33.25 in.
$\delta_{e_{trim}}$	-5 deg.	S_e/S_H	0.10

Table G.1-2: Summary of Lateral Stability and Control Parameters

$C_{n\beta}$	0.069/deg.	vertical volumetric tail ratio	0.213
$C_{n\delta_r}$	-0.009/deg.	vertical tail surface area	0.73 sq. ft.
Cl_{δ_r}	0.0002/deg.	vertical tail span	13.4 in.
Cl_p	0.012/deg.	vertical tail surface moment arm	36.1 in.
Cl_{δ}	-0.0021/deg.	S_e/S_v	0.58

G.2 Design Requirements and Objectives

Improved stability and control was not the avenue by which our design group attempted to overtake the Aeroworld market currently occupied by the *HB-40*. However, this does not mean that stability and control can be neglected. For any aircraft, stability and control is a crucial design issue that drives the sizing of the empennage, the placement of the center of gravity and the sizing and number of control surfaces. To remain competitive, favorable stability and control characteristics must be attained. The following is list of some self-imposed requirements and objectives set in order to achieve, and hopefully surpass, the control characteristics of the *HB-40* while accomplishing our primary design objective of lowering the overall CPSPK of the aircraft:

- (1) Improved longitudinal and lateral control using only two control surfaces: an elevator and a rudder coupled with dihedral. This was decided upon due to the weight increase associated with having a third servo for the ailerons.
- (2) Ability for aircraft to cruise at zero angle of attack with a minimum elevator deflection in order to minimize the associated drag caused by a plane flying at an incidence angle.

G.3 Center of Gravity and Static Margin

The static margin (SM) of an aircraft is the distance between the neutral point and the aircraft center of gravity position in terms of percent chord:

$$SM = \frac{X_{np}}{c} - \frac{X_{cg}}{c} \quad (G.3-1)$$

The neutral point of an aircraft represents the aft most position the c.g. can be located for the aircraft to maintain a minimum of neutral stability. Therefore, the SM is a measure of the longitudinal static stability of the aircraft: the greater the distance between neutral point and the c.g., the greater the longitudinal stability. Further, it is a measure of the response time of an aircraft; the larger the SM, the slower the response to pilot input.

The data base revealed that for similar aircraft with good stability characteristics the c.g. needed to be located near $0.3c$ and the SM needed to be approximately 20%. Normally, transport planes fly at SM's of 5% to 10% but that is because the pilot is onboard the aircraft and can observe the results of his or her inputs. Our aircraft will employ a ground based pilot so the response time needs to be much slower. From eqn. G.3-1, this places the neutral point at $0.5c$.

Given a desired neutral point, a corresponding value of $C_{m\alpha}$ can be found from the relationship:

$$C_{m\alpha} = C_{L_{\alpha_w}} \left(\frac{X_{cg}}{c} - \frac{X_{np}}{c} \right) + C_{m_{\alpha_i}} \quad (G.3-2)$$

Static stability requires that the value of this slope be negative and the resulting curve must have a positive intercept. The slope needs to be negative because a positive angle of attack needs to cause a negative pitching moment. This will trim the plane back to the zero moment cruise configuration. Further, it needs to have a positive intercept so that the plane can be trimmed at positive angles of attack.

The data base showed that for similar planes the acceptable values for $C_{m\alpha}$ ranged from $-0.75/\text{rad.}$ to $1.25/\text{rad.}$ For our rectangular fuselage configuration and Wortmann lift-curve slope, a desired value of $0.5c$ for the neutral point corresponds to a $C_{m\alpha}$ of $-1.02/\text{rad.}$, or $-0.177/\text{deg.}$ Again, this value matches favorably to similar aircraft that had better than average handling qualities.

G.4 Longitudinal Stability

The sizing of the horizontal stabilizer was driven by the desire to place the neutral point at $0.5c$. Equations G.4-1 and G.4-2 were included in a computer code that varied the span and chord of the stabilizer to find combinations of the two dimensions that met the static stability requirements.

$$\frac{X_{NP}}{c} = \frac{X_{ac}}{c} - \frac{C_{m_{\alpha f}}}{C_{L_{\alpha w}}} + \eta V_H \frac{C_{L_{\alpha t}}}{C_{L_{\alpha w}}} \left(1 - \frac{d\epsilon}{d\alpha}\right) \quad (G.4-1)$$

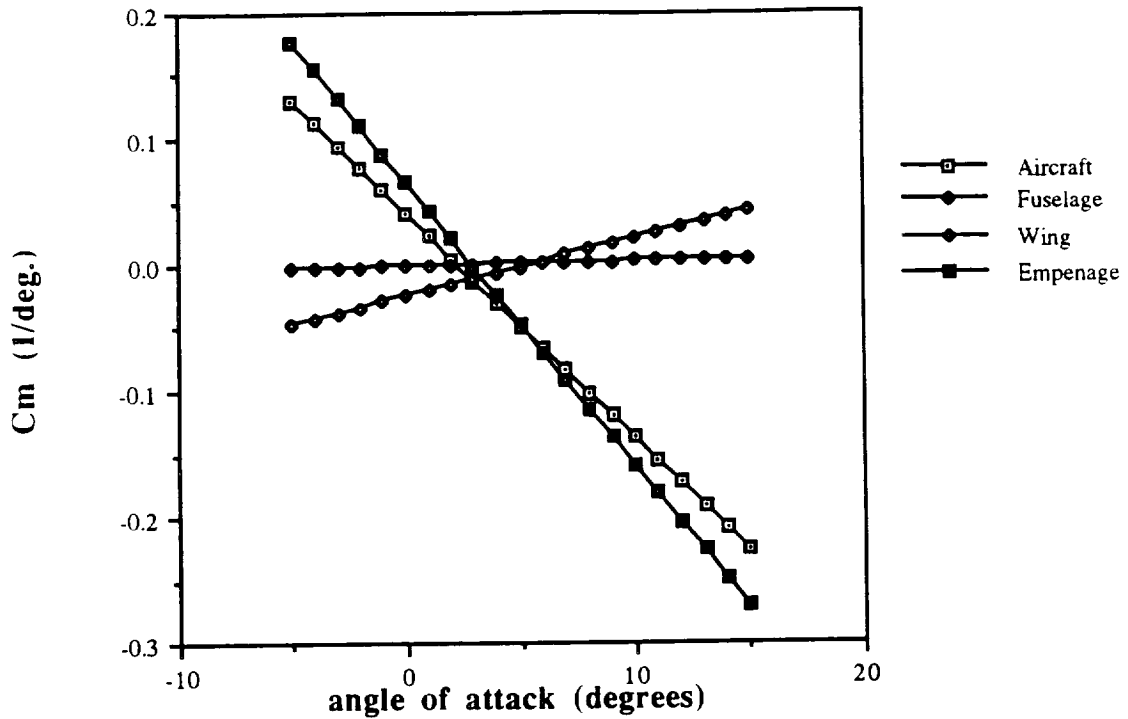
$$C_{m_{\alpha}} = C_{L_{\alpha w}} \left(\frac{X_{cg}}{c} - \frac{X_{ac}}{c}\right) + C_{m_{\alpha f}} - \eta V_H C_{L_{\alpha t}} \left(1 - \frac{d\epsilon}{d\alpha}\right) \quad (G.4-2)$$

Appendix III shows this program that was written to arrive at possible combinations of span and chord that would fulfill our design objectives. For the range of values tested, there were 15 combinations of the span and chord that accomplished this feat. Therefore, another figure of merit had to be considered to justify the choice of a tail size, namely control power.

The control power of an elevator is defined as the change in C_m that results from a given elevator deflection. This derivative is a function of the horizontal volumetric tail ratio and the lift-curve slope of the tail, which are both functions of the span and chord of the horizontal stabilizer. Since greater control power requires less elevator deflection to achieve the same effect, it was desired for the elevator to possess the greatest control power possible. Consequently, the combination of span and chord that was selected from the possible fifteen choices had the highest product of the volumetric ratio and lift-curve slope. Thus, a span of 25.8 in. and a chord of 9 in. were selected as the size of the stabilizer.

Figure G.4-1 is a plot of C_m for the three aircraft components, wing, tail, and fuselage, that contribute to the longitudinal stability.

Figure G.4-1: C_m vs. α for Individual Aircraft Components



Eqn. G.3-2 shows the derivation of the wing and tail contributions while the fuselage contribution is given by:

$$C_{m\alpha_f} = \frac{1}{36.5Sc} \sum w_f^2 \frac{\partial \epsilon}{\partial \alpha} \Delta x \quad (G.4-3)$$

The plot shows that both the fuselage and the wing are both destabilizers in terms of longitudinal stability. The horizontal stabilizer needs to be large enough to counteract the destabilizing effect of the other two components. The curve for the entire aircraft is also shown so that it can be compared to the individual components. This comparison shows that the tail is the major contributor to longitudinal static stability.

Static longitudinal stability also requires that the intercept of the curve be positive. Yet, both the wing and fuselage have negative intercepts. Therefore, the horizontal stabilizer must also be large enough to force the intercept of the entire aircraft to be positive. Equation G.4-4 shows that the intercept is directly related to incidence of the wing and the tail:

$$C_{mo} = C_{mo_w} + C_{mo_f} + \eta V_H C_{L_\alpha} (\epsilon_o + i_w - i_t) \quad (G.4-4)$$

The equations for the intercepts of the wing and fuselage are given by eqns. G.4-5 and G.4-6:

$$C_{mo_w} = C_{mac_w} + C_{Lo_w} \left(\frac{X_{cg}}{c} - \frac{X_{ac}}{c} \right) \quad (G.4-5)$$

$$C_{mo_f} = \frac{k_2 - k_1}{36.5 S c} \sum w_f^2 (\alpha_{ow} + i_f) \Delta x \quad (G.4-6)$$

These coefficients have values of -0.024 and -0.00039, respectively. For simplicity in design and construction, the wing was set at zero incidence relative to the fuselage. Although a wing incidence is needed for takeoff, it is unnecessary for cruise conditions for the design cruise speed. The additional lift provided by a wing mounted at an incidence during cruise would have to be compensated for by greater lift at the tail and a slower cruise speed. This analysis led to the decision to mount the wing at zero incidence.

An established wing incidence leaves the tail incidence as the only variable in determining C_{mo} of the entire aircraft. A tail incidence of zero would satisfy both the requirement of a positive C_{mo} and also make construction of the tail much easier. This yields a C_{mo} of 0.0408 for the entire aircraft and, given the slope of the curve, an equilibrium angle of attack of the aircraft of 2.5 degrees with no elevator deflection.

G.5 Longitudinal Control

Although the aircraft will fly with no elevator deflection, the drag created by the lift vector from flying at an angle of attack of 2.5 degrees is very costly in terms of lost power and could be eliminated by a small elevator deflection. Therefore, it was necessary to find the trim elevator angle, δ_e , that would allow the aircraft to fly at zero angle of attack while experiencing no pitching moment. The C_m of the entire aircraft is given by:

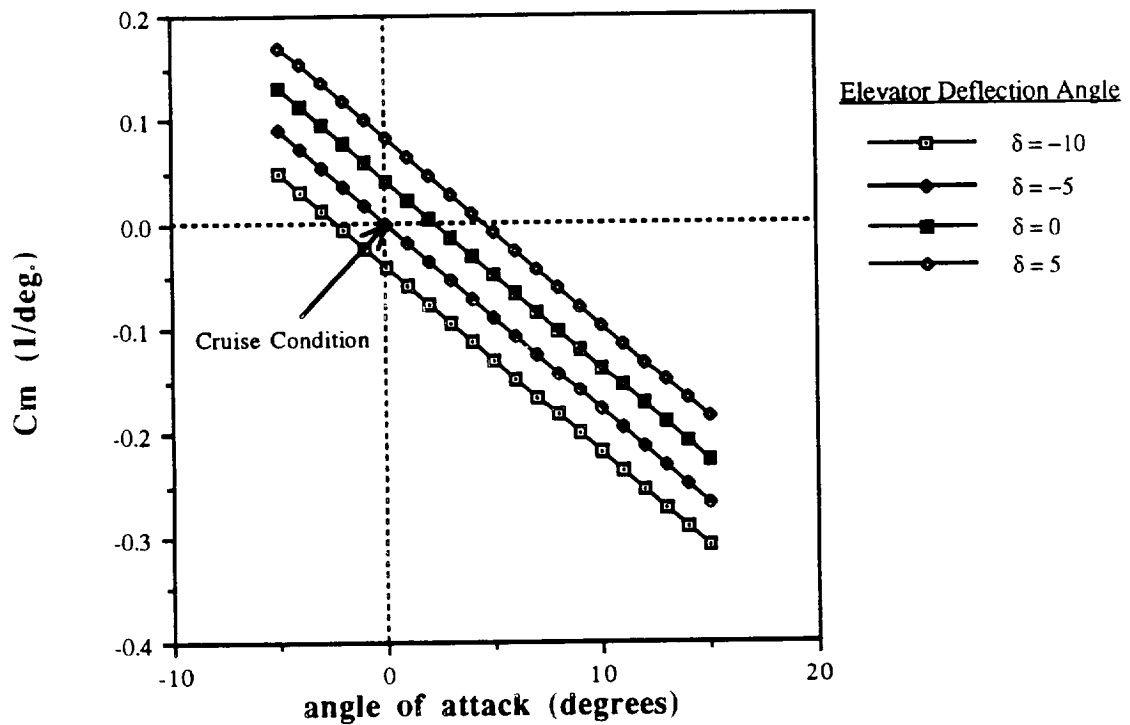
$$C_m = C_{mo} + C_{m\alpha} \alpha + C_{m\delta_e} \delta_e \quad (G.5-1)$$

$$C_{m\delta_e} = -\eta V_H C_{L_\alpha} \tau \quad (G.5-2)$$

where eqn. G.5-2 is referred to as the control power. To fly the plane at zero angle of attack and zero moment the trim angle must equal C_{m0} divided by the control power. Yet, the control power is dependent upon the ratio of elevator to stabilizer surface area, τ . Therefore, a relationship between δ_e and τ can be derived and a plot generated to show their dependence upon one another. Appendix III contains a program written to study this relationship between elevator size and deflection while varying the incidence of the wing and tail. This appendix also contains graph of the study's results. The study revealed that this aircraft could be trimmed straight and level if the wing with mounted at zero incidence to the fuselage. Further, at a tail incidence of zero degrees, the trade study revealed that for a -5 degree elevator deflection, τ would be 0.244, or the elevator to stabilizer surface area ratio would be 0.10. This means the chord of the elevator would be 1.0 in. over the entire span. This result met our design goals of being able to fly at zero angle of attack while remaining simple to construct given the zero incidence of the tail and wing.

Figure G.5-1 is a plot of C_m for the aircraft at four different elevator deflections.

Figure G.5-1: C_m vs. Alpha for Aircraft with Elevator Deflections

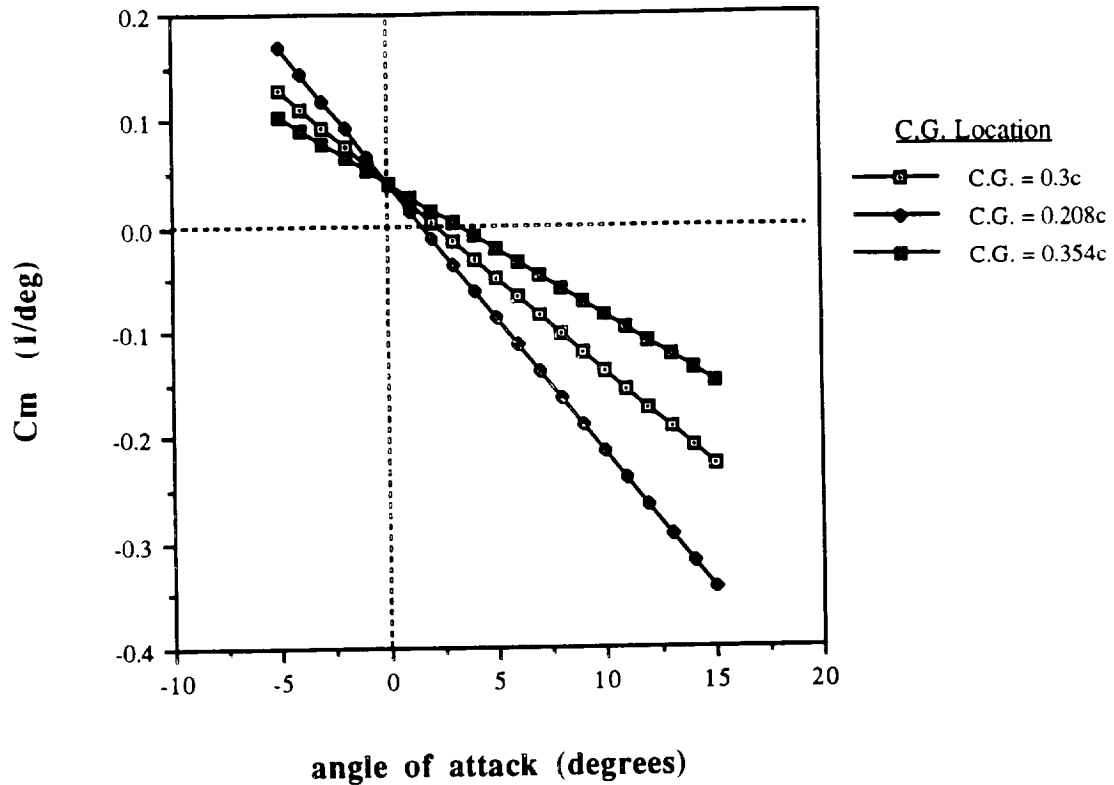


The design trim point, corresponding to an elevator deflection of -5 degrees, is shown to intersect at zero moment and zero angle of attack. This shows that the given configuration of elevator and stabilizer should provide sufficient longitudinal control enabling the aircraft to fly straight and level during cruise. Further, the sensitivity of the plane to a sudden elevator deflection is not a significant problem. The graph shows that for a 5 degree change in elevator angle the corresponding moment will cause the plane to increase to a 2.5 degree angle of attack. This is a small incidence and will not cause any problems during the validation phase of the project.

Another sensitivity analysis that was performed was the response of the aircraft in a less than full passenger loading situation. Although, we employ a movable battery pack, there is still some movement in the c.g. Further, if that critical technology does not work as effectively as planned, it is important for the plane to be able to fly at all loading configurations while maintaining adequate longitudinal stability.

An aircraft stability analysis shows that the c.g. can move 2 in. backward and still possess better than neutral stability. The envelope forward of the design c.g. is much greater than this. A weight analysis revealed that without employing the mobile pack, the c.g. moves a total of 1.5 in. forward of the design c.g. and 0.25 in. to the rear. Figure G.5-2 shows these two extreme cases for the longitudinal stability.

Figure G.5-2: C_m for Extreme C.G. Positions



This plot reveals that neither extreme loading configuration significantly effects the stability of the plane. For the aft-most c.g. position, the aircraft trim angle of attack with no elevator deflection rises from 2.5 degrees to 4 degrees. Similarly, for the forward most c.g. position the aircraft trim angle of attack decreases from 2.5 degrees to 1.5 degrees. This change in the slope of the curve does not present any difficulty with respect to the stability and control of the aircraft.

G.6 Lateral Stability

The task of sizing the vertical stabilizer was much easier than that of the horizontal stabilizer due to the given volumetric ratio given by ref. 7. For an aircraft of this size it is suggested to have a vertical tail volume ratio of 0.22 where this ratio is given by:

$$V_v = \frac{S_v L_v}{S_c} \quad (G.6-1)$$

This equation can not be fully utilized, though, until the chord is set because the tail area is a function of the chord.

The chord was sized through Reynolds number considerations at the tail. It was desired to keep the Reynolds number at the tail less than or equal to 100,000, since this is the regime the tail is desired to be in during flight. Therefore, the chord was set to correspond to a Re number of 100,000 at the tail, or 7.86 in. The tail was originally designed at a Re number of 70,000 but a preliminary trade study revealed that this did not provide enough lateral stability. With the tail chord established by the Reynolds number, the span was found to be 13.4 in. and the distance to the tail 36.1 in. using the volumetric ratio of 0.22.

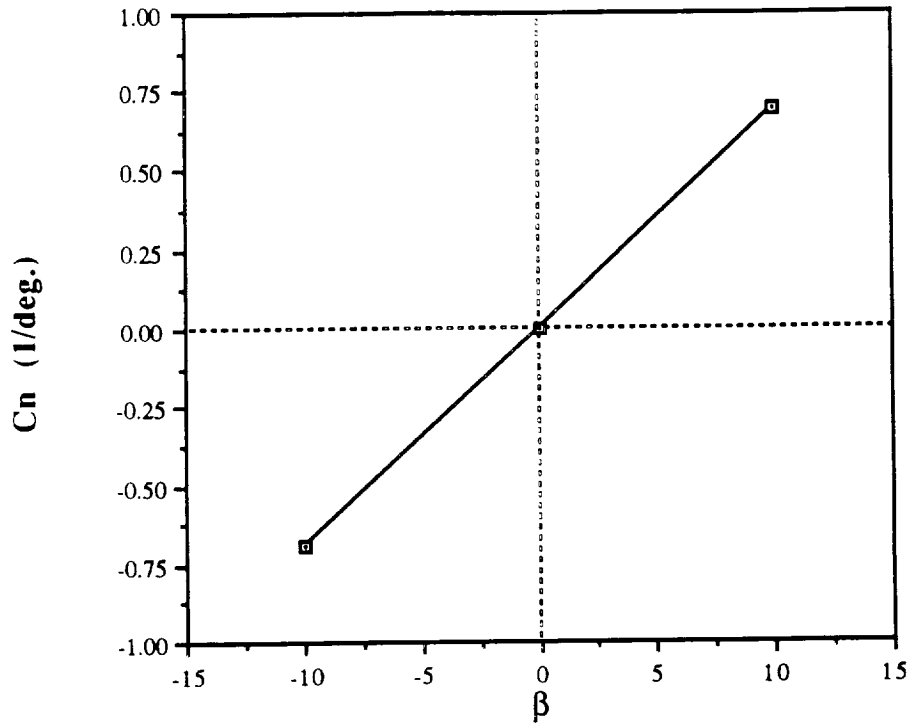
Once the vertical tail size was established, the lateral stability coefficients could be analyzed to ensure sufficient control. The primary control derivative for lateral control is $C_{n\beta}$, or yaw moment due to yaw angle. This derivative becomes extremely important when analyzing lateral control due to the fact that the aircraft must turn using only a rudder and dihedral; there are no ailerons present to create roll moment. The value of $C_{n\beta}$ must be positive for the plane to be laterally stable. This derivative is given by the equation:

$$C_{n\beta} = C_{n\beta wf} + \eta V_v C_{L\alpha v} \left(1 + \frac{d\sigma}{d\beta}\right) \quad (G.6-2)$$

$$C_{n\beta wf} = -k_n k_{RI} \frac{S_{fs} l_f}{S_w b} \quad (G.6-3)$$

where eqn. G.6-3, the fuselage term, although destabilizing, was negligible for this analysis and was discarded. Therefore, $C_{n\beta}$ can be reduced to a function solely of tail size. Figure G.6-1 is a plot of C_n vs. yaw angle using the vertical tail dimensions already established.

Figure G.6-1: Cn vs. Beta for Aircraft



It can readily be seen from this plot that the plane is stable with a value for the slope of this curve of 0.069/deg. The vertical tail size, arrived through the Reynolds number considerations, is large enough and far enough from the c.g. to maintain lateral stability.

G.7 Lateral Control

The required 60 foot radius turn at 25 ft/s was the main consideration when sizing the rudder and setting the dihedral angle. Although the turn requirement was for only 60 feet, a factor of safety was factored in so that the rudder and dihedral were sized to accomplish a 50 foot radius turn. The roll coefficient is the primary coefficient that governs lateral control and is given by the equation:

$$C_l = C_{l_p}p + C_{l_\beta}\beta + C_{l_{\delta_r}}\delta_r \quad (G.7-1)$$

where
$$C_{l_{\delta_r}} = \frac{S_v z_v \tau C_{L_{\alpha v}}}{S_w b} \quad (G.7-2)$$

$$C_{lp} = \frac{C_{L\alpha}}{12} \frac{1+3\lambda}{1+\lambda} \quad (G.7-3)$$

$$C_{l\beta} = \left(\frac{C_{l\beta}}{\Gamma}\right) \Gamma + \Delta C_{l\beta} \quad (G.7-4)$$

An adequate model for the necessary roll moment could not be established, so C_l was set to zero in order to solve for δ_r as a function of rudder size. The roll rate, p , is established by the necessary bank angle and the design time to reach the angle. For the smaller turn radius of 50 ft., a bank angle of 25 degrees was needed and the time to reach that angle was set at 0.5 sec. The C_{lp} and $C_{l\beta}$ are only functions of taper and dihedral which was fixed at 8 degrees for this analysis. The value for the yaw angle was given by setting C_n to zero and solving for b in terms of $C_{n\delta_r}$ and $C_{n\beta}$. The yaw angle reduces to the following:

$$\beta = \frac{\tau_v \delta_r}{\eta \left(1 + \frac{d\sigma}{d\beta}\right)} \quad (G.7-6)$$

It can now be shown that eqn. G.7-1 is reducible to a function of rudder area and deflection. Both values, area and deflection, should be minimized so as not to incur more drag than is necessary. A value of 0.58 was decided on for the ratio of rudder surface area to vertical tail surface area. This rudder will provide enough roll power to accomplish the turn at a rudder deflection of 15 degrees. The rudder area and deflection provide enough roll power to accomplish the turn yet still do not incur a large drag penalty.

G.8 Control Mechanisms

Our aircraft will employ two control surfaces, a rudder and an elevator, and two servos to operate them. The rudder will have a maximum deflection of 25 degrees and the zero-servo position will correspond to a zero rudder deflection. The elevators will have a maximum deflection of -15 to 10 degrees. The zero-servo position will correspond to a -5 degree deflection in the elevators since that is the cruise configuration. The servo should be able to overcome any hinge moment produced by the aerodynamics on the control surfaces.

H. Performance

The foundation for making these estimates was based on the aerodynamic forces associated with the aircraft (lift and drag) and the propulsion system (thrust). With the exception of weight, these were the main forces that determined the performance capabilities of the aircraft.

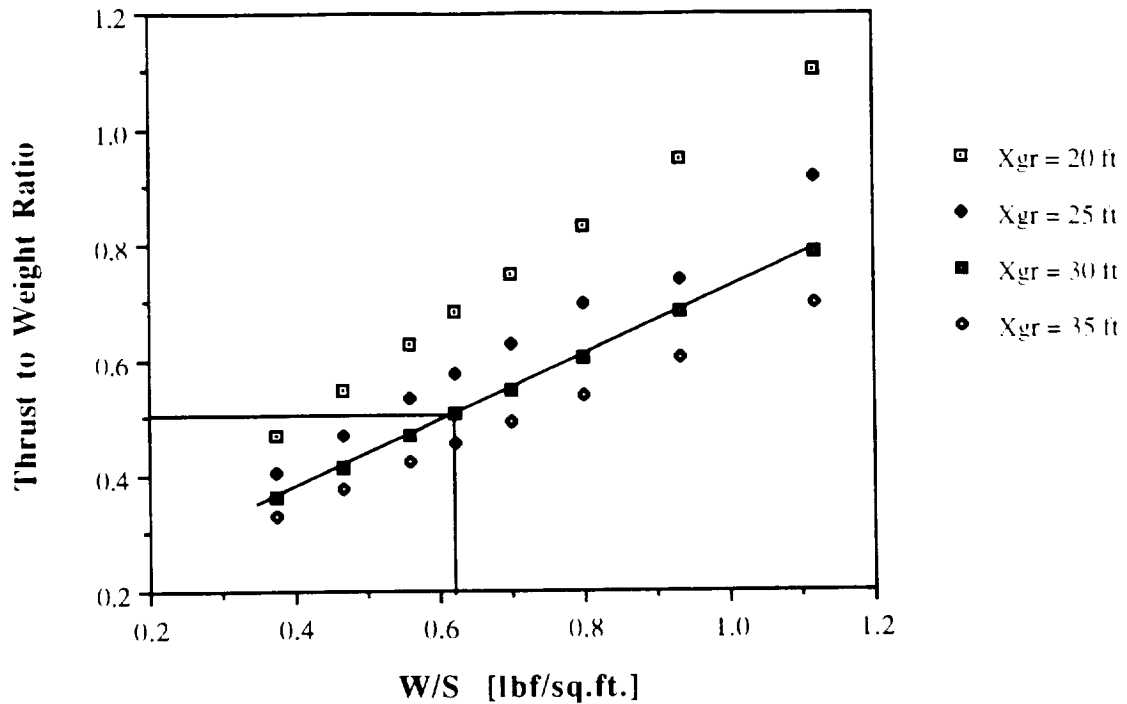
Most of the airplane performance estimates were calculated using the available computer software. These included a Propulsion Program and TK Solver (Electric Motor Performance) to determine endurance and range and a Takeoff Performance code. Hand calculations were also made to double check results such as takeoff distance and climb rates.

H.1 Takeoff and Landing Estimates

Using an equation developed in Flight Mechanics (eqn.H.1-1 Appendix IV) and setting the thrust equal to the static thrust, a distance of 27.4 feet for takeoff was calculated. With the aid of the software available, a more precise calculation was performed and the takeoff distance was calculated to be 30.96 feet. The calculation done using the TAKEOFF PERFORMANCE code is more precise because it accounts for the fact that the propeller is not actually producing the same thrust throughout takeoff. The difference between the two was about 11.5%. In either case the takeoff run does not exceed 32.0ft. A conservative estimate of 0.15 for the runway coefficient of friction was used and the takeoff distance was also based on an airplane weight of 5.6 pounds. Generally, takeoff distance includes a ground roll distance, a transition distance and an air distance. However, note that the takeoff distance here was simplified and defined as being the ground roll distance only. Further studies would have to be carried out to determine the unstick position and a reasonable obstacle height for this scale (i.e. RPV obstacle height) in order to compute the additional distances.

Initial studies were done to determine thrust to weight ratios for given wing loadings in order to accomplish takeoff in certain distances (eqn.H.1-2 Appendix IV). Figure H.1-1 shows that in order to takeoff in 32 feet with a reasonable wing loading of approximately 0.62 lbf/sq.ft., a thrust to weight ratio of about 0.5 would be required. The *Blue Emu* had a wing loading of about 0.56 lbf./sq.ft. with a thrust to weight ratio at takeoff of about 0.5. Takeoff performance is usually enhanced by ground effects but due to the difficulty involved in determining its extent, this was neglected.

Figure H.1-1: Thrust to Weight Ratio For Takeoff vs. Wing Loading

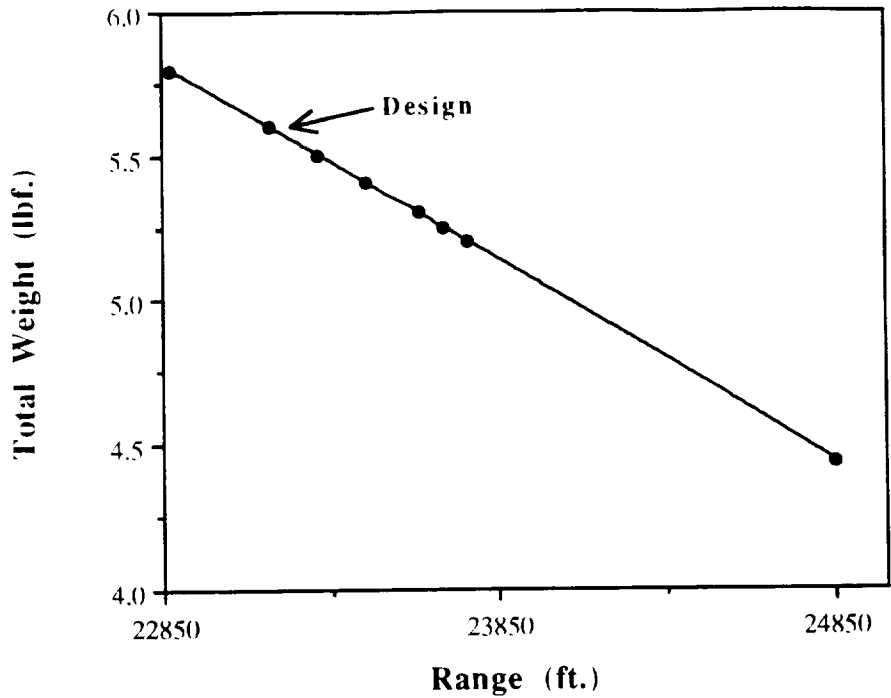


An estimate for the landing distance was determined using equation H.1-3 (Appendix IV). The velocity at touch-down is approximated as the stall velocity. The calculation yielded 41.2 feet as a minimum distance for the airplane to land. However, when equation H.1-4 was used to estimate the landing distance, a value of 51.3 feet was calculated. This is a problem because the airports that the *Blue Emu* is intended to service all have 32 ft. runways. However, this can be resolved if some sort of braking mechanism is employed.

H.2 Range and Endurance

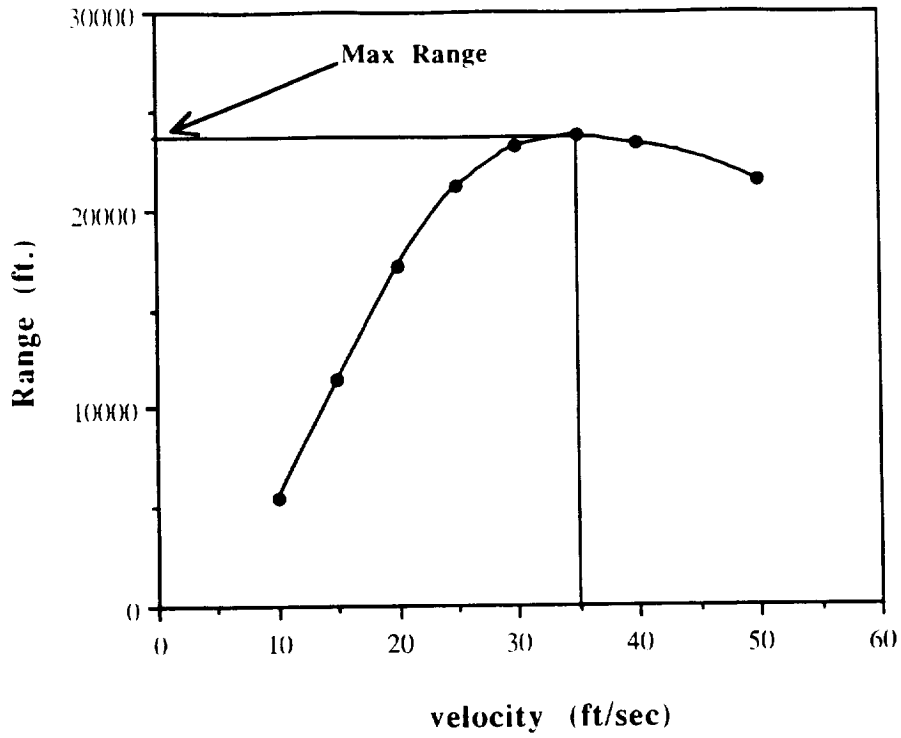
Based on weight estimates the maximum possible weight (with 60 passengers and crew) was originally 5.6 pounds. However, subsequent weight estimations yielded a lower overall weight of 4.79 pounds. All performance estimates were based on the original weight estimate. The minimum weight (without passengers) was not predicted to fall below 5.25 pounds. Figure H.2-1 shows how the range may vary with payloads at extremes of these estimates.

Figure H.2-1: Total Weight vs. Range



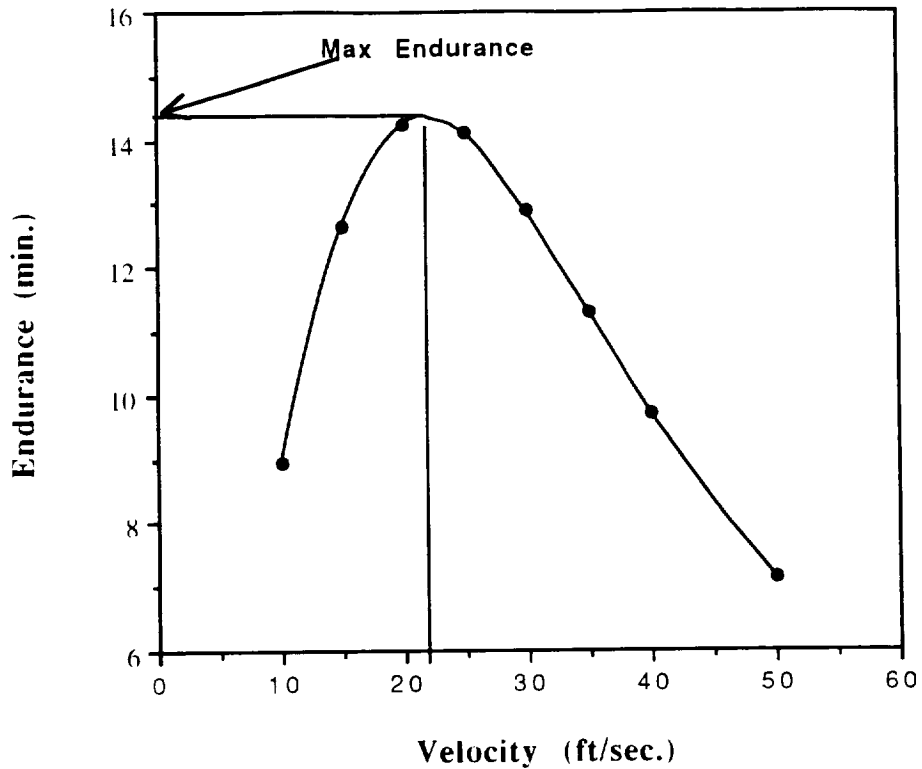
Range calculations relied almost exclusively on the software available. From the Electric Power application a maximum range of 23,667 feet was determined (see Fig.H.2-2). This value far exceeded the design range goal of 17,000 feet, including 2,000 ft. for loiter. The endurance at this range was 11.21 minutes. At first this seemed to be the result of inefficient engineering or possibly faulty codes. However, neither was the case. The reason for the large overshoot in range had to do with the availability of different battery pack capacities. A battery pack rated at 600mAhrs would have only allowed for a maximum range of 15,640ft.,and an additional 1,360ft was needed to satisfy the target range as stipulated in the design requirements and objectives. As it turned out, the next higher battery pack capacity was rated at 900mAhrs and this resulted in exceeding the design goal by such a large extent. With this additional range, the implication is that a purchaser may fly between any two cities in Aeroworld.

Figure H.2-2: Range vs. Velocity



The maximum endurance was achieved at the minimum current draw. This occurred while the airplane operated at a speed of approximately 23ft/sec. With a battery capacity of 900mAhrs. and a current draw of 3.71A, a maximum endurance of 14.3 minutes was calculated (see Fig.H.2-3).

Figure H.2-3: Endurance vs. Velocity



Even though the maximum current draw at takeoff and in climbing to 20 ft. was relatively high (10.82A), it was only for a very short period of time: 2.46 seconds for takeoff and 3.46 seconds to climb to 20 ft.. The battery “burn” during these two phases accounted for less than 2.5% of battery use. The corresponding range at this maximum endurance condition was computed to be 19,734 feet. For the *Blue Emu*’s chosen cruise velocity of 30ft./sec, the current draw was 4.11A, and this allowed an endurance of 12.87 minutes. The range at this cruise condition was 23,168 feet. Again, these values are higher than anticipated because of the low current draw and high battery capacity.

Figure H.2-4: Range and Endurance vs. Velocity

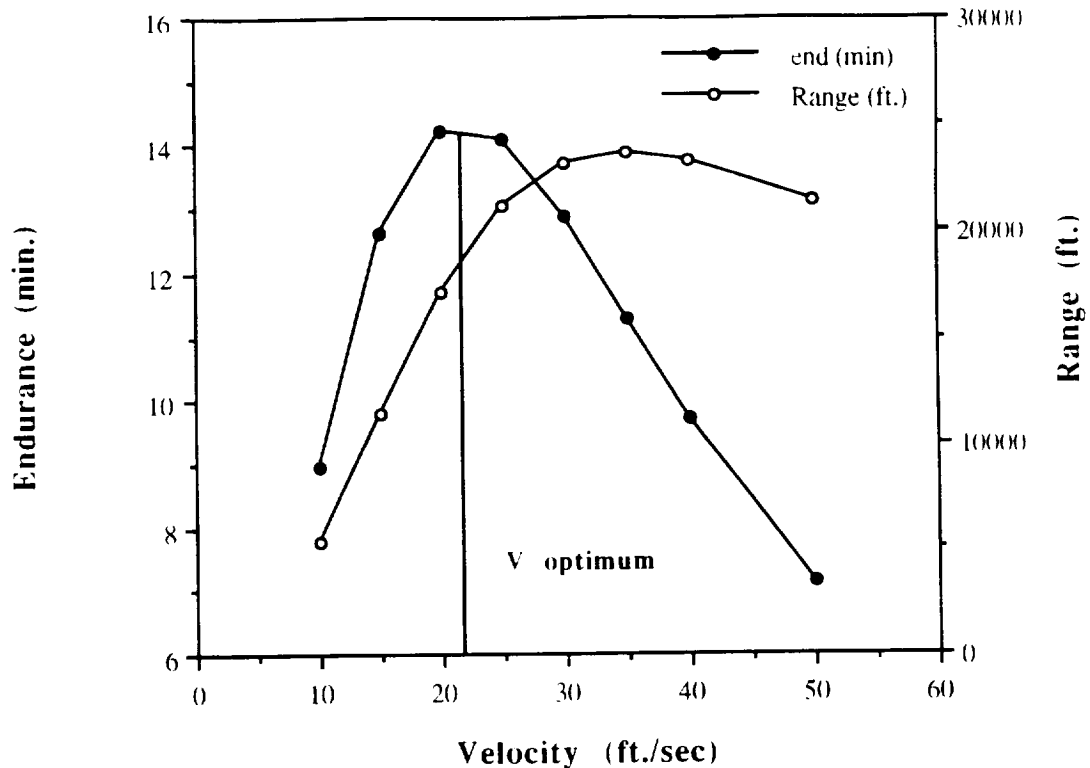


Figure H.2-4 shows the optimum velocity that the aircraft should operate at in order to achieve the best endurance-range combination. This was found to be about 27.86 ft./sec which is very close to the chosen cruising speed of 30 ft./sec. At the onset of the design process this cruising speed was agreed upon in order to be comparable to the *HB-40*.

H.3 Climbing and Gliding Performance

From power available and power required curves generated by the propulsion division, the maximum rate of climb was determined. The maximum rate of climb occurs at maximum excess power of 63.4W. The aircraft will be capable of achieving a maximum rate of climb of approximately 11.32 ft./sec.

The minimum glide path angle for the airplane occurs at the maximum lift to drag ratio for the aircraft. This is the same as maximum lift coefficient to drag coefficient ratio. This ratio was determined using

$$(L/D)_{\max} = [(C_{d0} \cdot \pi \cdot AR)^{-5}] / (2 \cdot C_{d0})$$

and found to be 17.4. Assuming that the airplane will commence gliding from a height of about 20 ft., the minimum glide angle given by

$$\tan \gamma_{\min} = 1/(L/D)_{\max}$$

is about 3.33 degrees. At this glide angle the *Emu* will cover a horizontal distance of 344 feet.

H.4 Turning

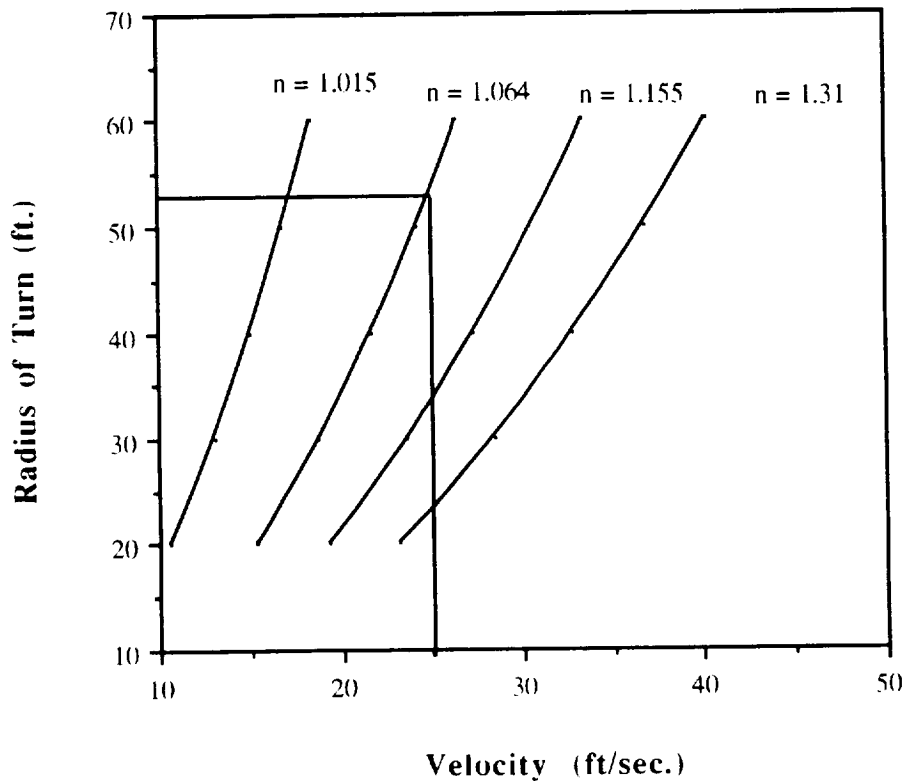
Due to the limited operating space for the technology demonstrator, the aircraft must be able to execute a turn within a 60 ft. radius. Also, the maximum speed allowed in the turn was 25 ft./sec. In order to avoid exceeding the structural limitations of the aircraft, load factors during the turn were to be as small as possible. In other words, the optimal situation is that most nearly a level turn.

The load factor and bank angle are related through

$$\cos\theta = 1/n.$$

Figure H.4-1 shows the various load factors encountered and the velocities involved in order to complete a turn in less than 60 ft.

Figure H.4-1: Radius of Turn vs. Velocity for Constant Load Factors



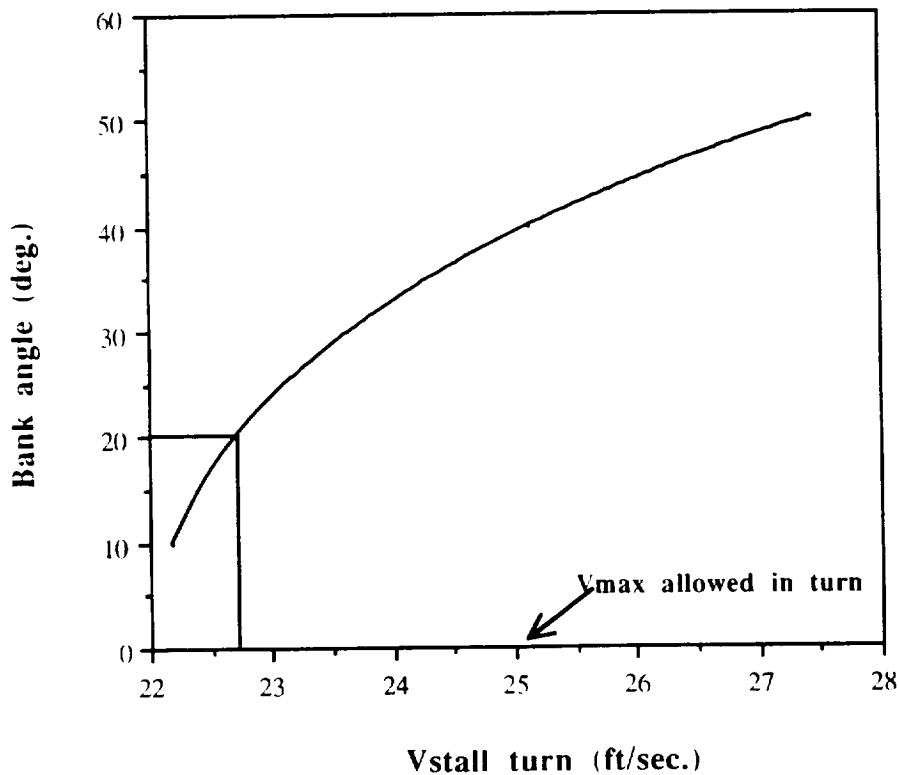
This graph shows that at a load factor of about 1.064 (bank angle = 20 deg.), the aircraft will complete the turn in about 53.5 ft while flying at the maximum prescribed turn velocity. To be on the safe side, the aircraft will be capable of banking at 30 degrees. A decision was made not to bank at more than 30 degrees because doing so would probably cause some discomfort to the passengers. In order to prevent banking more than 30 degrees the rudder will have a maximum deflection of 20 degrees in either direction.

Another issue that was addressed was the stall velocity in the turn. While not exceeding the 25 ft./sec maximum speed in the turn, the airplane has to maintain a speed greater than the stall speed in the turn. The stall speed in the turn is related to the stall speed during level flight operations by

$$V_{\text{stall turn}} = V_{\text{stall level}} \cdot n$$

Figure H.4-2 shows this relation. Larger bank angles incur higher stall velocities. At 20 degrees bank angle, the *Blue Emu* stalls at 22.7ft/sec. Banking beyond 30 degrees will put the airplane in a situation where, in order to avoid stalling, it will have to fly too close to the maximum velocity allowed in the turn.

Figure H.4-2: Bank Angle vs. Stalling Velocity in Turn



H.5 Performance Summary

Takeoff Velocity	25.32 ft/s
Takeoff Distance	30.96 ft
Time for takeoff	2.46 seconds
Current draw at takeoff	10.82 Amps
Takeoff thrust	2.08 lbf
Battery drain	18.34 mAhrs
Maximum endurance	14.3 minutes
Range at max endurance	19,734 ft
Maximum range	23,667 ft
Endurance at max range	11.21 minutes
Endurance at cruise	12.87 minutes
Range at cruise	23,169 ft

I. Structural Analysis

The main objective is to provide the preliminary structural design of an aircraft that will satisfy the requirements set forth in the Group Design Requirements and Objectives. One of the general requirements is to provide a structure that will be able to withstand extreme normal loads. The maximum load that has been calculated is 175.38 oz/in². Another factor that is to be taken into consideration is that of the factor of safety. This factor of safety is set at 1.3.

I.1 Producibility

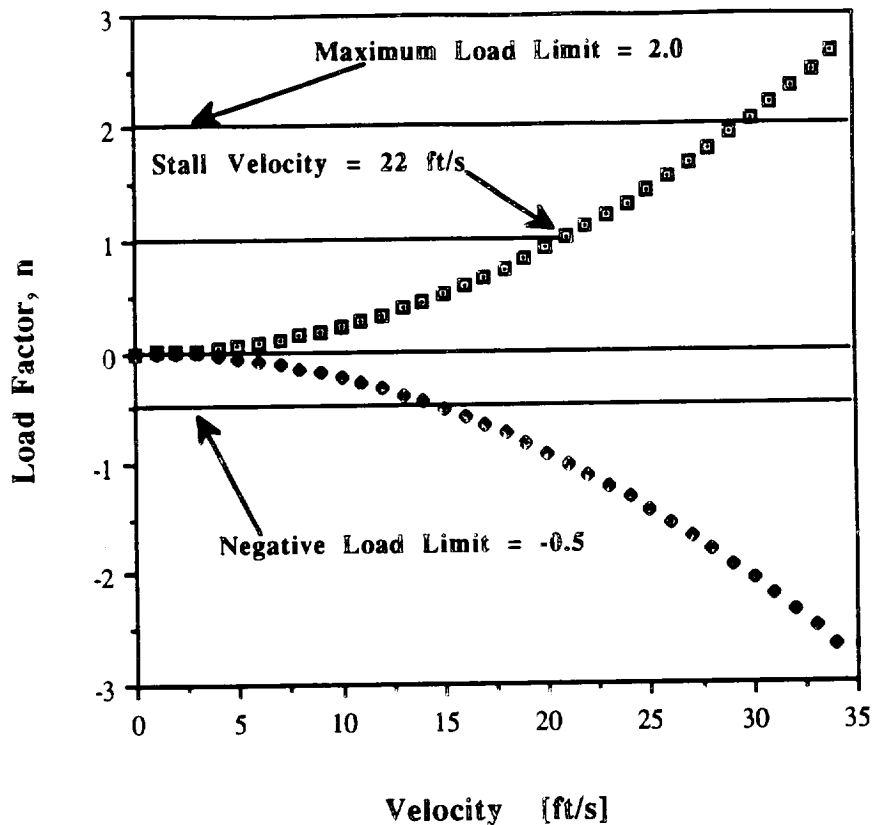
One of the main factors affecting the design of this aircraft is its producibility. This airplane must be both easy and economical to construct and reproduce. By constructing a monoplane, high-wing airplane some problems encountered in the basic construction of the airplane have been eliminated. The only section of the airplane that will be difficult to construct is the wing. Due to its taper, producing the wing will increase the amount of person hours needed. However, the overall reduction in weight and material will compensate in the total final cost.

The fuselage will be the simplest of the airplane's sections to construct because of its simple box cross-section design and minimum amount of material. This minimal material will also benefit the final weight and cost of the airplane. Thus, the airplane will be easier and more profitable to reproduce.

I.2 V-n Diagram

Figure I.1-1 presents the V-n diagram for the *Blue Emu*. The *Blue Emu* will have to perform between 22ft/sec and approximately 55ft/sec. Any speed below 22ft/sec is not possible. Any speed higher than 55ft/sec will cause structural damage to the aircraft. The maximum load factor was set at 2.0 to compensate for a possible extraordinary recovery maneuver with some factor of safety. Similarly, the minimum load factor was arbitrarily set at a minimum value of -0.5 due to the absence of any maneuvers producing negative loads.

I.1-1: V-n Diagram for the Blue Emu



I.3 Wing Structure

The wing is shown in Fig. I.2-1 and is composed of three frontal spruce spars of 1/16th in. thickness near the root of the wing, and 1/8th in. thickness near the tip of the wing. The reason for using a thicker spar at the root is to compensate for the larger moments and loads that the wing will experience at this location. The rear of the wing will be formed by a spruce wedge. Its skin will be the same as the skin of the entire airplane which will be a monocoque covering. The wing will be divided into 35 sections in the spanwise direction. Each subsection near the root of the wing will be strengthened by a birch panel between the ribs. The same reasoning follows for the spar webs at the root since most of the loads will occur at this location. Since the wing will be a simple lifting structure and not used as an engine mount it can be strengthened with the simplest conventional cross-sections. These cross-sections will be made from balsa wood since these do not need as much strength as other portions of the structure such as the spars in the wing and fuselage. The ribs will be constructed in the shape of the Wortzmann airfoil.

The chord length of the root cross section is 1.25 feet, while the tip will be .75 feet. This in turn leads to a reduction in weight which will approximately be 14.38 ounces.

This wing structure uses three thin spars. This was done because of the finer and more evenly distributed structure that will be built. This will reduce the critical stresses at the skin and at the spanwise supports. Therefore, the structure can be optimized to redistribute the stresses more easily and reduce the weight. Also, as seen in several sources such as **F-24 Stingray: A Low Cost High-Performance Export Fighter**, the stresses will be concentrated at the fuselage root with thicker and fewer bars. This will in turn lead to material fatigue. There will still be higher stresses at the root of the wing than at the tips. Therefore, the roots will be reinforced with birch spar webs. About midway along the span of the wing, the birch spar webs will no longer be used since the stresses in the wing decrease along the span.

The tapering of the wing was also decided not only for better aerodynamic performance, but also in order to reduce the weight at the tips, and thus eliminate the bending and shearing forces in the wing. Since the length of the wing is large, 10ft, the reduction of the deflection is important. Thus the tapering will also decrease the amount of wing deflection that will occur.

I.4 Vertical and Horizontal Tail Structure

The detailed structure for both the vertical and horizontal tails are similar to each other as can be seen in Figs. I.3-1 and I.3-2. Their design was decided to be a flat plate design. This will make it easier to produce since there is no need for a complex wing structure. Since this part of the airplane will not experience heavy loads, and if the aircraft is trimmed, it will not experience any moment. Therefore, there is no need for a complex structure. Both of these wing structures will be comprised of a thin balsa sheet, and a balsa and spruce structure. For the vertical tail, the total height is 13.40in. with a width of 7.86in. The width of the balsa sheet will be 5.93in. For the horizontal tail, the total length is 25.8in. and the width is 9.0in. The total width of the balsa sheet is 1.8in. The balsa beams will be placed 2in. apart in the balsa-spruce configuration for both the horizontal and vertical tails.

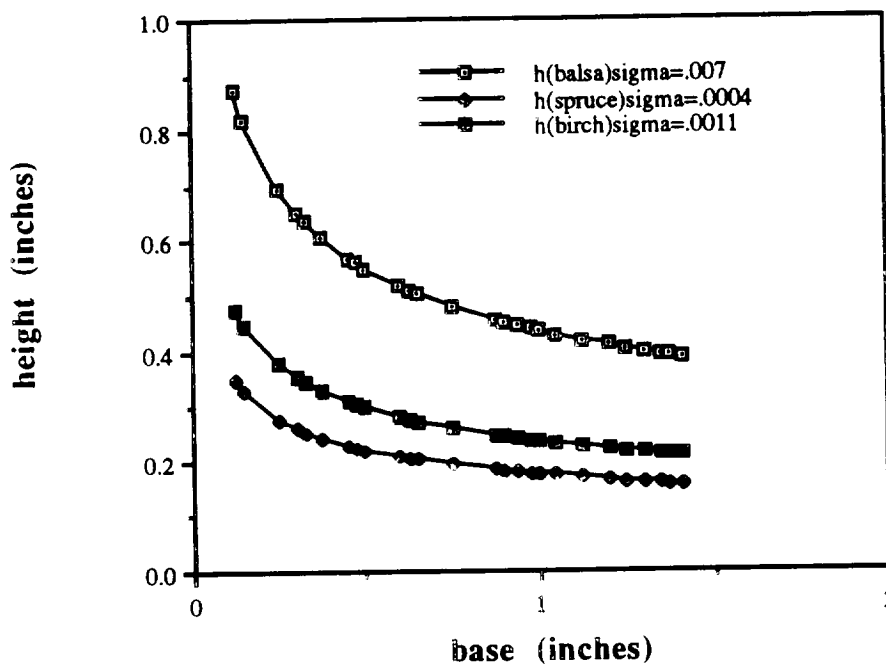
Deflections of the vertical and horizontal tails will be relatively small. Therefore, a slight re modification may occur later on in the building process to the spruce-balsa structure. The total weight of the empennage will be 4.2oz.

I.5 Fuselage

The principle of reducing the cost while satisfying the Design Requirements and Objectives, was one of the main purposes for this proposal. This will primarily be done through the construction of the fuselage and wing. Since the wing has more restrictions because of its duties, the fuselage is where most cost reduction will occur.

The fuselage consists of a simple box cross-section. Its width is 6.1in and its height will be 3.5in. Its total length will be 60.5in. It will be shaped by four spruce spars. Each spruce bar will be .25in thick. This decision was based upon the third individual trade study that found that spruce will withstand the largest loads and yet still be light enough to be considered as profitable to use. As can be seen in Fig.I.5-1, the most reasonable thickness of wood to use is spruce.

Figure I.5-1: Height of Longeron Cross-Section vs. Base at Maximum Normal Stress for Various Materials



It is stronger than balsa which for the same amount of strength would need a very thick cross-section. Also, spruce is lighter than birch. The individual cross section and truss beams will be made of balsa. These locations require less strength and balsa is the lightest of the materials.

Each subsection on the sides and bottom of the fuselage will also be box shaped 5in. long. This configuration can be seen in Fig. I.4-1 However, the truss section will be alternating in diagonal directions. The top of the fuselage will not contain these truss sections. Examining the older models, the top sections did not seem to require much structural strength. The front section of the fuselage will be tapered in order to reduce frontal drag. Similarly the aft of the fuselage will be tapered along the bottom to eliminate drag also.

The total stress distribution along the fuselage will be greatest slightly behind the wing. At this location the greatest shear and moment occur as can be seen in the shear-moment diagram in Fig. I.5-2. Thus the most careful analysis of the construction will occur at this location. The overall stress distribution is relatively small compared to the stresses on the wing. This can be seen from Fig.I.5-3 which shows that across the entire fuselage, when a specific wall-thickness has been selected, the spars will undergo similar stresses.. The total fuselage weight is therefore 9.337oz.

I.6 Landing Gear Design

The design of the landing gear is one of the most important components of the airplane, since the airplane will experience the highest force at landing. The main function of the landing gear is to absorb landing shocks and taxi shocks, thus transmitting these loads to the airframe. The tires are subjected to rather severe static and dynamic loads during taxiing, take-off roll, and landing roll. They also provide the ability for ground maneuvering at four different times: taxi, takeoff roll, landing roll, and steering. The most critical time for this aircraft will be at takeoff and landing.

At takeoff and landing the landing gear will experience three types of loads: vertical loads caused by non-zero touchdown rates and taxiing over rough surfaces, longitudinal loads caused by spin-up loads and friction loads, and finally lateral loads which are caused by "crabbed landings," cross-wind taxiing and ground turning. The least important of these loads will be the lateral loads since there is no cross-wind in Loftus and there will not be much ground turning. The one load which will be very important since our "airport" surface area is extremely rough is the vertical load. Each tire will thus be designed to operate at a maximum allowable static load.

Using a descent velocity of 10ft/sec, which is typical for transport aircraft, it was decided to go with a simple configuration. The supporting structure will be a thin metal rod of approximately 0.15 in. diameter and 7 in. length. The wheel will also be approximately 1.5 in. in thickness and 2.5 in. in diameter. Two wheels will be located at the front of the fuselage and one at the aft of the fuselage. The landing gear

configuration for the aft of the airplane will be a metal bar of 0.15 in in diameter but will only be five inches in height since, as stated before, most of the force will be at the front of the aircraft. The rear wheel will be .5 in. in thickness and 1.0-1.5 in. in diameter depending on the availability of wheel sizes. These sizes were based on: weight, minimum size, customer preference, and finally wear and tear characteristics.

The reason for the larger landing gear at the front of the aircraft is because these must not exceed values which will cause structural damage to the airplane, cause tire damage, cause runway damage, or excessive surface deformation. They must also have a minimal normal force which must be less than 0.8% of the weight acting on the nose gear for appropriate levels of friction forces needed for steering. Therefore, the nose gear must be designed for maximum allowable dynamic loads.

Figure 1.2-1 Wing Structure

Balsa Airfoil Sections
Spruce Spar Caps
Spruce Leading and Trailing Edge

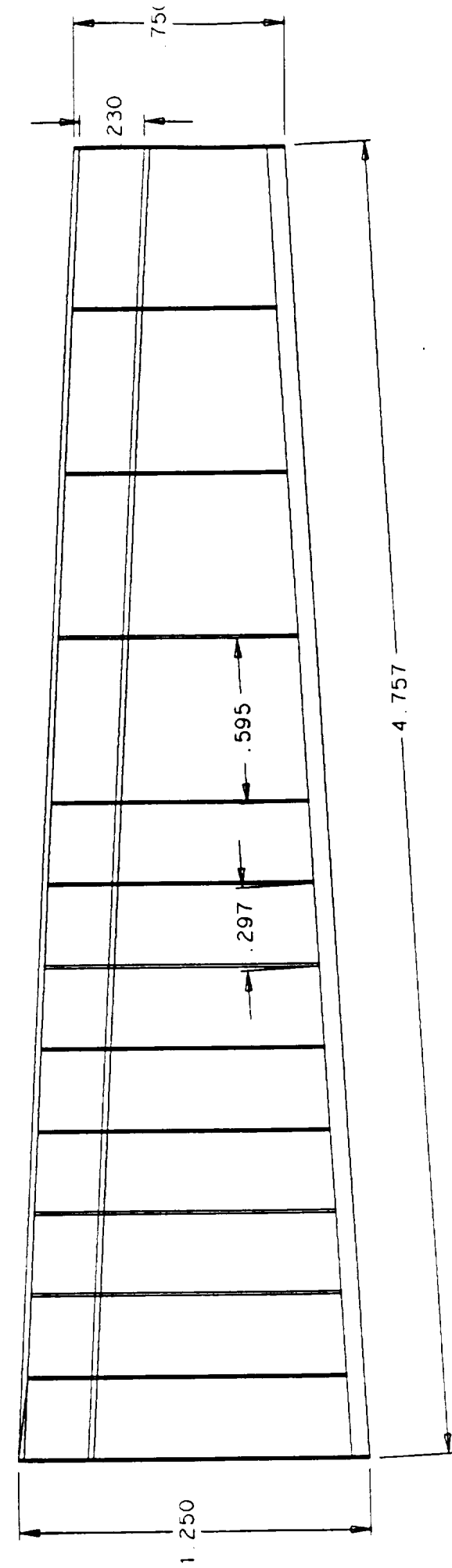


Figure 1.3-1 Vertical Tail Surface

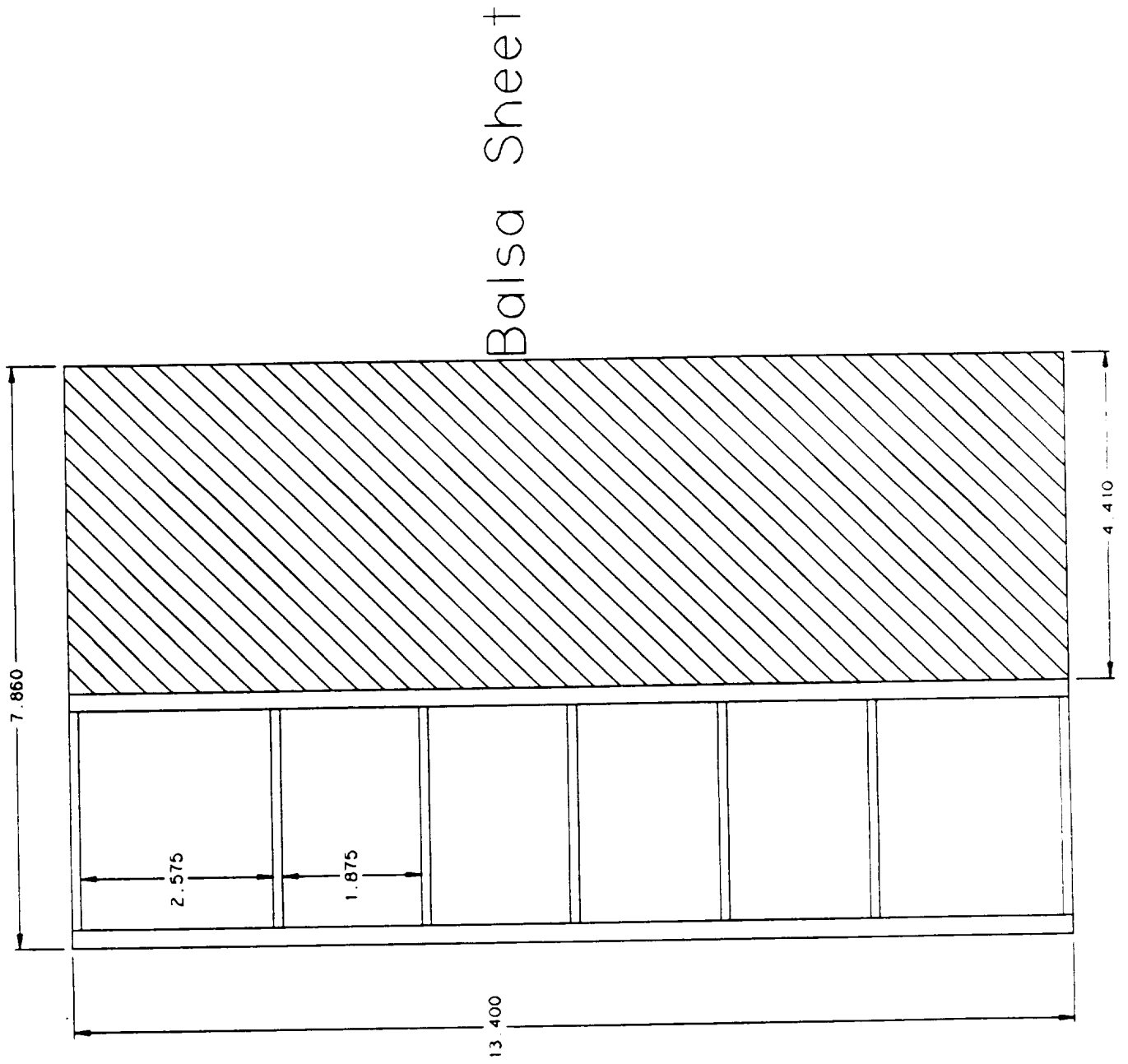


Figure 1.3-2 Horizontal Tail Structure

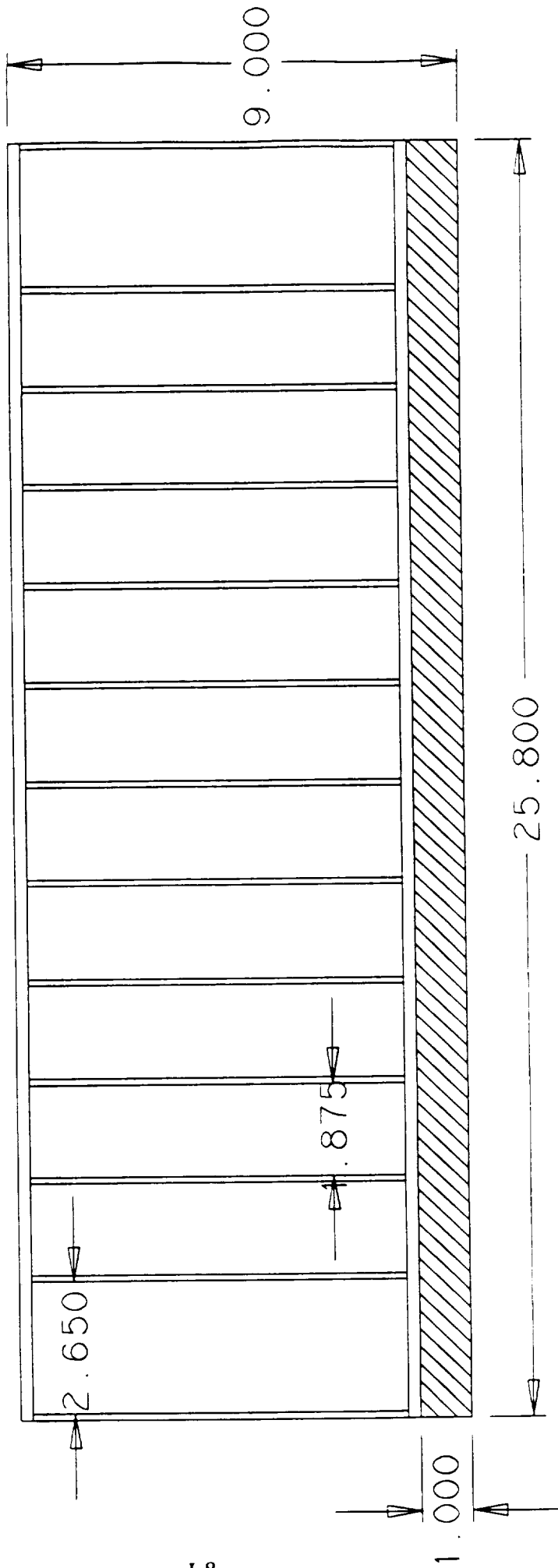
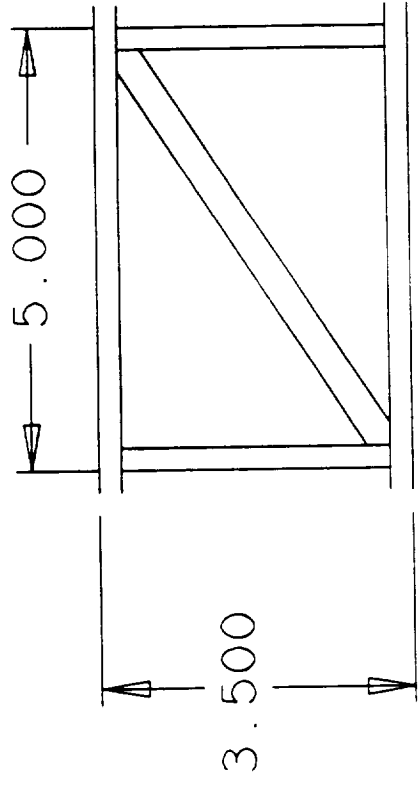
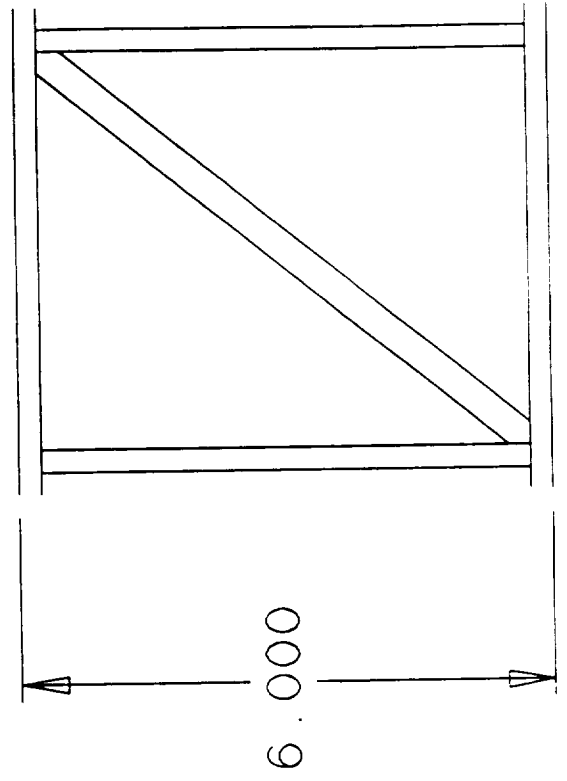


Figure 1.5-2 Fuselage Structure



Spruce Longerons and Spars
Balsa Trusses



J. Economic Analysis

J.1 Introduction and Tabular Summary

The cost efficiency of any aircraft is a chief concern in its design. In Aeroworld, certain economic parameters are defined. Some of these parameters are fixed costs which the engineers cannot influence. The parameters which are capable of being manipulated alter the cost of building, flying and maintaining the aircraft. The following discussions investigate which parameters largely influence the economy of the aircraft and the magnitude of their cost effectiveness. Also, a new type of economic analysis which explores the fuel cost per passenger will be explained and its significance related to the aircraft's payload. Finally, a brief economic comparison with the *HB-40* is presented to end the Economic Analysis.

The Direct Operating Costs (DOC) and the cost per seat per 1000 ft (CPSPK) are defined as follow:

$$\text{DOC} = \text{Depreciation} + \text{Operation} + \text{Fuel Costs}$$

$$\text{CPSPK} = \text{DOC}/(\text{Design Range} * \text{max \#passengers})$$

This section will primarily use CPSPK for cost effective measurement since it is the only comparable economic parameter to the *HB-40*. A tabular summary of the projected costs for the aircraft is presented below. Note how the DOC components are broken into their sub-costs. Operations Costs have limited means to influence its cost (#servos, max#passengers). Because of its nominal influence and lack of manipulative factors it shall not be discussed; but rather, the focus shall be on Depreciation and Fuel Costs.

Table J.1-1 Depreciation Sub-Costs

Man-hours for Project	95
Personnel [\$]	\$950
Tooling [\$]	\$300
Manufacturing [\$]	\$1240

Table J.1-2 Operation Sub-Costs per Flight

Flight Crew [\$]	0.20
Maintenance	0.05

Table J.1-3 Fuel Costs & DOC.

\$/amp hr	\$2.00/amp hr
Fuel Costs [\$]	0.64
Depreciation Costs [\$]	5.33
Operation Costs [\$]	0.25
DOC. [\$]	\$6.18
CPSPK [\$]	0.0061
Cost of the Aircraft	\$1700

J.2 Depreciation Costs: The Economy and Effect of its Components

Depreciation costs embody 85% of the DOC. It is certainly the most significant of the DOC triad. The bulk of Depreciation costs are involved in Manufacturing costs as is seen in Figure J.2-1. The 21% Subsystems cost is fixed which limits cost efficiency to Raw Materials and Manufacturing. A closer look dissects the Manufacturing costs into Tooling and Personnel (Labor) Costs (Figure J.2-2). With a labor rate of \$10.00 per man-hour, the Personnel costs -- which incorporate 76% of the Manufacturing costs -- quickly increase the aircraft's expenses. Tooling costs are based on both the time and frequency of machinery use. This particular cost is difficult to estimate due to lack of manufacturing experience. Estimates for Tooling costs are included in Appendix V.

Figure J.2-1 Depreciation Cost Percentages

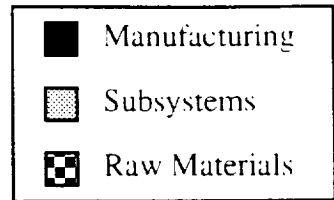
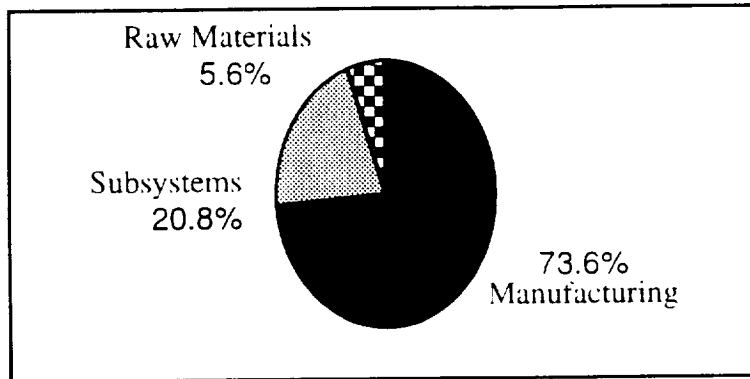
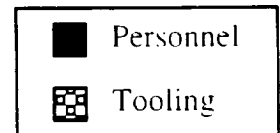
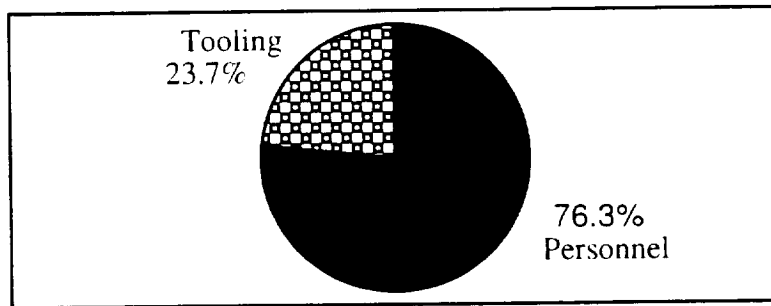


Figure J.2-2 Manufacturing Cost Percentages

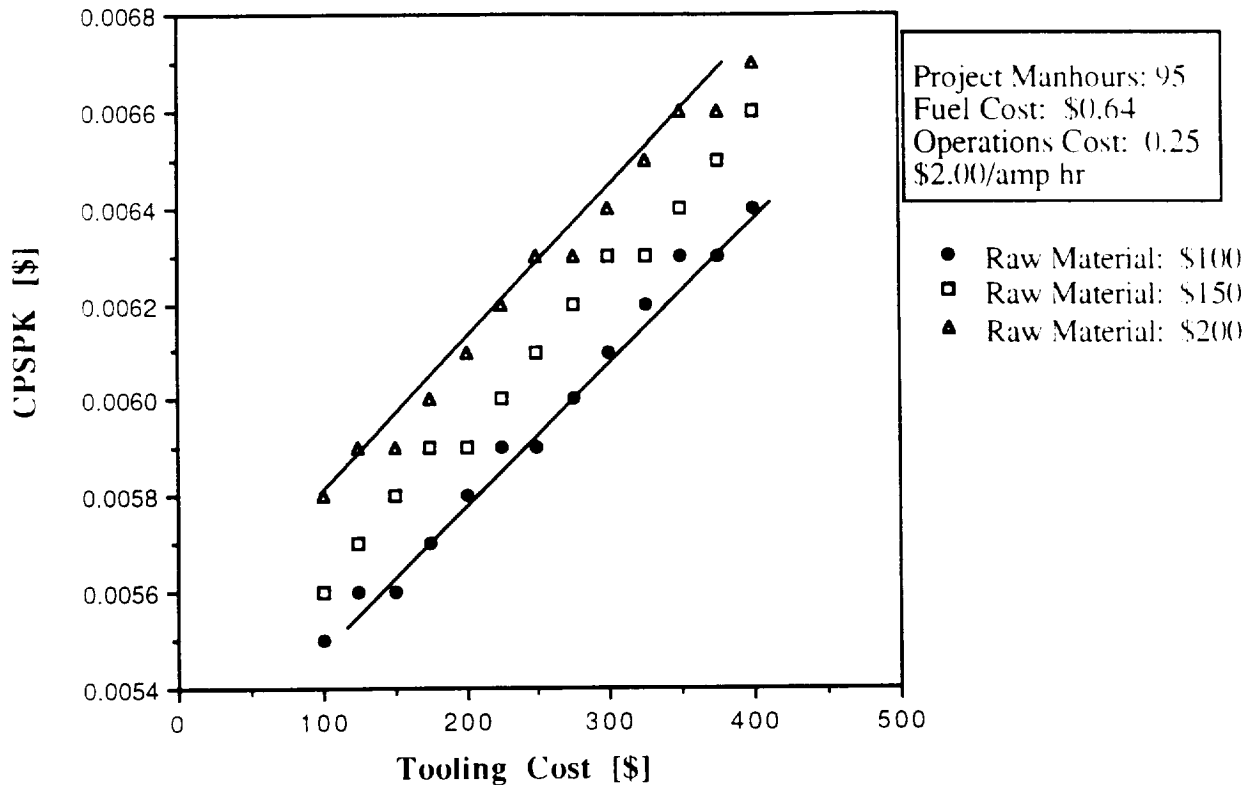


Raw materials are the smallest portion of the Depreciation Costs. Current estimates for material procurement are given in Appendix V; however, the engineer is advised to look up the current costs of materials since Aeroworld is not immune to inflation.

To show the cost effectiveness in the various Depreciation cost components, Figures J.2-3 and J.2-4 plot different values of raw materials cost and project man-hours on a CPSPK versus Tooling cost graph. This type of graph will also be extremely useful when the Technical Demonstrator is completed and will facilitate the assessment of the

related costs. Tooling cost, a difficult cost estimate, can then be quickly located on the graph along with the other respective costs. CPSPK is chosen for the vertical axis since it is the only economic parameter that is comparable with the *HB-40*.

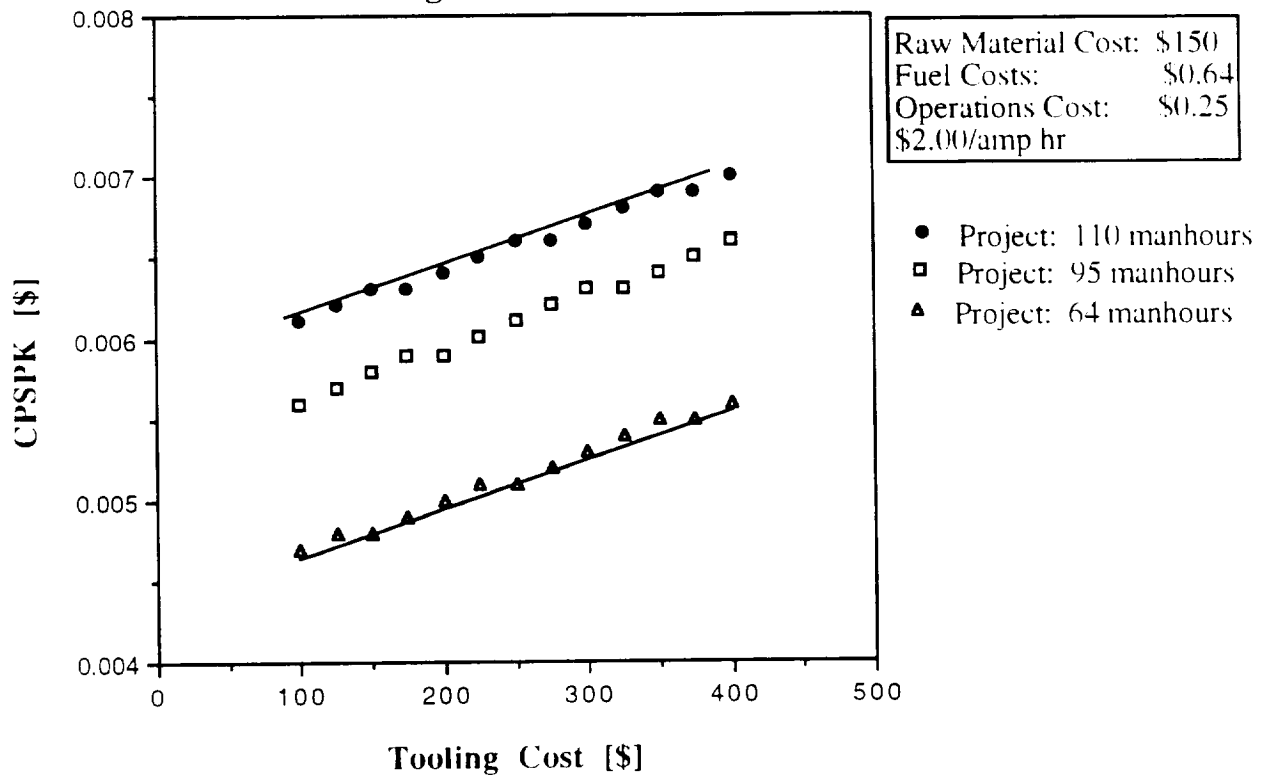
Figure J.2-3: Effect of Tooling Cost and Raw Materials on CPSPK



The effect of changing the Raw Materials cost by \$100 changes the CPSPK by less than 6% (Figure J.2-3). A \$100 increment is a large step to yield such a nominal savings. Again, it should be remembered that Raw Materials make up less than 6% of the Depreciation costs which presents a difficulty in having its cost-efficient presence felt. Personnel costs, however, provide a different story. If each member of a 6 person design team works a little less than 4 hours more per week or better put, approximately 30 minutes more each day (for a 2 week construction period), the CPSPK is increased by nearly 40% (Figure J.2-4). Such a costliness must be respected and methods to achieve cost effectiveness should be employed during construction. Such methods include 1) a detailed set of construction deadlines (e.g. fuselage will be built by . . .), 2) a detailed duty roster which assigns certain members to specific tasks (time spent guessing what to do is money wasted), and 3) precise careful measurements and attention to detail during

construction (fixing a mistake usually takes ten times longer than making it). Employment of these methods will provide an effective way to lower Depreciation costs, the major component of the DOC. A target construction time of 95 man-hours is set for the Technology Demonstrator. This is 5 man-hours below the *HB-40* and should result in an approximate 9% savings on CPSPK.

Figure J.2-4: Effect of Manhours and Tooling Costs on CPSPK

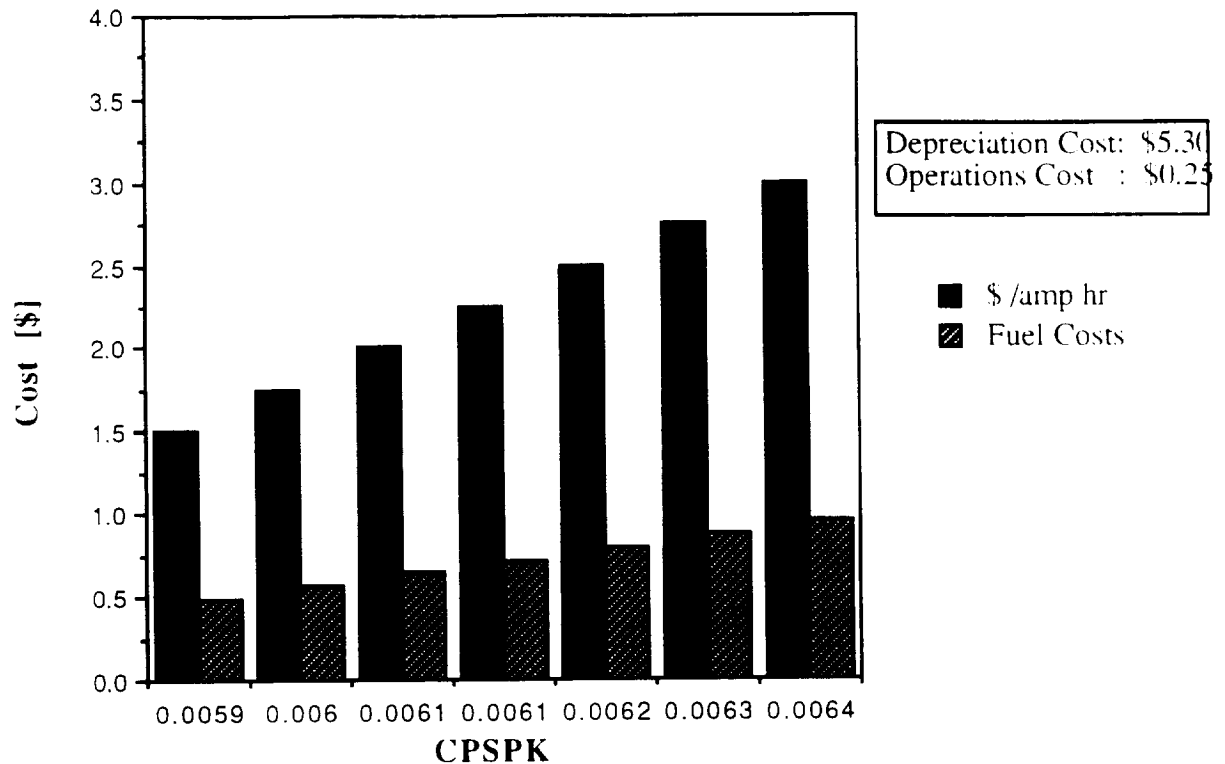


J.3 Fuel Costs: The Effect of Cost/Amp Hr Variation

One economic parameter to which the engineer is subordinate is the Fuel Cost Rate [\$/amp hr]. A similar example of this parameter is price of gasoline for a car (e.g. \$1.19/gallon). The cost can fluctuate from \$1.50/amp hr to \$3.00/amp hr. Fuel costs for the aircraft therefore fluctuate with this rate as does the CPSPK. Notice above in the summary Table J.1-3 that an average \$2.00/amp hr was used to determine the CPSPK of this aircraft. The fuel cost rate at which the *HB-40* calculated its CPSPK, \$0.009, is unknown. Figure J.3-1 relates how even at the most expensive fuel cost rate, \$3.00/amp hr, the *Blue Emu* is more cost efficient in this area by 40% yielding a CPSPK of \$0.0064. One should observe that the fuel costs only rise \$0.48 for a \$1.50/amp hr change in the fuel cost rate. Such an increase might be perceived as insignificant as it changes the

CPSPK by only \$0.0005 for the full range. The significance is only understood when a different type of economic analysis is performed.

Figure J.3-1: Effect of Fuel Cost Rate [\$/amp hr] on Fuel Costs and CPSPK



J.4 Fuel Cost per Passenger

As discussed above, the CPSPK appears to be callous to the fluctuation in the fuel cost rate [\$/amp hr]. So where does this parameter show any significance? To answer this question requires knowledge of the fuel cost per passenger.

The fuel cost per passenger is the product of two ratios. The first is the weight per passenger (wt/psngr) and the second is the fuel costs[\$] per weight. The fuel cost is a function of maximum weight, thereby, the ratio 1.2 oz/passenger would remain constant for any payload. This of course is a falsity since the ratio of weight/passenger will become larger with smaller payload. If this reality is held accountable in Aeroworld, then the true significance of a fluctuating fuel cost rate begins to appear.

Before showing this graphically, it must be understood how this analysis was performed. Below is a succinct, empirical explanation of how the real fuel market is impressed upon Aeroworld.

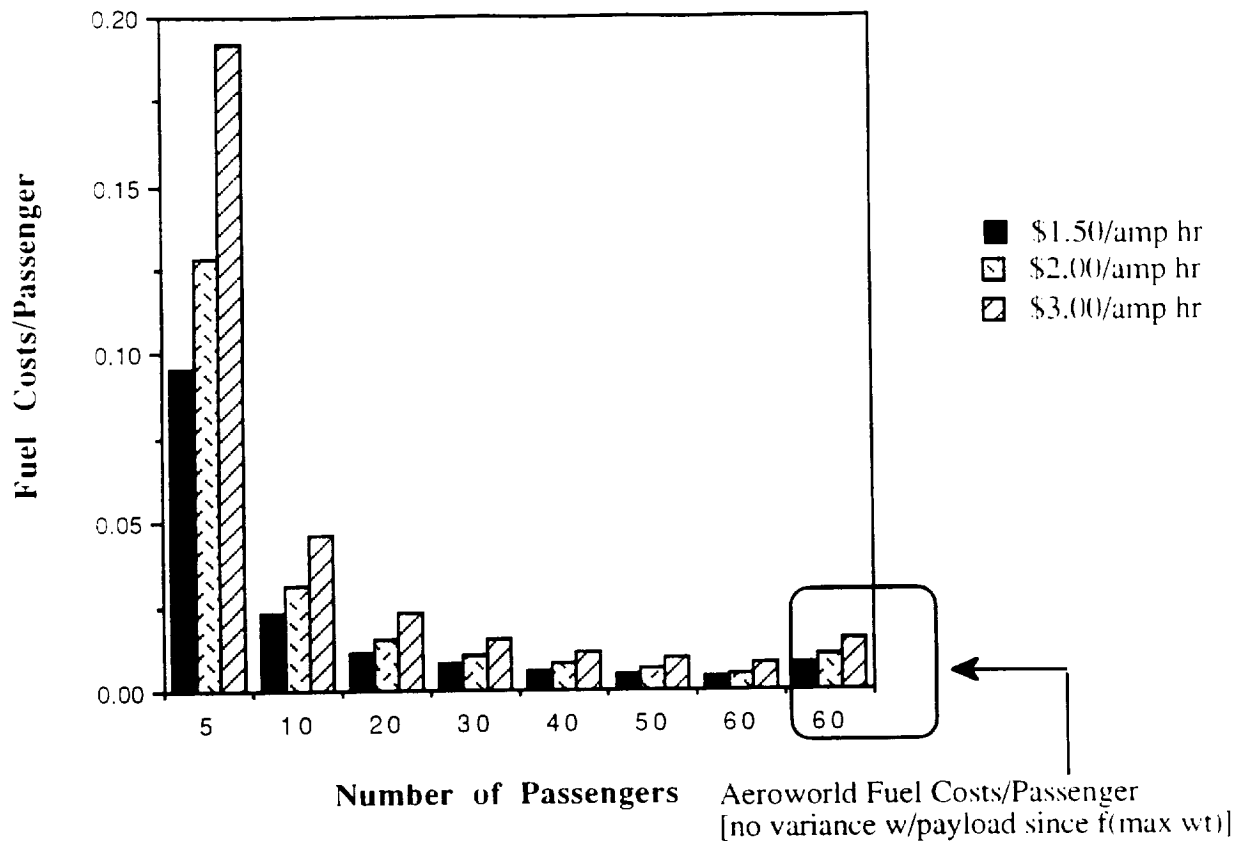
$$\frac{\text{Fuel Costs}}{\text{Passenger}} = \frac{\text{Weight}}{\text{Passenger}} * \frac{\text{Fuel Costs}}{\text{Weight}}$$

$$\frac{\text{Weight}}{\text{Passenger}} = \frac{\text{A/C Weight}}{\# \text{ Passengers}} \quad \text{fixed for Aeroworld, variable in reality}$$

$$\frac{\text{Fuel Costs}}{\text{Weight}} = \frac{\text{max weight} * V_{\text{cruise}} * \text{fuel cost rate } [\$/\text{amp hr}] * \text{flight time}}{\text{L/D} * 1.36 * \text{weight}}$$

Note that the fuel costs/ weight ratio uses the maximum weight in the fuel costs calculation as it is defined in Aeroworld. To compensate for the variance in payload, the weight in the denominator is the real weight. The Aeroworld fuel costs/wt ratio uses the maximum weight in the denominator and the weight/passenger ratio is always 1.2 oz/passenger (this is to yield a Fuel Costs/Passenger ratio for Aeroworld based on maximum weight). This is graphically portrayed in Figure J.4-1 which shows the drastic difference between a low payload flight and an Aeroworld maximum capacity flight, approximately 86% difference at one point! Also, the fuel cost rate [\$/amp hr] becomes less significant as the plane fills up with passengers. This is due to more passengers sharing the cost for the fuel.

Figure J.4-1: Fuel Cost/Passenger as it Varies for Different Payloads & Fuel Costs Rates



Again, the purpose of this analysis was to show that the fuel cost rate [\$/amp hr] is more significant once variation in aircraft weight due to different payloads is accounted for. This was best represented through the determination of the Fuel Costs/Passenger ratio.

J.5 Brief Economic Comparison with HB-40

The *HB-40* was set to a different economical standard than that of the *Blue Emu*. The only true parameter for comparison is the CPSPK for which *Blue Emu* yielded a 32% lower cost. The DOC for the *HB-40* can be determined from the equation in Section J.1. The *HB-40*'s DOC is \$6.12 while the DOC for the *Blue Emu* is \$6.18 at a fuel cost rate of \$2.00/amp hr. This is another complication which obscures comparison of these two aircraft economically. If the less expensive fuel cost rate, \$1.50/amp hr, is chosen to evaluate the DOC, the *Blue Emu* triumphs with a low \$6.02. Below is table which tries to represent some of the disadvantages and advantages of both aircraft and what cost area

is affected by the differences. Again, since the economic standards differ, a more quantitative analysis is difficult.

Table J.5-1 *Blue Emu* and HB-40 Economic Advantages/Disadvantages

Cost	The <i>Blue Emu</i> has
Material Cost	3.5 inch longer fuselage & 26% larger wing
Maintenance Cost	22 more passengers
Fuel Costs	7.09 oz more weight than HB-40
Fuel Costs	has a higher L/D @ cruise
Personnel Cost	targeted 5 less man-hours

The *Blue Emu* is a larger aircraft, therefore, material cost will be higher than its competitor. However, as discussed earlier, the material cost requires a \$100 difference to change the CPSPK by only 6%. Therefore, material cost will not be a significant disadvantage to the *Blue Emu*.

Maintenance cost is higher than the *HB-40* due to the larger number of passengers. In the DOC triad, maintenance cost is a subcost of Operations Cost. Operations Cost embodies only 4% of the DOC and therefore is not a significant enough factor to decrease the cost efficiency of the aircraft. The fuel costs is a function of current draw. Current draw is calculated by multiplying a constant with the ratio maximum weight/(Lift/Drag)_{cruise}. The competitor has a lower weight but also a lower L/D of approximately 12. The *Blue Emu*'s L/D is slightly over 16 which translates into a 17% savings on fuel cost. All equations for the various costs are included in Appendix V.

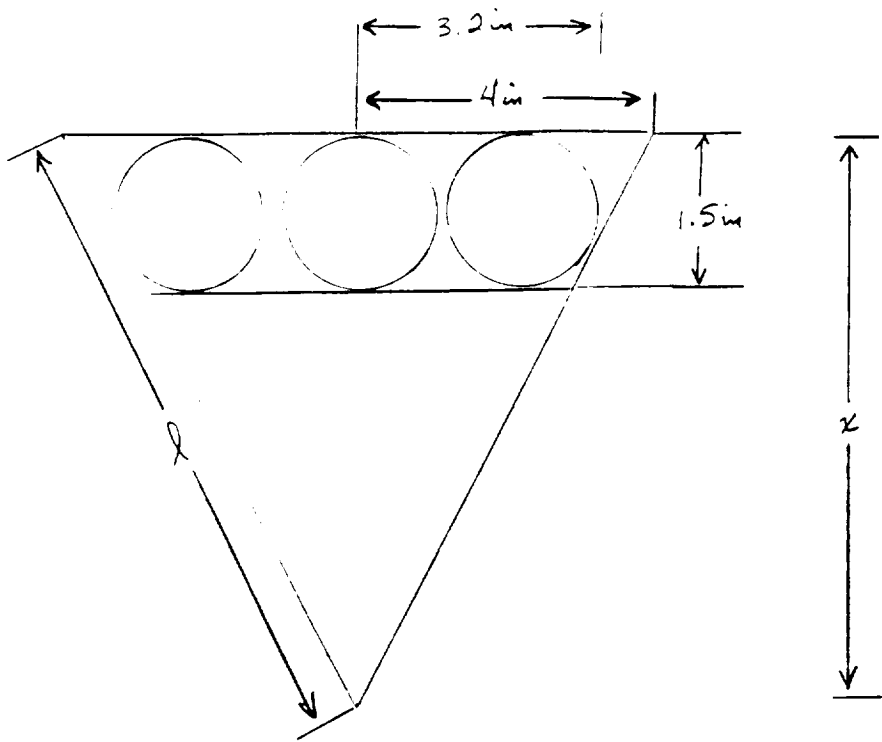
The *Blue Emu* is a more cost efficient aircraft. Cost efficiency is achieved through employment of efficient labor methods for low personnel cost and attaining good aerodynamic performance (L/D) to reduce fuel costs.

K. References

- 1) Anderson, John D., Fundamental of Aerodynamics, McGraw-Hill, New York, 1991, pp. 153-390.
- 2) Batill, Steven, TAKEOFF, computer program, University of Notre Dame, 1991
- 3) Dunn, Patrick F., "AE454 Lecture Notes", Notre Dame, Indiana, 1992.
- 4) Hoerner, Sighard F., Fluid-Dynamic Drag, 1958, p. 13-14.
- 5) Jensen, Daniel T., "A Drag Prediction Methodology For Low Reynolds Number Flight Vehicles", Master's Thesis, University of Notre Dame, pp. 17-31.
- 6) McCormick, Barnes J., Aerodynamics, Aeronautics, and Flight Mechanics, Wiley and Sons, New York, 1979, pp. 61-235, 477-605.
- 7) Nelson, Robert C., Flight Stability and Automatic Control, McGraw-Hill, New York, 1989, pp. 39-172.
- 8) Selig, Michael; Donovan, John F. and Fraser, David B., Airfoils at Low Speeds, H. A. Stokely Publisher, Virginia, 1989.
- 9) Young, Barry, PROPELLER, computer program, University of Notre Dame, 1991.
- 10) AE441 Lecture Notes

APPENDICES

Appendix I. Concept Selections



$$\frac{x}{4} = \frac{1.5}{0.8} \rightarrow x = \frac{1.5(4)}{0.8}$$

$$x = 7.5 \text{ in}$$

$$l = \sqrt{x^2 + 4^2}$$

$$= \sqrt{(7.5)^2 + 4^2}$$

$$l = 8.5 \text{ in}$$

Appendix II. Aerodynamics

METHOD II

$$\overline{C_{D_0}} = \sum \frac{C_{D_0} FF_{\pi} S_{wet, \pi}}{S_{ref}}$$

$$C_{D_0} = \frac{1.328}{\sqrt{Re_{\pi}}}$$

$$FF_{\pi} = \left[1.0 + \frac{0.6}{(x/c)} \left(\frac{t}{c}\right) + 100 \left(\frac{t}{c}\right)^4 \right] \left[1.34 m^{0.18} \right]$$

FUSELAGE

$$l = 4.9 \text{ ft}$$

$$S_{wet} = 7.99 \text{ ft}^2$$

$$C_{D_0} = \frac{(2.62 \text{ ft})(.00304) + (2.28 \text{ ft})(.00620)}{4.9 \text{ ft}^2}$$

$$= \underline{0.00452}$$

$$FF_{\pi} = \left(1.0 + \frac{60}{(9.64)^2} + \frac{9.64}{400} \right)$$

$$= \underline{1.091}$$

$$C_{D_0 \text{ fuse}} = \frac{(0.00452)(1.091)(7.99 \text{ ft}^2)}{10 \text{ ft}^2}$$

$$= \underline{0.00394}$$

HORIZONTAL TAIL

$$Re = 1.908 \times 10^5 c$$

$$= 1.43 \times 10^5$$

$$C_f = \frac{1.328}{\sqrt{1.43 \times 10^5}}$$

$$C_{D_0} = \underline{0.0035}$$

$$FF_{\pi} = \left[1.0 + \frac{.6}{.25} \left(\frac{.25}{9}\right) + 100 \left(\frac{.25}{9}\right)^4 \right] \left[1.34 (.027)^{0.18} \right]$$

$$FF_{\pi} = \underline{0.746}$$

$$S_{wet, \pi} = 3.226 \text{ ft}^2$$

$$C_{D_0, HT} = \frac{(0.0035)(0.746)(3.226 \text{ ft}^2)}{10 \text{ ft}^2}$$

$$C_{D_0, HT} = \underline{0.000855}$$

$$Re = 1.908 \times 10^5$$

$$= 1.25 \times 10^5$$

$$C_D = \sqrt{1.25 \times 10^5}$$

$$C_{D_T} = 3.00376$$

$$S_{wet_T} = 1.362 \text{ ft}^2$$

$$FF_T = \left[1.0 + \frac{.6}{.35} \left(\frac{.25}{7.86} \right) + 100 \left(\frac{.25}{7.86} \right)^4 \right] \left[1.34 (.027)^{2.18} \right]$$

$$FF_T = 3.752$$

$$C_{D_{VT}} = \frac{(3.00376)(3.752)(1.362 \text{ ft}^2)}{10 \text{ ft}^2}$$

$$C_{D_{VT}} = 3.00385$$

LANDING GEAR

$$\text{WHEEL} \Rightarrow C_D = \frac{C_{D_T} A_T}{S_{ref}}$$

$$C_{D_T} = 0.12$$

$$A_T = 0.013 \text{ ft}^2$$

$$C_D = \frac{(0.12)(0.013 \text{ ft}^2)}{10 \text{ ft}^2}$$

$$C_D = 0.00156 / \text{wheel}$$

STRUT

$$C_{D_T} = 0.25$$

$$A_T = 0.006 \text{ ft}^2$$

$$C_D = \frac{(0.25)(0.006 \text{ ft}^2)}{10 \text{ ft}^2}$$

$$C_D = 0.000152 / \text{strut}$$

$$C_{D_0} = 3.006104 + C_{D_{wing}}$$

$$= 3.006104 + .007$$

$$= 3.013104 (1.15)$$

→ interference

$$C_{D_0} = 3.0151$$

$$\frac{1}{e} = \frac{1}{e_{\text{wind}}} + \frac{1}{e_{\text{body}}}$$

$$\bar{E}_{\text{body}} = e_{\text{body}} \frac{S_{\text{body}}}{S_{\text{ref}}} \Rightarrow e_{\text{body}} = \bar{E}_{\text{body}} \frac{S_{\text{ref}}}{S_{\text{body}}}$$

$$= \frac{(0.5 \times 10)}{0.148}$$

$$e_{\text{body}} = 33.78$$

$$\frac{1}{e} = \frac{1}{.85} + \frac{1}{33.78}$$

$$e = 0.829$$

Appendix III. Stability and Control

Code to find horizontal tail span and chord that would satisfy our neutral point requirement of $.5c$

```
real cma(99,99),xnp(99,99),lv(99),clah(99,99),cp(99,99),vh(99,99)
real cmde(99,99),arh(99,99),sh(99,99),sv(99,99),ch(99),bh(99,99)
```

```
b = 10
c = 1.0
sw = b*c
ar = b/c
tap = .6
xac = .25
xcg = .3
claw = 5.1
cmaf = .022
deda = 2*claw/(3.14*ar)
dih = .0872
```

Begin loops to vary chord, span and dist. to tail (Horz.)

```
do 5 i=1,26
  ch(i) = .5+.01*(i-1)
do 10 j=1,11
  bh(i,j) = 2.0+.05*(j-1)
arh(i,j)=bh(i,j)/ch(i)
sh(i,j)=bh(i,j)*ch(i)
clah(i,j) = (6.14*arh(i,j))/(2+arh(i,j))
lv(i)=(40-.75*ch(i))/12
vh(i,j) = lv(i)*sh(i,j)/(sw*c)
```

Horizontal Tail Surface

Pitching moment due to a.o.a. (neg. stable)

```
cma(i,j) = claw*(xcg-xac)+cmaf-vh(i,j)*clah(i,j)*(1-deda)
```

Position of neutral point ($\sim .5c$)

```
xnp(i,j) = xac-(cmaf/claw)+vh(i,j)*(clah(i,j)/claw)*(1-deda)
cp(i,j) = vh(i,j)*clah(i,j)
```

```
10 continue
5 continue
```

```
write(*,*) 'Horizontal Tail Results'
```

```
write(*,*) 'Cma          Neutral Point          b          c'
```

```
do 35 l=1,26
```

```
do 40 m=1,11
```

```
write(*,*) cma(l,m),xnp(l,m),bh(l,m),ch(l),sh(l,m),vh(l,m),cp(l,m)
```

```
40 continue
```

```
35 continue
```

```
stop
```

```
end
```

Appendix III

Code to find relationship between elevator size, deflection and the incidence of the tail and wing

```

program incidence
real iw(99),tau(99,99,99),de(99,99,99),it(99,99),cmot(99,99,99)
real cmo(99,99,99)

```

```

open(220,file='wing0')
open(221,file='wing1')
open(222,file='wing4')
open(223,file='wing5')
open(224,file='wing6')
open(225,file='wing7')

```

```

cmof = -.00039
cmow = -.024
vh = .53
clat = .068
eo = 1.95
cma = -.0187
do 10 i=1,8
    iw(i) = 0+(i-1)
do 20 j=1,9
    it(i,j) = 0.0+(j-1)
do 30 k=1,15
    tau(i,j,k) = .15+.025*(k-1)
cmot(i,j,k) = vh*clat*(eo+iw(i)-it(i,j))
cmo(i,j,k) = cmot(i,j,k)+cmof+cmow
de(i,j,k) = cmo(i,j,k)/(vh*clat*tau(i,j,k))
30 continue
20 continue
10 continue

```

```

do 40 l=1,9
do 50 m=1,15
write(220,*) tau(1,l,m),de(1,l,m)
write(221,*) tau(2,l,m),de(2,l,m)
write(222,*) tau(3,l,m),de(3,l,m)
write(223,*) tau(4,l,m),de(4,l,m)
write(224,*) tau(5,l,m),de(5,l,m)
write(225,*) tau(6,l,m),de(6,l,m)
50 continue
40 continue

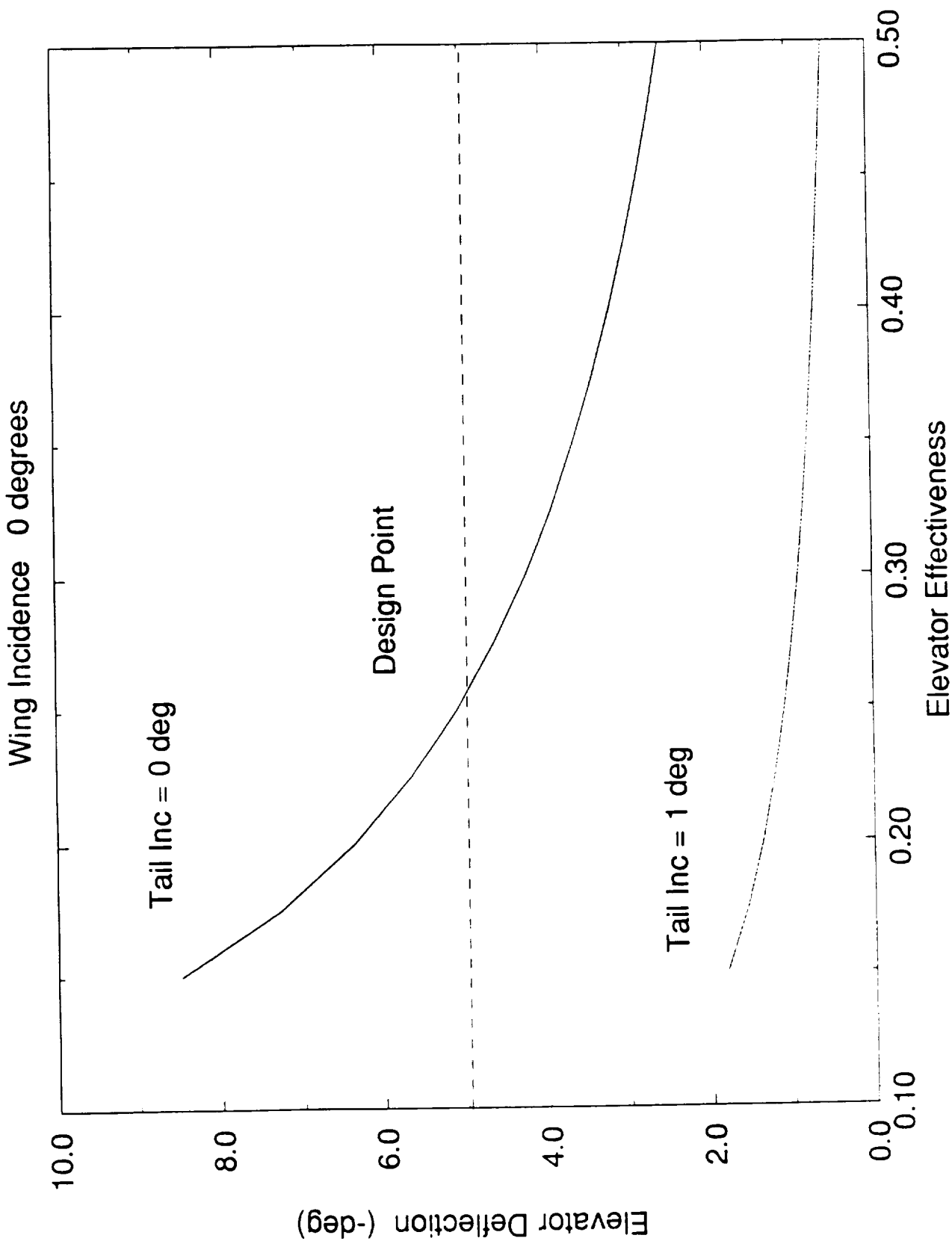
```

```

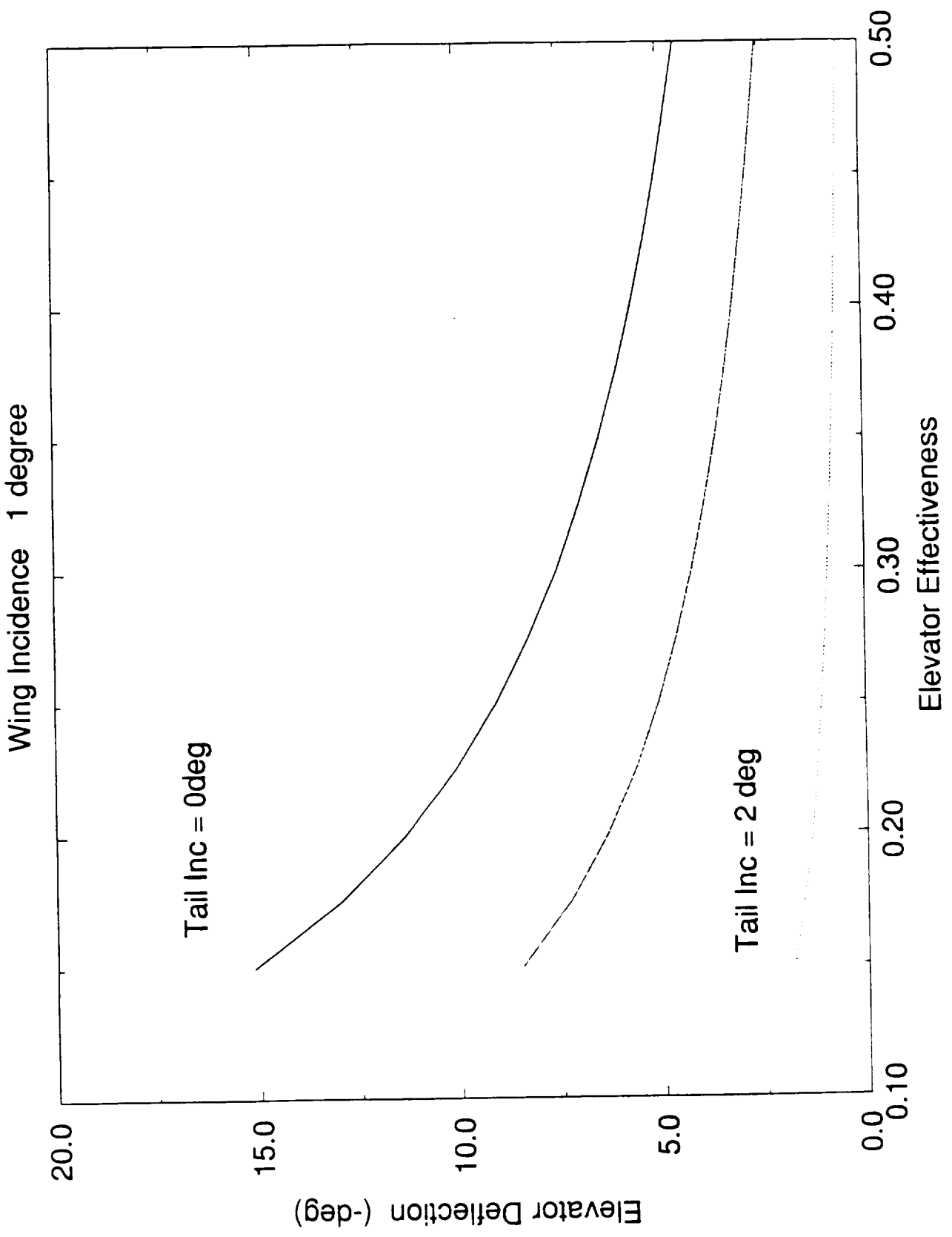
close(220)
close(221)
close(222)
close(223)
close(224)
close(225)
stop
end

```

Appendix III -- Figure 1



Appendix III -- Figure 2



Appendix IV. Performance

Eqn. H.1-1

$$X_{gr} = [1.44/(g.r.Cl_{max})].(W/S)/[T_o/W - m]$$

$$Cl_{max} = 1.1$$

$$T_o = 2.8 \text{ lbf}$$

$$m = 0.15$$

Eqn. H.1-2

$$T_o/W = [1.44/(\rho g C_{Lmax})]*[(W/S)/X_{gr}] + \mu$$

Eqn. H.1-3

Referenced from the *Prime Mover*

$$X_L = W/(g.2B). \ln[1 + (B/A).V_{TD}^2]$$

$$A = m.W$$

$$B = C_D.(1/2).r.S \quad (C_D = 0.0673)$$

$$V_{TD} \sim V_{stall} = 22.0 \text{ ft/sec.}$$

$$W = 5.6 \text{ lbf}$$

$$X_{Landing} = 41.2 \text{ ft.}$$

Eqn. H.1-4

$$\text{Landing distance} = (1.69 W^2)/(r.g.S.Cl_{max}.[D + m(W - L)])$$

Reference

Anderson, John D. Introduction to Flight. New York: McGraw-Hill 1985,
pg.306 - 311

Appendix V. Economics

I. The DOC Network

$$\begin{array}{c}
 \text{DOC} = \\
 \text{Depreciation} + \text{Operation} + \text{Fuel Costs} \\
 \left| \qquad \qquad \qquad \right| \qquad \qquad \qquad \left| \qquad \qquad \qquad \right| \\
 \text{cost per a/c} / \# \text{flights in life} \quad \text{flt crew} + \text{maintenance} \quad \text{crnt draw} * \text{FAC3} * \text{flt time} \\
 \left| \qquad \qquad \qquad \right| \qquad \qquad \qquad \left| \qquad \qquad \qquad \right| \\
 \qquad \qquad \qquad 50(\text{hrs}) / \text{flight time} \quad \text{max\# pas} * \text{flt tm} * \text{FAC2} \\
 \left| \qquad \qquad \qquad \right| \qquad \qquad \qquad \left| \qquad \qquad \qquad \right| \\
 \text{fixed+materials+manufacturing} \quad \# \text{servos} * \text{FAC1} \quad \text{max wt} * \text{cruise spd} / (\text{L/D}) * 1.36 \\
 \left| \qquad \qquad \qquad \right| \\
 \text{personnel + tooling}
 \end{array}$$

* note: FAC1,2,3 are constants given

II. Fixed Systems Cost

Fixed Subsystems

a.	Radio Transmitter	\$ 75
b.	Radio Receiver	\$ 35
c.	Avionics Battery	\$ 10
d.	Switch Harness	\$ 5
e.	Miniature Servo	\$ 35
f.	Electronic Speed Control	\$ 50
g.	Astro 15 geared	\$107
h.	NiCad batteries(11)	\$ 33
i.	Motor power wiring	\$2/ft

III. Manufacturing Rates

Personnel	\$10/man-hour	
Tooling	TURN ON	\$/MIN
1) Large band saw	\$10	2.00
2) Large scroll saw	\$ 1	0.25
3) Small scroll saw	\$0.5	0.10
4) Drill press	\$ 1	0.10
5) Sander	\$0.25	0.25
6) Monokote Iron	\$0.00	0.25

IV. Raw Material Estimates

Balsa ~ \$0.16/in ³	project estimate ~ \$26.00
Bass/Spruce ~ \$0.28/in ³	
Beams ~ \$0.16/in ³	project estimate ~ \$10.00
Glue ~ \$15.00	
Monokote ~ \$20.00	
Gear ~ \$3.00	

V. Tooling Cost Estimates

1) Large band saw	\$90
2) Large scroll saw	\$93
3) Small scroll saw	\$25
4) Drill press	\$13
5) Sander	\$13
6) Monokote Iron	\$60

Appendix VI

Manufacturing Plan & Review

VI.1. Introduction

After all the analytical calculations and engineering predictions have been given and recorded, the challenge of producing a three-dimensional product from two-dimensional numbers and drawings presents itself. If there is an engineer who has experience in such an area, she or he is a vital resource. However, if this is the first confrontation with manufacturing, this appendix will serve as a guideline on methods which were employed for the construction of *the Blue Emu*. First, the primary structural components will be discussed; as will the sequence and methods for their fabrication and assembly. Tactics for keeping good manufacturing schedules and labor records will then be suggested. Finally, plans for accounting and control of costs are examined along with the risk of surplus material versus disposal cost.

VI.2 Primary Structural Components

The fuselage, empennage and the wing certainly come to the forefront of one's thoughts when discussing primary structural components. However, the details of the wing and fuselage become more complex as these large structures are broken down into sub-structures. For example, the fuselage is not simply a long box; rather, it has three sections: 1) cockpit 2) cabin and 3) fuselage-empennage. The wing has both the main planform area on the left and right as well as a carry-through structure.

Careful planning and material predictions are crucial for both an understanding of how the manufacturing will be accomplished and, more importantly, procurement of the needed materials. Below, Table VI.2-1 summarizes structural material predictions needed to construct the primary structural components. The fuselage and wing structures are presented schematically in the blue-prints which will be used for construction. Reference Figures I.3-1 and Figure I.3-2 to remember the structure of the vertical and horizontal tail.

Table VI.2-1 Primary Structural Components

Fuselage	Structural Material Predictions
Cockpit	1/4" x 1/4" Spruce: 17 inches
Cabin	1/4" x 1/4" Spruce: 400 inches 3/16" x 1/8" Balsa: 220 inches 1/16" Balsa sheet : 545 sq inches
Empennage (minus v. and h. tail)	1/4" x 3/8" Spruce: 74 inches **
Wing	
Planform, left & right	1/16" Birch sheet: 270 sq inches 1/16" Balsa sheet: 360 sq inches 1/4" x 3/8" Balsa: 480 inches ** 1/4" x 1" Balsa Trailing Edge 1/2' x 3/8" Balsa Leading Edge
Carry-through Structure	1/4" diameter dowel: 15 inches 1/16" Balsa sheet: 170 sq inches 1/4" x 1/4" Spruce: 12 inches 1/4" x 3/8" Spruce: 13 inches 4 rubber bands
Empennage	
Horizontal Tail	1/16" Balsa: 52 sq inches 3/16" x 1/8" Balsa: 104 inches 1/4" x 1/4" Spruce: 52 inches
Vertical Tail	1/16" Balsa: 119 sq inches 3/16" x 1/8" Balsa: 28 inches 1/4" x 1/4" Spruce: 28 inches

The items which are preceded by a double asterix denote those materials which were procured but not specified in the original design. Such adaptability is necessary when the source of material is limited. Fortunately, most of the materials were procured early enough in advance that such complications were limited to only two occurrences. In the case fo the spar caps for the wing, the substitutions involved using a lighter material, balsa in place of spruce. This balsa-for-spruce substitution was also accompanied by an increase in original cross-section of 1/8". Strength and structural integrity is not as much a concern since the basa spar caps will be reinforced by birch

spar webs. The major concern is how this lighter material will affect the center of gravity of the aircraft. As of yet, no new calculations in this regard have been done; however, the variability of the battery pack position along with the increased weight of the wing's carry-through will hopefully keep this material alteration and its resulting c.g. affects to a minimal significance.

The primary structural components and their respective materials have been discussed. Complications arise when questions concerning a) structural discontinuity (what to do if material is not long enough -- e.g. a 10 ft wing spar cap is not available) or b) the connection of cabin to the empennage, or c) the employment of dihedral, and d) methods of mounting the high-wing. The blueprints for the fuselage and the wing structure are most crucial sources of information concerning the manufacturing of these primary structural components. Well drawn and planned out blueprints are the bridge between thoughts and a real product. A discussion on the sequence and methods of assembly follows next.

VI.3 Sequence and Methods of Assembly & Fabrication

The advantage of using a high-wing design is the opportunity it presents to build the primary structural components separately and then bring them together for the final product: the technology demonstrator. Three separate manufacturing teams will be assigned to the three primary structural components. In a sense, the teams will specialize in the manufacturing of their component, yet still communicate openly with the other teams to make sure that the integration of the three separate components is possible. Therefore, the sequence of primary structural components is obscured by the opportunity for their separate construction. What is not obscured sequentially are the methods of assembly, i.e. cutting, cementing, Monokoting. The order of these operations are examined now with a special interest in cutting the raw materials.

Construction demands the cutting of the truss members, airfoils and control surfaces to the required sizes. Therefore, a detailed and complete cutting order must be supplied to the manufacturers. Remember, there is a limited amount of material so the "measure twice and cut once" philosophy is the most favorable and wise advice given. On the blueprints of the primary structural material are *Structural Material/Cuts Orders*. These orders inform the laborer the material to cut, amount to cut and what excess remains. Below is an example which is used for the fuselage cabin.

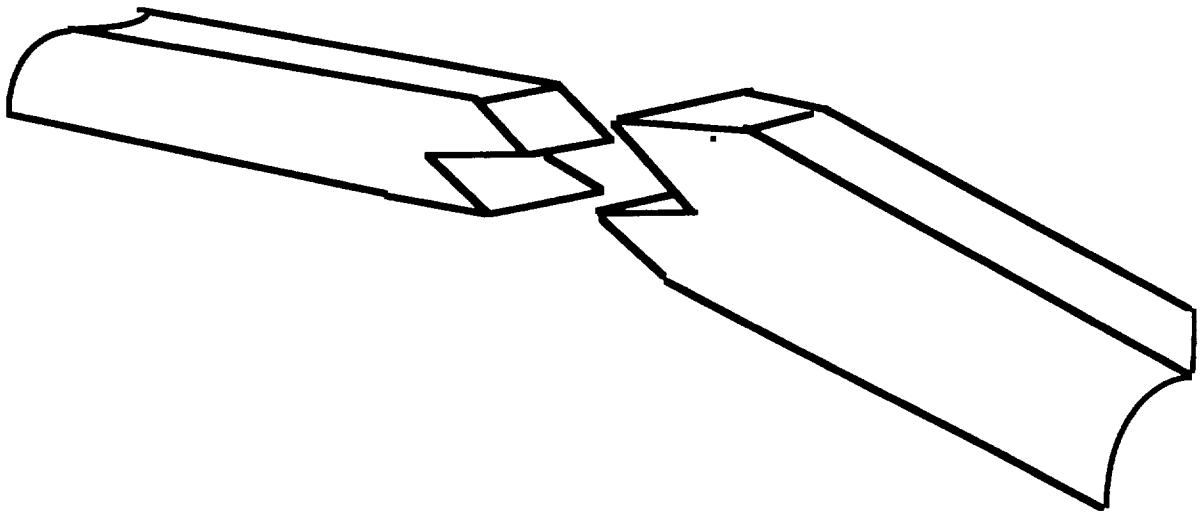
Table VI.3 - 1 Sample of *Structural Material/ Cut Order*

* 1/4" x 1/4" Spruce			
i)	2 uncut,	36"	2 beams
ii)	2 cut,	10.5"	
	5 cut,	3.0"	1 beam
iii)	12 cut,	3.0"	1 beam
iv)	5 cut,	3.0"	
	3 cut,	5.6"	1 beam (with 4.2" left over)
v)	6 cut,	5.6"	{ 1 beam x 3 }
	[18 cuts,	5.6"	3 beams (with 2.4 " left over/ beam)]
vi)	1 cut,	5.6"	1 beam (with 30.4" left over)
46 cuts total			9 beams total

The above example is only for 1/4" x 1/4" spruce and a similar cut order follows for 3/16"x1/8" balsa and the 1/16" balsa sheet. The demand and necessity for manufacturing planning becomes first apparent when faced with the challenge of procuring the materials and secondly when manipulation of those limited materials is required to start construction. Once the cutting is finished, the task of assembling the cut materials presents itself.

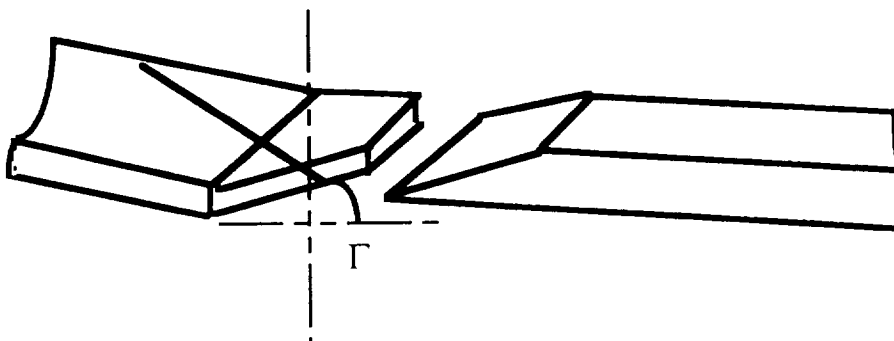
One area of particular interest is structural discontinuity. In other words, what is to be done if it is impossible to procure a solid 10 foot piece of balsa (which it is in most cases) and shorter segments must be combined. A method of assembly must be determined which will best present a solution. One possible solution, which will be used for the construction of this technology demonstrator, is to join the discontinuity with a tongue in groove joint. Figure VI.3-1 illustrates such a joint. Cut orders must compensate if such a technique is employed to combine structural discontinuities.

**Figure VI.3-1 Tongue in Groove Joint:
Solution for Structural Discontinuity**



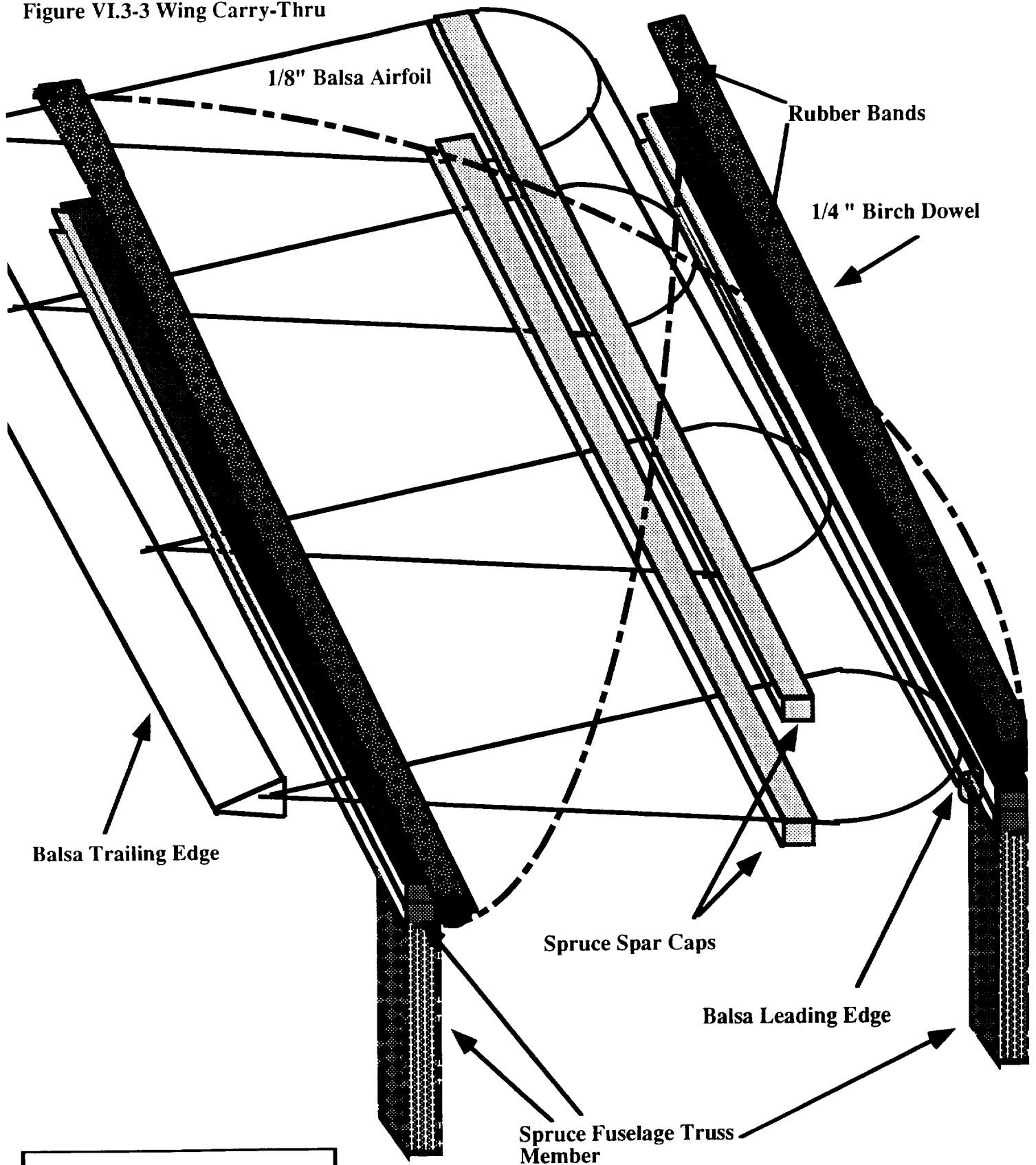
By increasing the surface area for adhesion, the strength of the bond increases. Another method is to glue the two surface along a an angle cut where they would join. The same principle is involved here as well. Combination of the fuselage-cabin to the fuselage-empennage will employ the latter technique so as to yield a tapering effect as well as a joint. Likewise, dihedral is acheived through the same technique (Figure VI.3-2). To reinforce the joint, right triangles cut from 1/32" birch plywood can attached bridging the discontinuity.

**Figure VI.3-2 Assembling Truss Members at Angles:
Solution for Dihedral and Empennage/Cabin Combination**



A method of assembly for employing dihedral will use the technique of cementing along an angle as mentioned above. The carry-through structure will rest flat on top of the fuselage cabin (Figure VI.3-3).. As a result, the airfoils will have to be cut with flat bottoms. To increase the structural integrity of this section, the 4 airfoils will be two-ply

Figure VI.3-3 Wing Carry-Thru



Not Pictured:

- 1) 1/16" Balsa sheet over top
- 2) 1/32" Birch spar webs

1/16" balsa [resulting in 1/8" airfoil]. In addition, the balsa spar caps of the left and right planforms will attach to 1/4" x 3/8" spruce carry-through spars. Birch spar webs will also aid in strengthening this section.

The wing will be mounted via a crossing pattern of rubber bands over the carry-through structure which will "tie off" to four protruding 1/4" diameter birch dowels. Figure VI.3-3 illustrates this method of assembly. In order to strengthen the top surface of the carry-through from any stresses which might be imparted upon it by the rubber bands, a 1/16" balsa sheet will cover the top surface of the carry through and provide it with a substantial shape and form. Each dowel will be attached to two spruce truss members which run transversely across the fuselage near the leading and trailing edges of the wing. The blueprints again will be most helpful in assisting construction.

The importance of a blueprint cannot be over stressed. The blueprint should contain an enlarged, detailed scaled drawing of the primary or sub-structural component. A *structural material/cuts order* as well as a tool and material list should be included on the blueprint. This informs the laborers of everything they need to manufacture the component properly. Also, balloon-windows which enlarge complicated or detailed areas should be included on the blueprint. The key to manufacturing is communication and an effective tool for communication is through a blueprint. It is the bridge between a two-dimensional idea and a three-dimensional product.

Most, but not all of the manufacturing material will be used and the cost for its disposal must be addressed. The following section evaluates both the impact of disposal cost and the risk of buying materials during construction at an expensive rate.

VI.4 Economics of Manufacturing

The importance of keeping good records is true in many different ventures or situations. In manufacturing accurate records are vital for economic considerations which include tooling and personnel costs as well as raw materials cost. As mentioned in Section J of the proposal these costs are included Depreciation costs which embody 85% of the DOC. Therefore, the more accurate the records kept, the more accurate and credible will be the final DOC.

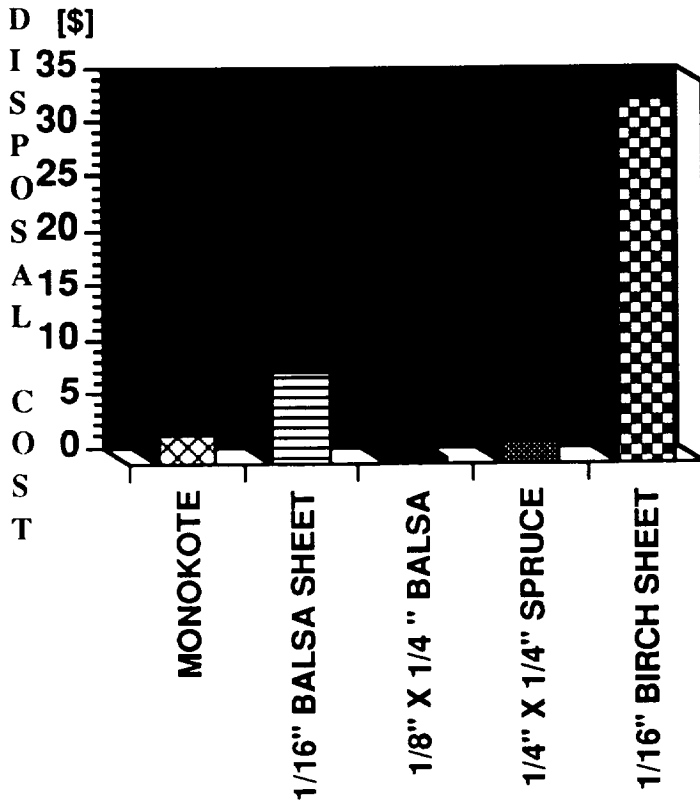
Tooling and labor costs are based upon timely rates, e.g. \$10/man-hour. A suggested method for this type of record keeping is to have a clipboard available at the work sight. On this clipboard will be a chart which looks as follows:

NAME	TIME IN	TIME OUT	TOOL	#turn ons/time
Ken Novak	1700 hrs	1800 hrs	lg band saw	2/ 25 minutes

Thus both the tooling and personnel costs can be accounted for on one table. Scheduling the specific laborers to specific times is most difficult without knowledge of their available times. It is to be certain that once the available times of all the laborers is known, some sort of regimen will be developed so as to guide the manufacturing to completion and take advantage of the most work-efficient times of the laborer.

The DOC is not only affected by tooling, personnel and raw materials cost but disposal cost as well. Disposal cost is to be accounted for as well as the penalty for buying materials during manufacturing (3 times the cost penalty). Below, Figure VI.4-1 shows the effect of buying 1 square foot or 1 foot more of the various materials. The disposal cost rate of \$10/oz makes the penalty more significant the heavier the material.

Figure VI.4-1 "What's One More Foot?"

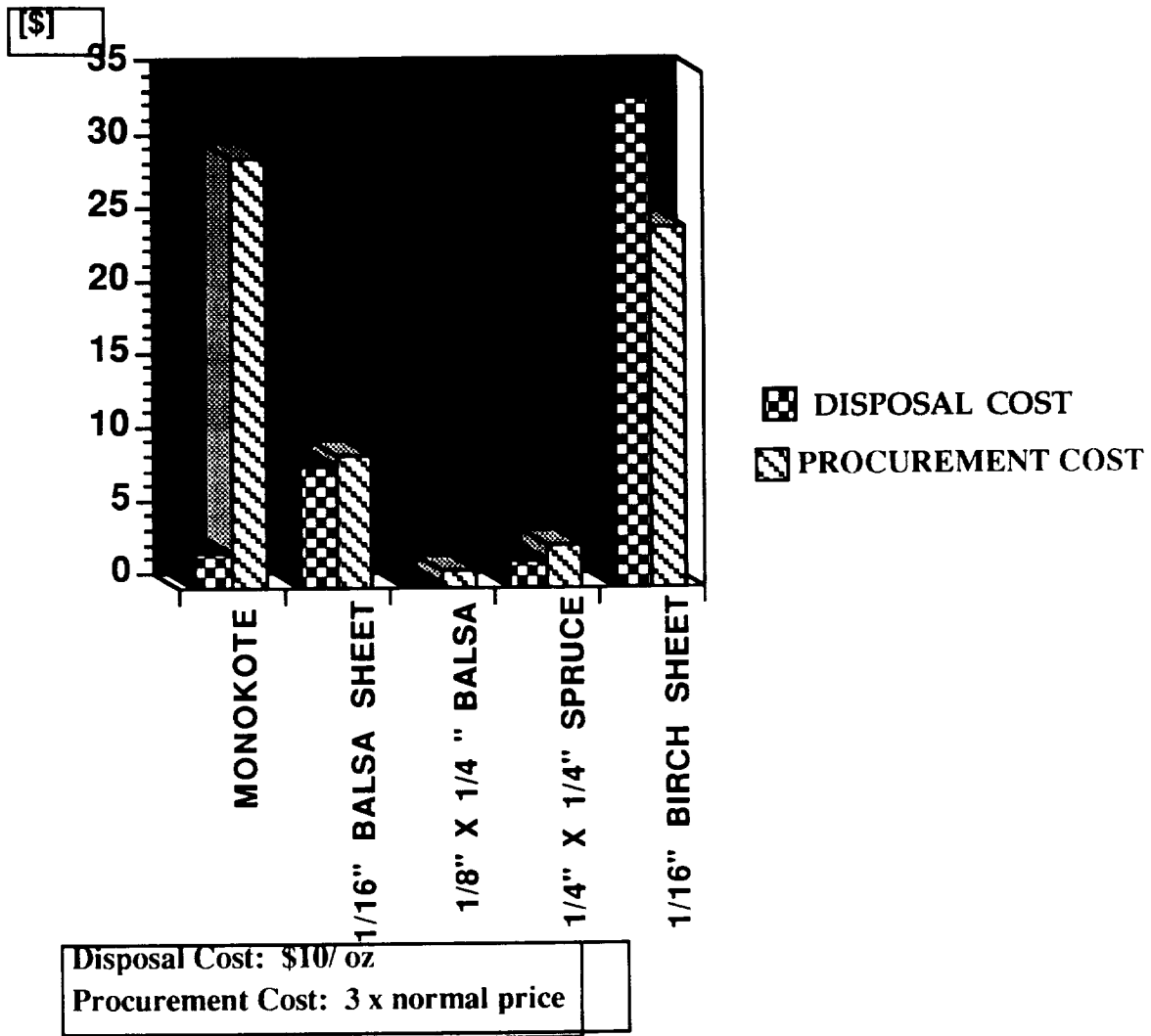


* Disposal Cost: \$10 per oz

* The above Graph shows the cost of disposing 1 foot or 1 square foot of excess material.

If disposal cost is compared with buying the material during manufacturing (Figure VI.4-2) the choice between the two penalties becomes ambiguous. Surplus is better in many cases because the amount needed is not always the amount which can be purchased. Both penalties are usually levied; however, certain situations would lean toward the old paradox, "more is less". Consider the following situation.

Figure VI.4-2 Comparing Penalties



Assume for example that you have a materials cost totaling \$134. The technology demonstrator requires more skin to cover the fuselage. If only one more square foot of Monokote is needed but you have to purchase 1872 square inches at three times the normal price you have increased your \$134 raw materials cost by 14% (Monokote ~ \$9.00/ roll). If you have to dispose of 1 square foot the disposal cost will be \$2.52, less than 2% of a \$134 raw materials cost. Remember also, if you have to buy a whole roll to

use a small portion of it, not only is the roll being procured at 3 times its normal cost but you must also dispose of the unused portion. If only 1 square foot is used on a 26" x 72" roll of Monokote, the cost to dispose the unused portion will be \$30. That extra roll of Monokote will increase your raw materials cost by 36%. Both surplus and shortage will result in both penalties more than likely. This can only be avoided if the amount of material needed can be procured at exactly the dimensions required. A situation of exact measurements and availability is very rare. Careful detailed materials list prior to procurement is the only way to minimize the penalties of too little and too much. Prediction of disposal cost is complicated by materials such as glue (epoxy). An estimate of \$40 disposal cost, .i.e. 4 oz of unused material is predicted.

Economics is certainly a concern. However, remember that it takes about \$100 difference in raw material cost to change the CPSPK by 6%. Therefore, the economy of raw materials is important, but more important is the structural integrity and safety of the aircraft. A list of the actual materials cost is attached to the end of this review.

In summary, the primary structural components were identified along with their sequence and methods of assembly. Manufacturing scheduling and the importance of a detailed blueprint were then discussed. Finally, the economic control and accounting concluded the manufacturing plan and review.

HOBBYLAND INC.
620 W. EDISON RD.
MISHAWAKA, IN
46545
219-255-1722

HOBBYLAND INC.
620 W. EDISON RD.
MISHAWAKA, IN
46545
219-255-1722

TE 04/08/93 11:17
VOICE NO: 37604

DATE 04/12/93 39:40
INVOICE NO: 38234

CLERK - BRIAN

CLERK - JEFF RIDGE

EM #	QTY DESCRIPTION	PRICE
76417	1 MID EPOXY 15 MIN 9 0	10.99T1
32920	1 LITE WHEELS 1-3/4"	4.50T1
31434	1 NYLON CNTL HORNS	.09T1
61989	1 #2X1/2" SCREWS	.79T1
36987	5 PEARL BLUE	29.37T1
35102	4 1/4 x 1/4 x 36" SPRU	4.00T1
85072	2 1/4 x 1 x 36" TR EDG	2.88T1
62107	4 1/2 x 3/8 LEADING ED	7.20T1
85072	2 1/4 x 1 x 36" TR EDG	2.88T1
384962	1 1/4 x 36" BIRCH DOME	.72T1
385102	8 1/4 x 1/4 x 36" SPRU	8.00T1
384989	1 1/8 x 1/4 Balsa STIC	.40T1
384988	10 1/8 x 3/16 Balsa STI	3.20T1
385155	1 1/32 x 12 x 14" 3-PL	8.19T1
385054	6 1/16 x 8 x 36" Balsa	18.00T1
46	SUB TOTAL	102.21
	SALES TAX	5.11
	INVOICE TOTAL	107.32
	VISA/MASTER	107.32
	AMT TENDERED	107.32

ITEM #	QTY DESCRIPTION	PRICE
836994	1 12 x 6 POWER POINT P	3.29T1
281567	1 HOOK & LOOP STUFF	3.45T1
364603	1 TAIL WHEEL ASSEMBLY	2.11
342279	1 1/8 LOG BEAR CLAMP	1.29
281452	1 1/8 WHL COLLARS	1.49
281451	1 3/32 WHL COLLARS	1.49
281651	1 1 1/4" TAIL WHEEL	1.70
792148	1 SEMI-FLEX. PUSH ROD	5.15
385001	14 1/4 x 3/8 x 36" BALS	8.96
385103	3 1/4 x 3/8 x 36" SPRU	3.60
481022	1 1/8" MUSIC WIRE	.87
35	SUB TOTAL	33.39
	SALES TAX	1.67
	INVOICE TOTAL	35.06
	VISA/MASTER	35.06
	AMT TENDERED	35.06

HOBBYLAND INC.
620 W. EDISON RD.
MISHAWAKA, IN
46545
219-255-1722

DATE 04/12/93 39:47
INVOICE NO: 38234

CLERK - BRIAN

ITEM #	QTY DESCRIPTION	PRICE
196419	1 INSTA-CUVE (+) 1OZ.	4.99T
1	SUB TOTAL	4.99
	SALES TAX	.25
	INVOICE TOTAL	5.24
	VISA/MASTER	5.24
	AMT TENDERED	5.24

THANK YOU

THANK YOU

THANK YOU

Rest. Person: Van D...

ORIGINAL PAGE IS OF POOR QUALITY

Appendix VI. Fabrication

Primary Problems in Construction:

- 1) Needed a more detailed schedule for the production of the *Blue Emu*.

The construction of the *Blue Emu* would have proceeded much more efficiently had more rigid component dead-lines been set. Without such a detailed schedule, there was a definite increase in total man-hours worked. The goal was 95 hours; the actual number was over 160.

- 2) Needed more detailed "cutting orders".

A problem arose in terms of which cuts were to come from which pieces of wood. As a result, there was a lot of scrap wood due to inefficient use of pieces that had already been cut. On top of this problem, it was unclear at times as to which pieces of wood were to be used for specific structural components of the aircraft, i.e., the fuselage, wing, nose, etc.

- 3) Should have exercised greater care in the production of airfoil sections.

Due to a tapered wing, a Xerox machine was used to scale down a master airfoil section to the appropriate size for placement on the wing. However, some of the wing tip airfoils were thicker at their trailing edges than those at the root. This is believed to be the result of neglecting to cut the cusp in the Wortmann airfoil.

- 4) Needed to monokote components more carefully.

Some components warped when the monokote was applied, namely the root chord airfoil section. The monokote is very strong, and as such, it can easily warp weak aspects of the aircraft. A number of groups had this problem.

- 5) Should have originally constructed a stronger tail section.

Many groups attempted to save weight by producing a light tail structure. However, it is also necessary to produce a structure that can withstand the loads of flight. The supports of the tail must be quite strong. Most groups had to reconstruct their horizontal and vertical tails as a result of the weak nature of the original construction.

Weight and Center of Gravity Concerns

1) Component Weights

Wings (both halves) :	1.36 lbs
Fuselage (with avionics and battery pack) :	4.01 lbs
<u>Carry through structure</u>	: <u>0.60 lbs</u>
total	: 5.97 lbs

This final weight represents an increase of approximately 0.4 lbs over the original weight estimate of 5.6 lbs. Prior to the submission of the draft proposal, the weight dropped to approximately 4.8 lbs, yet the group was informed that the final weight would most probably be closer to the original weight estimate. This is clearly the case for the *Blue Emu*.

2) Center of Gravity

Without the inclusion of the battery pack, the final position of the center of gravity of the *Blue Emu*, is approximately 20.0 inches aft of the tip of the propeller. The position of the battery pack was variable in order to compensate for motion of the aircraft's center of gravity for stability considerations. With the available motion of the battery pack, the center of gravity can be positioned at approximately 30% of the mean aerodynamic chord.